Line operators in theories of class $\mathcal{S}$, quantized moduli space of flat connections, and Toda field theory

Ioana Coman,[a,d] **Maxime Gabella**[a,b,c] **and Jörg Teschner**[a]

[a]*DESY, Theory Group,*
 Notkestrasse 85, Building 2a, 22607 Hamburg, Germany

[b]*Department of Mathematics, University of Hamburg,*
 Bundesstrasse 55, 20146 Hamburg, Germany

[c]*Institute for Advanced Study,*
 Einstein Drive, Princeton, NJ 08540, U.S.A.

[d]*Department of Theoretical Physics, NIPNE,*
 Str. Reactorului 30, 077125, Magurele, Romania

 E-mail: ioana.coman@desy.de, gabella@ias.edu, joerg.teschner@desy.de

ABSTRACT: Non-perturbative aspects of $\mathcal{N} = 2$ supersymmetric gauge theories of class $\mathcal{S}$ are deeply encoded in the algebra of functions on the moduli space $\mathcal{M}_{\text{flat}}$ of flat SL(N)-connections on Riemann surfaces. Expectation values of Wilson and 't Hooft line operators are related to holonomies of flat connections, and expectation values of line operators in the low-energy effective theory are related to Fock-Goncharov coordinates on $\mathcal{M}_{\text{flat}}$. Via the decomposition of UV line operators into IR line operators, we determine their noncommutative algebra from the quantization of Fock-Goncharov Laurent polynomials, and find that it coincides with the skein algebra studied in the context of Chern-Simons theory. Another realization of the skein algebra is generated by Verlinde network operators in Toda field theory. Comparing the spectra of these two realizations provides non-trivial support for their equivalence. Our results can be viewed as evidence for the generalization of the AGT correspondence to higher-rank class $\mathcal{S}$ theories.

doi:10.1007/JHEP10(2015)143

Contents

1 Introduction

There has been a lot of recent progress in the study of $\mathcal{N} = 2$ supersymmetric field theories in four dimensions (see [1] for a survey). Highlights include exact results on the expectation values of certain observables like Wilson and 't Hooft loop operators, and powerful algorithms for the computation of the spectra of BPS states. Many of these results are deeply related to mathematical structures on the moduli spaces of vacua.

A rich and interesting class of $\mathcal{N} = 2$ theories, often referred to as class $\mathcal{S}$, arises from the twisted compactification of the six-dimensional $(2,0)$ theory with Lie algebra $\mathfrak{g}$ on a Riemann surface $\mathcal{C}_{g,n}$ of genus g with n punctures [2, 3]. Class $\mathcal{S}$ theories of type $\mathfrak{g} = A_1$ admit weakly-coupled Lagrangian descriptions specified by pair of pants decompositions of $\mathcal{C}_{g,n}$. Each of the $3g - 3 + n$ cutting curves defining the pants decomposition corresponds to an SU(2) gauge group, while each of the n punctures corresponds to an SU(2) flavor group. Alday, Gaiotto, and Tachikawa (AGT) made the striking observation that the four-sphere partition functions of A_1 theories can be expressed in terms of the correlation functions of Liouville conformal field theory on $\mathcal{C}_{g,n}$ [4].

An important goal is the generalization of the AGT correspondence to higher rank. The origin of class $\mathcal{S}$ theories from the six-dimensional $(2,0)$ theory suggests that the relations to two-dimensional conformal field theory may have interesting generalizations for $N > 2$. In particular, A_{N-1} theories are expected to be related to SU(N) Toda field theory [5], and a lot of evidence has been accumulated for this conjecture, including [6–20]. It has been proven in [14] for a particular subclass of the A_{N-1} theories in class $\mathcal{S}$ which can be represented as quiver gauge theories with linear or circular quiver diagrams. However, neither side of this higher-rank AGT correspondence is well-understood. Usual methods do not apply because class $\mathcal{S}$ theories of type $\mathfrak{g} = A_{N-1}$ with $N > 2$ do not have Lagrangian descriptions in general. It is therefore unclear what should play the role of instanton partition functions in these non-Lagrangian theories. Similarly, the Toda conformal blocks seem to be poorly understood at the time of writing.

Parallel developments came from the insight of Gaiotto, Moore, and Neitzke (GMN) that the BPS spectrum of a class $\mathcal{S}$ theory is encoded in geometrical structures on the moduli space $\mathcal{M}_{\mathrm{vac}}$ of vacua of the theory on $\mathbb{R}^3 \times S^1$ [3, 21–23]. The six-dimensional description of class $\mathcal{S}$ theories implies that $\mathcal{M}_{\mathrm{vac}}$ is isomorphic to Hitchin's moduli space
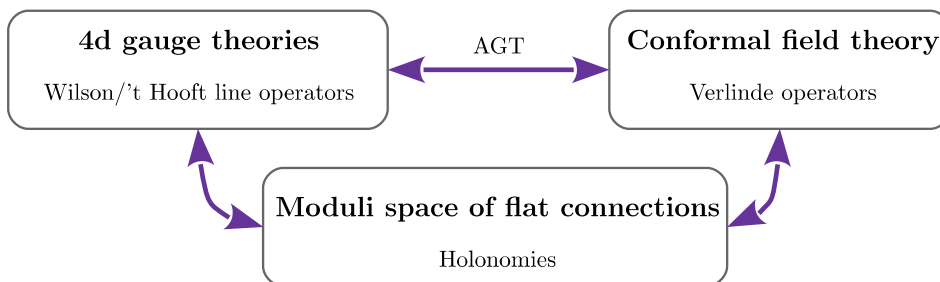
Figure 1. Triangle of relations between 4d $\mathcal{N} = 2$ supersymmetric gauge theories labeled by Riemann surfaces $\mathcal{C}_{g,n}$ (*left*), conformal field theory (Liouville or Toda) on $\mathcal{C}_{g,n}$ (*right*), and the moduli space of flat $\mathrm{SL}(N, \mathbb{C})$-connections on $\mathcal{C}_{g,n}$ (*bottom*). We also indicate the interpretation of line defects in each description.

$\mathcal{M}_{\mathrm{H}}$ of solutions to the self-duality equations on $\mathcal{C}_{g,n}$ (see [24] for a review). This space has a hyperkähler structure, and in one of its complex structures it can be identified with the moduli space $\mathcal{M}_{\mathrm{flat}}$ of complex flat connections. This leads to the key relation

$$\mathcal{M}_{\mathrm{vac}}(\mathbb{R}^3 \times S^1) = \mathcal{M}_{\mathrm{flat}}(\mathcal{C}_{g,n}) \ . \tag{1.1}$$

An important manifestation of this relation is that vacuum expectation values of BPS line operators in class $\mathcal{S}$ theories can be expressed as holonomies of flat connections on $\mathcal{C}_{g,n}$.

It has subsequently been observed in [25] that the origin of the AGT correspondence can be understood from the relation to $\mathcal{M}_{\mathrm{flat}}$ (see [26]). Thus there appears to be a triangle of relations between $\mathcal{N} = 2$ supersymmetric gauge theories, conformal field theories, and moduli spaces of flat connections, as depicted in figure 1.

In this paper, we make the first steps towards a generalization of this triangle of relations to higher rank. Given the difficulties in tackling directly higher-rank gauge theories and Toda field theory, we focus first on flat connections. We will describe in detail the quantum algebra $\mathcal{A}^{\mathrm{flat}}$ of functions on the moduli space of flat $\mathrm{SL}(N, \mathbb{C})$-connections, which the arguments of GMN relate to the algebra $\mathcal{A}^{\mathrm{line}}$ of quantized line operators in class $\mathcal{S}$ theories of type A_{N-1}. We will moreover show that $\mathcal{A}^{\mathrm{flat}}$ can be identified with the algebra $\mathcal{A}^{\mathrm{Ver}}$ of Verlinde loop and network operators in $\mathrm{SU}(N)$ Toda field theory. Given the central role played by these algebras in the approach of [25], we may regard the relations

$$\mathcal{A}^{\mathrm{line}} \simeq \mathcal{A}^{\mathrm{flat}} \simeq \mathcal{A}^{\mathrm{Ver}} \tag{1.2}$$

as support for a higher-rank AGT correspondence.

Before summarizing our results in more detail, we now give some background about line operators and their role in the AGT correspondence.

Line operators and framed BPS states. BPS line operators in class $\mathcal{S}$ theories are supersymmetric generalizations of Wilson and 't Hooft line observables, describing the effect of inserting heavy dyonic probe particles labeled by electric and magnetic charge
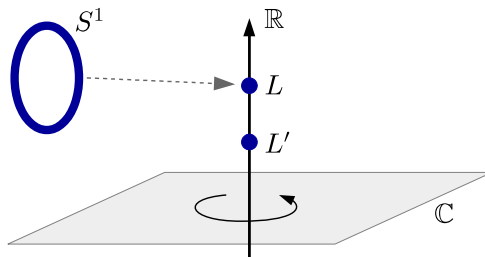
Figure 2. The algebra of line operators can be quantized by twisting $\mathbb{R}^3 \times S^1$ such that a plane $\mathbb{C} \subset \mathbb{R}^3$ rotates as one moves along the S^1. BPS line operators wrap S^1 and align along the axis $\mathbb{R}$ at the origin of $\mathbb{C}$.

vectors.[1] Such a line operator can be viewed as descending from a surface operator in the six-dimensional $(2,0)$ theory, which is labeled by a representation $\mathcal{R}$ of $\mathfrak{g}$ and supported on $\Sigma = S^1 \times \wp$, with $\wp$ a path in $\mathcal{C}_{g,n}$. This leads to a relation between the vacuum expectation value (vev) of the line operator $L(\mathcal{R}; \wp)$ on S^1 and the classical holonomy of a flat connection $\mathcal{A}$ along the path $\wp$ on $\mathcal{C}_{g,n}$:

$$\big\langle L(\mathcal{R}; \wp) \big\rangle = \mathrm{tr}_{\mathcal{R}} \mathrm{Hol}_{\wp} \mathcal{A} \,. \tag{1.3}$$

BPS line operators thus provide natural coordinate functions on $\mathcal{M}_{\mathrm{flat}}$.

As argued in [22, 29], the vev of a UV line operator L can be represented in the IR in terms of a set of vevs of line operators $\mathcal{X}_\gamma$ with charge γ defined using the low-energy abelian gauge fields:

$$L \rightsquigarrow \sum_\gamma \overline{\Omega}(L, \gamma) \mathcal{X}_\gamma \,. \tag{1.4}$$

The coefficients $\overline{\Omega}(L, \gamma)$ are integers which count the BPS states supported by the line operator L, called *framed BPS states*. The IR line operators $\mathcal{X}_\gamma$ are Darboux coordinates on $\mathcal{M}_{\mathrm{flat}}$ that are closely related to the coordinates constructed by Fock and Goncharov in their study of higher Teichmüller spaces [30].

The line operators can be quantized by twisting $\mathbb{R}^3 \times S^1$ into the fibered product $\mathbb{R} \times \mathbb{C} \times_q S^1$ such that a coordinate z on $\mathbb{C}$ rotates as $z \to qz$ after going around S^1 [22, 31, 32]. BPS conditions then constrain line operators on S^1 to be located at points along the axis $\mathbb{R}$ and at the origin of $\mathbb{C}$ (see figure 2). The relation (1.4) between UV and IR line operators becomes

$$\hat{L} \rightsquigarrow \sum_\gamma \overline{\Omega}(L, \gamma; q) \hat{\mathcal{X}}_\gamma \,, \tag{1.5}$$

where the noncommutative variables $\hat{\mathcal{X}}_\gamma$ satisfy the relation $\hat{\mathcal{X}}_\gamma \hat{\mathcal{X}}_{\gamma'} = q^{\frac{1}{2}\langle \gamma, \gamma' \rangle} \hat{\mathcal{X}}_{\gamma+\gamma'}$ appearing in the quantization of the algebra of functions on higher Teichmüller spaces. The coefficients $\overline{\Omega}(L, \gamma; q)$ are the *framed protected spin characters* defined in [22] as

$$\overline{\Omega}(L, \gamma; q) = \mathrm{tr}_{\mathcal{H}_L^{\mathrm{BPS}}} q^{J_3} (-q^{\frac{1}{2}})^{2I_3} \,, \tag{1.6}$$

---

[1] Note that allowed sets of "mutually local" line operators are specified by a certain topological data, which impose some restrictions on the representations [22, 27, 28]. This subtlety will not affect our conclusions in an essential way, as noted for the A_1 case in [26].

where $\mathcal{H}_L^{\mathrm{BPS}}$ is the Hilbert space of framed BPS states, and J_3 and I_3 are generators of the SO(3) and SU(2)$_R$ symmetries. GMN conjectured that framed BPS states have $I_3 = 0$ ("no exotics conjecture"), which implies in particular that the $\overline{\Omega}(L, \gamma; q)$ are linear combinations of su(2) characters with positive integral coefficients. The coefficients of $q^m X_\gamma$ in the decomposition (1.5) of a line operator are dimensions of Hilbert spaces graded by the IR electromagnetic charges γ and the so(3) spins m.

The noncommutative algebra of IR line operators $\hat{\mathcal{X}}_\gamma$ determines via (1.5) the algebra of UV line operators, which can be represented by relations of the form

$$\hat{L} * \hat{L}' = \sum_{L''} c(L, L', L''; q)\hat{L}'' \ . \tag{1.7}$$

The order in which we multiply operators corresponds to their ordering along the axis $\mathbb{R}$. The algebra generated by the operators $\hat{L}$ can be viewed as a noncommutative deformation of the algebra of functions on $\mathcal{M}_{\mathrm{flat}}$, with q the deformation parameter. For A_1 theories, it was argued in [22] that this algebra is isomorphic to the algebra of quantum geodesic length operators in quantum Teichmüller theory.

The role of line operators in the AGT correspondence. Expectation values of line operators in A_1 theories on the four-ellipsoid $E_{\epsilon_1,\epsilon_2}^4 = \{x_0^2 + \epsilon_1^2(x_1^2 + x_2^2) + \epsilon_2^2(x_3^2 + x_4^2) = 1\}$ can be calculated by localization [33–35] and take the schematic form

$$\left\langle L \right\rangle_{\epsilon_1,\epsilon_2} = \int \mathrm{d}a \, (\Psi(a))^* \, \mathsf{L} \, \Psi(a) \ . \tag{1.8}$$

The integration is performed over variables $a = (a_1, \ldots, a_h)$ representing the zero modes of the $h = 3g - 3 + n$ scalar fields in the vector multiplets. $\Psi(a)$ represents the contribution of the path integral over the lower half-ellipsoid with $x_0 < 0$, and L is a finite difference operator acting on the variables a. It is natural to interpret the right hand side of (1.8) as an expectation value in an effective zero-mode quantum mechanics. By localization, this quantum mechanics in finite volume can be shown to represent the exact result for $\langle L \rangle_{\epsilon_1,\epsilon_2}$. The functions $\Psi(a)$ can be identified with the instanton partition functions (see [36] for a review and references) that were found to be related to Liouville conformal blocks by AGT.

The approach proposed in [25] establishes the relation between the wave-functions $\Psi(a)$ in (1.8) and the Liouville conformal blocks without using the relation to the instanton partition functions observed in [33]. It is based on the observation that the effective zero-mode quantum mechanics in which line operators take the form (1.8) coincides with the quantum-mechanical system obtained by quantizing a real slice $\mathcal{M}_{\mathrm{flat}}^{\mathbb{R}}$ in $\mathcal{M}_{\mathrm{flat}}$. This follows from the fact that the algebra $\mathcal{A}_{\epsilon_1\epsilon_2}^{\mathrm{line}}$ generated by the supersymmetric line operators on $E_{\epsilon_1,\epsilon_2}^4$ factorizes as $\mathcal{A}_{\epsilon_1\epsilon_2}^{\mathrm{line}} \simeq \mathcal{A}_{\epsilon_1/\epsilon_2}^{\mathrm{flat}} \times \mathcal{A}_{\epsilon_2/\epsilon_1}^{\mathrm{flat}}$ into two copies of the noncommutative algebra $\mathcal{A}_{\hbar}^{\mathrm{flat}}$ obtained in the quantization of the algebra of coordinate functions on $\mathcal{M}_{\mathrm{flat}}$, as argued for instance in [37]. The two copies correspond to line operators supported on $x_0 = x_1 = x_2 = 0$ and $x_0 = x_3 = x_4 = 0$, respectively. The same conclusion can be reached from the observation made in [32] that the algebra of line operators supported on $x_0 = x_1 = x_2 = 0$, for example, is isomorphic as a noncommutative algebra to the algebra of line

operators in $\mathbb{R}^3 \times S^1$ defined via (1.7) with $\hbar = \epsilon_1/\epsilon_2$. The twisting of $\mathbb{R}^3 \times S^1$ inducing the noncommutativity models the residual effect of the curvature near the support of the line operators on $E^4_{\epsilon_1,\epsilon_2}$.

Duality invariance of the expectation values (1.8) can then be combined with the representation theory of $\mathcal{A}^{\text{line}}_{\epsilon_1\epsilon_2}$ to obtain a precise mathematical characterization of the wave functions $\Psi(a) \equiv \Psi_\tau(a)$, now considered as multivalued analytic functions of the gauge coupling constants $\tau = (\tau_1, \ldots, \tau_h)$ [25]. It was furthermore shown in [25] that the Virasoro conformal blocks represent the same mathematical objects. Within conformal field theory one can, in particular, define a natural family of operators called the Verlinde loop operators representing the action of the quantized algebra of functions on $\mathcal{M}_{\text{flat}}$ on spaces of conformal blocks.

Having established the relation between wave-functions $\Psi_\tau(a)$ and the Liouville conformal blocks it remains to notice that the functions $\Psi(a)$ in (1.8) must coincide with the instanton partition functions defined in [38]. Different arguments in favour of this identification can be found in [33] and in [37]. This line of argument establishes the validity of the relations between conformal blocks and instanton partition functions conjectured in [4] for all A_1 theories of class $\mathcal{S}$.[2] A crucial role is played by the relation of the algebra $\mathcal{A}^{\text{flat}}_\hbar$ to the algebra $\mathcal{A}^{\text{Ver}}$ generated by the Verlinde line operators. This relation is generalized to theories of higher rank in our paper, thereby supporting the natural generalization of the AGT correspondence to class $\mathcal{S}$ theories of type A_{N-1}.

Overview. In this paper, we start a program to generalize the AGT correspondence to higher rank based on the central role of line operators and the moduli space of flat connections in the approach of [25].

The six-dimensional origin of class $\mathcal{S}$ theories of type A_{N-1} suggests that there should exist a family of line operators that correspond to coordinate functions on the moduli space $\mathcal{M}^N_{g,n} \equiv \mathcal{M}^{\text{SL}(N,\mathbb{C})}_{\text{flat}}(\mathcal{C}_{g,n})$ of flat $\text{SL}(N,\mathbb{C})$-connections. While for A_1 theories traces of holonomies along simple closed loops as in (1.3) were enough to parameterize $\mathcal{M}^2_{g,n}$, for higher rank we consider in addition some functions associated with *networks* on $\mathcal{C}_{g,n}$. These network functions are constructed from a collection of holonomies along open paths that are contracted at junctions with $\text{SL}(N)$-invariant tensors. Such networks arise naturally from products of simple curves by applying $\text{SL}(N)$ skein relations at their intersections. The algebra $\mathcal{A}^N_{g,n}$ of functions on $\mathcal{M}^N_{g,n}$ can be described in terms of a set of generators (loop and network functions) and the relations that they satisfy (section 2). A standard way to quantize $\mathcal{A}^N_{g,n}$ into a noncommutative algebra is to use quantum skein relations to resolve intersections in a product of operators (this deformation can be defined using the Reshetikhin-Turaev construction of knot invariants in terms of quantum group theory). This gives a product of the form (1.7), where the operators $\hat{L}$ may also be network operators.

In section 3, we give several explicit examples of algebras $\mathcal{A}^N_{g,n}$ and their quantizations for basic surfaces: three-puncture sphere $\mathcal{C}_{0,3}$, one-punctured torus $\mathcal{C}_{1,1}$, four-punctured sphere $\mathcal{C}_{0,4}$. Using pants decompositions of surfaces $\mathcal{C}_{g,n}$, we can build the algebras $\mathcal{A}^N_{g,n}$ from these building blocks, in the spirit of the "tinkertoys" approach [40].

---

[2]A somewhat similar approach to the case $\epsilon_2 = 0$ had previously been outlined in [39].

In section 4, we describe an explicit representation of the algebra $\mathcal{A}_{g,n}^N$ in terms of Fock-Goncharov coordinates [30]. Loop and network functions are expressed in terms of positive Laurent polynomials, as in the relation (1.4) between UV and IR line operators. The natural quantization of Fock-Goncharov coordinates then determines uniquely the quantization of $\mathcal{A}_{g,n}^N$. For all the cases that we compared, we find that the resulting quantum relations coincide with the ones obtained from skein quantization. Furthermore, the existence of such quantum relations turns out to lead to a unique quantization of the Fock-Goncharov polynomials, as in (1.5). This allows us obtain many examples of framed protected spin characters (1.6) in higher-rank theories.

In section 5, we define Verlinde network operators, which are natural generalizations of Verlinde loop operators [41, 42] acting on spaces of conformal blocks in Toda field theory. We show that the algebra $\mathcal{A}^{\mathrm{Ver}}$ generated by the Verlinde network operators can be identified with the quantized algebra $\mathcal{A}_{g,n}^N$. To see this, we first observe that the braiding matrix in Toda field theory, from which the Verlinde network operators are built, is related via a twist to the standard R-matrix of the quantum group $\mathcal{U}_q(sl_N)$. In turn, this R-matrix is used to construct the quantum skein algebra defining the quantized version of $\mathcal{A}_{g,n}^N$.

As an outlook, we make a few observations in section 6 about the comparison of the spectra of the operators representing the skein algebra in Toda field theory and in the quantum theory of the moduli space of flat connections, respectively. The appendices collect some background about Fock-Goncharov coordinates and about quantum groups.

2 Algebra of loop and network operators

This section describes relevant background on the algebra $\mathcal{A}_{g,n}^N$ of functions on the moduli space $\mathcal{M}_{g,n}^N$ of flat connections on a punctured Riemann surface $\mathcal{C}_{g,n}$, which can be described in terms of generators and relations. We construct a set of generators for $\mathcal{A}_{g,n}^N$ consisting of functions associated with simple loops and networks naturally associated with a pair of pants decomposition of $\mathcal{C}_{g,n}$. Other functions can then be obtained by taking products of generators and resolving intersections with skein relations. The number of generators obtained in this way typically exceeds the dimension of the moduli space, as is reflected in the existence of polynomial relations between the coordinate functions. The algebra $\mathcal{A}_{g,n}^N$ has a Poisson structure, and it can be deformed into a noncommutative algebra $\mathcal{A}_{g,n}^N(q)$ by applying the skein relations that encode the representation theory of the quantum group $\mathcal{U}_q(sl_N)$. We study in detail the case of pair of pants $\mathcal{C}_{0,3}$, which is the building block for any $\mathcal{C}_{g,n}$. This will illustrate the crucial role of networks at higher rank. We also present some results for the punctured torus $\mathcal{C}_{1,1}$ and the four-punctured sphere $\mathcal{C}_{0,4}$. Using pants decompositions one can use these results to get a set of coordinates allowing us to cover $\mathcal{M}_{g,n}^N$ at least locally.

2.1 Moduli space of flat connections

The close relationship between 4d $\mathcal{N} = 2$ supersymmetric theories in class $\mathcal{S}$ and Hitchin systems is revealed by compactifying on a circle S^1. The moduli space $\mathcal{M}_{\mathrm{vac}}$ of vacua of such theories with gauge group G on $\mathbb{R}^3 \times S^1$ can be identified with the moduli space of

solutions to Hitchin's equations on $\mathcal{C}_{g,n}$ [3, 22]. These equations imply that the complex connections $\mathcal{A}(\zeta)$ built out of a connection A and a one-form φ,

$$\mathcal{A}(\zeta) = R\zeta^{-1}\varphi + A + R\zeta\bar{\varphi}\,, \tag{2.1}$$

are flat for all values of the parameter $\zeta \in \mathbb{C}^*$ (R is the radius of S^1).[3] $\mathcal{M}_{\text{vac}}$ is a hyper-Kähler space, and with the appropriate choice of complex structure it is identified with the moduli space of flat $G_{\mathbb{C}}$-connections on $\mathcal{C}_{g,n}$, with singularities at the punctures. We will only consider the cases where the singularities at the punctures are of regular type.[4] Flat connections modulo gauge transformations are then completely characterised by the representation of the fundamental group $\pi_1(\mathcal{C}_{g,n})$ generated by the holonomy matrices. The holonomy of a flat $G_{\mathbb{C}}$-connection $\nabla = \mathrm{d} + \mathcal{A}$ along a closed curve $\gamma \in \pi_1(\mathcal{C}_{g,n})$ is given by $\mathrm{Hol}(\gamma) = \mathcal{P}\exp\int_{\gamma}\mathcal{A} \in G_{\mathbb{C}}$. The moduli space $\mathcal{M}_{\text{vac}}$ is thereby identified with the space of representations of $\pi_1(\mathcal{C}_{g,n})$ into $G_{\mathbb{C}}$ called the character variety:

$$\mathcal{M}_{\text{vac}} \simeq \mathrm{Hom}\big(\pi_1(\mathcal{C}_{g,n}), G_{\mathbb{C}}\big)/G_{\mathbb{C}}\,. \tag{2.2}$$

More explicitly we have

$$\mathcal{M} = \left\{ (\mathbf{A}_1, \ldots, \mathbf{A}_g, \mathbf{B}_1, \ldots, \mathbf{B}_g, \mathbf{M}_1, \ldots, \mathbf{M}_n) \,\middle|\, \prod_{i=1}^{g}\mathbf{A}_i\mathbf{B}_i\mathbf{A}_i^{-1}\mathbf{B}_i^{-1} = \prod_{a=1}^{n}\mathbf{M}_a \right\}\middle/ G_{\mathbb{C}},$$

where $\mathbf{A}_i, \mathbf{B}_i \in G_{\mathbb{C}}$ are holonomy matrices for based loops going around the A- and B-cycles for each of the g handles, and $\mathbf{M}_a \in G_{\mathbb{C}}$ are holonomy matrices for based loops going around each of the n punctures. These matrices are considered modulo the action of $G_{\mathbb{C}}$ by simultaneous conjugation.

For 4d $\mathcal{N} = 2$ theories of type A_{N-1}, the complexified gauge group is $G_{\mathbb{C}} = \mathrm{SL}(N, \mathbb{C})$. We are thus interested in the moduli space $\mathcal{M}_{g,n}^N \equiv \mathcal{M}_{\text{flat}}^{\mathrm{SL}(N,\mathbb{C})}(\mathcal{C}_{g,n})$ of flat $\mathrm{SL}(N, \mathbb{C})$-connections on a Riemann surface $\mathcal{C}_{g,n}$, modulo gauge transformations. It has a dimension given by

$$\dim[\mathcal{M}_{g,n}^N] = -\chi(\mathcal{C}_{g,n})\dim[\mathrm{SL}(N, \mathbb{C})] = (2g + n - 2)(N^2 - 1)\,, \tag{2.3}$$

with the Euler characteristic $\chi(\mathcal{C}_{g,n}) = 2 - 2g - n$. We can furthermore fix the conjugacy classes of the holonomies $\mathbf{M}_a$ around the punctures (as we will see, this amounts to restricting to a symplectic leaf of the Poisson variety $\mathcal{M}_{g,n}^N$). The moduli space $\bar{\mathcal{M}}_{g,n}^N$ of flat connections with $\mathbf{M}_a$ in fixed conjugacy classes has the dimension

$$\begin{aligned}\dim[\bar{\mathcal{M}}_{g,n}^N] &= -\chi(\mathcal{C}_{g,n})\dim[\mathrm{SL}(N, \mathbb{C})] - n\,\mathrm{rank}[\mathrm{SL}(N, \mathbb{C})] \\ &= (2g + n - 2)(N^2 - 1) - n(N - 1)\,. \tag{2.4}\end{aligned}$$

2.2 Trace functions

The algebra $\mathcal{A}_{g,n}^N \equiv \mathrm{Fun}^{\mathrm{alg}}(\mathcal{M}_{g,n}^N)$ of algebraic functions on $\mathcal{M}_{g,n}^N$ can be described in terms of generators and relations, as we now review. Traces of holonomy matrices provide

---

[3]We will restrict to the case $\zeta = 1$ henceforth.

[4]Regularity means that the connection is gauge-equivalent to a meromorphic connection with simple poles at the punctures.

coordinate functions for $\mathcal{M}_{g,n}^N$ (see e.g. [43] for a review). They can be expressed as traces of words made out of letters given by the holonomy matrices $\mathbf{A}_i, \mathbf{B}_i, \mathbf{M}_a$. The relation coming from the fundamental group $\pi_1(\mathcal{C}_{g,n})$ allows us to eliminate one of the holonomy matrices, say $\mathbf{M}_n$, which leaves $(1-\chi)$ independent letters (for $n > 0$). General upper bounds are known for the maximal length of words that form a generating set of $\mathcal{A}_{g,n}^N$. The generators can be taken to be traces of words with lengths up to $N(N+1)/2$ for $N \le 4$, or up to N^2 for $N > 4$ (see references in [44]). The difference between the number of generators and the dimension of $\mathcal{M}_{g,n}^N$ is then accounted for by the existence of polynomial relations $\mathcal{P}_\alpha = 0$, which are consequences of the Cayley-Hamilton theorem. The algebra $\mathcal{A}_{g,n}^N$ is thus described as the polynomial ring generated by trace functions quotiented by polynomial relations:

$$\mathcal{A}_{g,n}^N = \mathbb{C}\left[\text{tr}\mathbf{A}_i, \text{tr}\mathbf{A}_i\mathbf{B}_j, \cdots\right]/\{\mathcal{P}_\alpha\}. \tag{2.5}$$

Note that this algebraic structure of $\mathcal{M}_{g,n}^N$ does not distinguish between different surfaces with the same number of letters. For example, the description of $\mathcal{A}_{g,n}^N$ in terms of generators and relations is the same for the one-punctured torus $\mathcal{C}_{1,1}$ and for the three-punctured sphere $\mathcal{C}_{0,3}$, which both have $(1-\chi) = 2$ letters.

Examples for $N = 2$: let us first consider the particularly simple example of SL$(2,\mathbb{C})$-connections on the one-punctured torus $\mathcal{C}_{1,1}$. The moduli space is given by

$$\mathcal{M}_{1,1}^2 = \{(\mathbf{A},\mathbf{B},\mathbf{M})|\mathbf{A}\mathbf{B}\mathbf{A}^{-1}\mathbf{B}^{-1} = \mathbf{M}\}/\text{SL}(2,\mathbb{C}) . \tag{2.6}$$

The algebra of functions $\mathcal{A}_{1,1}^2$ is generated by the trace functions

$$\text{tr}\mathbf{A}, \ \text{tr}\mathbf{B}, \ \text{tr}\mathbf{AB} . \tag{2.7}$$

Since the dimension of $\mathcal{M}_{1,1}^2$ is 3, there is no relation between these 3 generators. However, the generators are related to the trace of the holonomy around the puncture via

$$(\text{tr}\mathbf{A})^2 + (\text{tr}\mathbf{B})^2 + (\text{tr}\mathbf{AB})^2 - \text{tr}\mathbf{A}\text{tr}\mathbf{B}\text{tr}\mathbf{AB} = -\text{tr}\mathbf{M} + 2 , \tag{2.8}$$

and therefore they do satisfy a relation once we fix the conjugacy class of $\mathbf{M}$ to obtain $\bar{\mathcal{M}}_{1,1}^2$.

A more typical example is the sphere $\mathcal{C}_{0,4}$ with four punctures, which we label by A, B, C, D. The moduli space is

$$\mathcal{M}_{0,4}^2 = \{(\mathbf{A},\mathbf{B},\mathbf{C},\mathbf{D})|\mathbf{A}\mathbf{B}\mathbf{C}\mathbf{D} = \mathbf{I}\}/\text{SL}(2,\mathbb{C}) . \tag{2.9}$$

The holonomies $\mathbf{A}$, $\mathbf{B}$, $\mathbf{C}$ can be taken to be 3 independent letters, while $\mathbf{D} = (\mathbf{A}\mathbf{B}\mathbf{C})^{-1}$. The algebra of functions $\mathcal{A}_{0,4}^2$ is generated by traces of words with maximal length equal to 3:

$$\mathbf{A}, \ \mathbf{B}, \ \mathbf{C}, \ \mathbf{AB} \equiv \mathbf{S}, \ \mathbf{BC} \equiv \mathbf{T}, \ \mathbf{CA} \equiv \mathbf{U}, \ \mathbf{ABC} = \mathbf{D}^{-1}, \ \mathbf{CBA} . \tag{2.10}$$

These 8 trace functions satisfy 2 polynomial relations (we use the notation $A_1 \equiv \text{tr}\mathbf{A}$):

$$D_1 + \text{tr}\mathbf{CBA} = A_1 T_1 + B_1 U_1 + C_1 S_1 - A_1 B_1 C_1 , \tag{2.11}$$

$$\begin{aligned} D_1 \cdot \text{tr}\mathbf{CBA} = {} & S_1 T_1 U_1 + S_1^2 + T_1^2 + U_1^2 + A_1^2 + B_1^2 + C_1^2 \\ & - A_1 B_1 S_1 - B_1 C_1 T_1 - C_1 A_1 U_1 - 4 . \end{aligned}$$

The first relation allows to eliminate $\mathrm{tr}\mathbf{CBA}$ since it is linear. The algebra of functions $\mathcal{A}^2_{0,4}$ is then described as the quotient of the polynomial ring

$$\mathbb{C}[A_1, B_1, C_1, D_1, S_1, T_1, U_1] \tag{2.12}$$

by the quartic polynomial

$$\begin{aligned}
\mathcal{P}_1 = \ & S_1 T_1 U_1 + S_1^2 + T_1^2 + U_1^2 + A_1 B_1 C_1 D_1 + A_1^2 + B_1^2 + C_1^2 + D_1^2 \\
& -(A_1 B_1 + C_1 D_1)S_1 - (B_1 C_1 + D_1 A_1)T_1 - (C_1 A_1 + B_1 D_1)U_1 - 4 \ .
\end{aligned} \tag{2.13}$$

This gives a 6-dimensional quartic hypersurface in $\mathbb{C}^7$.

In general, the number of words in r letters of length up to 3 is

$$r + \binom{r}{2} + \binom{r}{3} = \frac{r(r^2 + 5)}{6} \ . \tag{2.14}$$

This number of generators becomes quickly much larger than the dimension $3(r-1)$ of $\mathcal{M}^2_{g,n}$, which implies that there are many polynomial relations.

Example for $N = 3$: the description of $\mathcal{A}^3_{g,n}$ for surfaces with 2 letters is very similar to that of $\mathcal{A}^2_{g,n}$ for surfaces with 3 letters (see for example [45] and references therein). The generators of $\mathcal{A}^3_{1,1}$ can be taken to be the traces of the 10 following words with length up to 6 (note that the Cayley-Hamilton theorem implies that $\mathbf{A}^{-1} \sim \mathbf{A}^2$ so it counts as 2 letters):

$$\mathbf{A}^{\pm 1}, \ \mathbf{B}^{\pm 1}, \ (\mathbf{AB})^{\pm 1}, \ (\mathbf{AB}^{-1})^{\pm 1}, \ (\mathbf{ABA}^{-1}\mathbf{B}^{-1})^{\pm 1} \ . \tag{2.15}$$

These generators satisfy 2 relations (similar to the relations (2.11) for $\mathcal{A}^2_{0,4}$):

$$\begin{aligned}
\mathrm{tr}\mathbf{ABA}^{-1}\mathbf{B}^{-1} + \mathrm{tr}\mathbf{BAB}^{-1}\mathbf{A}^{-1} &= (\dots), \\
\mathrm{tr}\mathbf{ABA}^{-1}\mathbf{B}^{-1} \cdot \mathrm{tr}\mathbf{BAB}^{-1}\mathbf{A}^{-1} &= (\dots) \ .
\end{aligned} \tag{2.16}$$

Eliminating $\mathrm{tr}\mathbf{BAB}^{-1}\mathbf{A}^{-1}$ with the first relation, we can then describe $\mathcal{A}^3_{1,1}$ as an 8-dimensional sextic hypersurface in $\mathbb{C}^9$.

2.3 Poisson structure

There is a Poisson structure on the moduli space $\mathcal{M}^N_{g,n}$, see [46] for a review and further references. Note that unlike the algebraic structure described in the previous subsection, the Poisson structure does distinguish between surfaces with the same $\chi(\mathcal{C}_{g,n})$. Goldman gave a general formula for the Poisson bracket of trace functions in terms of intersections of curves [47]:

$$\{\mathrm{trHol}(\alpha), \mathrm{trHol}(\beta)\} = \sum_{p \in \alpha \cap \beta} \epsilon(p; \alpha, \beta)\left[\mathrm{trHol}(\alpha_p \beta_p) - \frac{1}{N}\mathrm{trHol}(\alpha)\mathrm{trHol}(\beta)\right], \tag{2.17}$$

where $\epsilon(p; \alpha, \beta) = \pm 1$ is the oriented intersection number at the point p, and α_p, β_p are the curves α, β based at p.
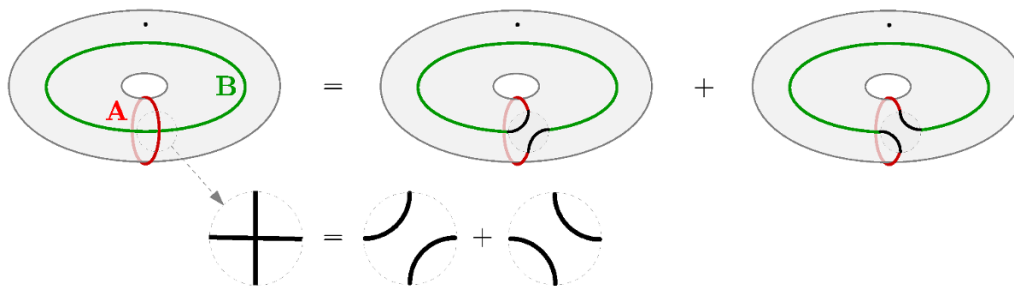
Figure 3. *Top*: the product of the trace functions for the A- and B-cycles on $\mathcal{C}_{1,1}$ gives the trace functions associated with the curves obtained by resolving the intersection. *Bottom*: locally, the crossing is replaced by two pairs of non-intersecting segments. This is the classical skein relation for $N = 2$.

As an illustration we can consider $\mathcal{C}_{1,1}$ with $N = 2$. Since the A- and B-cycles intersect once, Goldman's formula gives

$$\{\mathrm{tr}\mathbf{A}, \mathrm{tr}\mathbf{B}\} = \mathrm{tr}\mathbf{AB} - \frac{1}{2}\mathrm{tr}\mathbf{A}\mathrm{tr}\mathbf{B} \ . \tag{2.18}$$

Note that the right-hand side can be written as the derivative of the relation (2.8) by $\mathrm{tr}\mathbf{AB}$. This indicates that the Poisson structure on $\mathcal{M}_{1,1}^2$ is compatible with its structure as an algebraic variety. The Poisson algebra for the traces functions (2.15) on $\mathcal{M}_{0,3}^3$ and $\mathcal{M}_{1,1}^3$ has been studied in [48].

2.4 Classical skein algebra

Relations between functions in $\mathcal{A}_{g,n}^N$ have a topological origin. Let us take again the example of $\mathcal{C}_{1,1}$ with $N = 2$. The product of the traces associated with the A- and B-cycles is given by

$$\mathrm{tr}\mathbf{A}\mathrm{tr}\mathbf{B} = \mathrm{tr}\mathbf{AB} + \mathrm{tr}\mathbf{AB}^{-1} \ . \tag{2.19}$$

Graphically, we can interpret this as resolving the intersection of the A- and B-cycles into a pair of curves that curl up around the torus in two ways (see figure 3). This procedure is reminiscent of the classical skein relations in knot theory, which are linear relations between knot diagrams (projections of knots onto a plane) that differ only locally around an intersection. In fact, skein relations are nothing else than graphical representations of ϵ-tensor identities such as $\epsilon_{ab}\epsilon^{cd} = \delta_a^c\delta_b^d - \delta_a^d\delta_b^c$, which can be used to derive the relation (2.19).

The SL(2) skein relation implies that $\mathcal{A}_{g,n}^2$ can be described in terms of simple curves without self-intersections. In the case of $\mathcal{C}_{0,3}$ with $N = 2$, the trace function $\mathrm{tr}\mathbf{AB}^{-1}$, which corresponds to a figure-8 curve surrounding the punctures A and B and intersecting itself once, can be expressed in terms of non-intersecting curves as

$$\mathrm{tr}\mathbf{AB}^{-1} = \mathbf{A}_d^a\mathbf{B}^{-1b}{}_c\delta_a^c\delta_b^d = \mathbf{A}_d^a\mathbf{B}^{-1b}{}_c(\epsilon_{ab}\epsilon^{cd} + \delta_a^d\delta_b^c)$$
$$= -\mathrm{tr}\mathbf{AB} + \mathrm{tr}\mathbf{A}\mathrm{tr}\mathbf{B} \,, \tag{2.20}$$

where we used $\mathbf{B} = -\epsilon(\mathbf{B}^{\mathrm{t}})^{-1}\epsilon$ and $\mathrm{tr}\mathbf{B}^{-1} = \mathrm{tr}\mathbf{B}$. Similarly, $\mathrm{tr}\mathbf{CBA}$ on $\mathcal{C}_{0,4}$ corresponds to the Pochhammer curve with three self-intersections and can be expressed in terms of simple curves by applying the skein relation, as in (2.11).
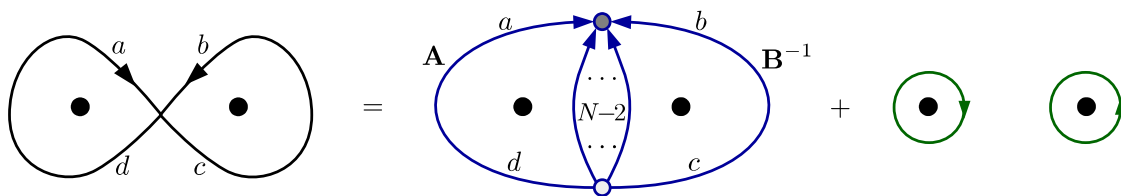
Figure 4. The application of the skein relation for general N to a self-intersecting curve produces a network with two N-valent junctions connected by an edge with multiplicity $N - 2$.

An important difference for $N > 2$ is that the skein relations involve N-valent junctions, associated with $SL(N)$-invariant ϵ-tensors (see for example [49]). In the case $N = 3$, the ϵ-tensor identity

$$\delta_a^c \delta_b^d = \epsilon_{abm} \epsilon^{cdm} + \delta_a^d \delta_b^c \tag{2.21}$$

corresponds to the skein relation expressed graphically as

$$\tag{2.22}$$
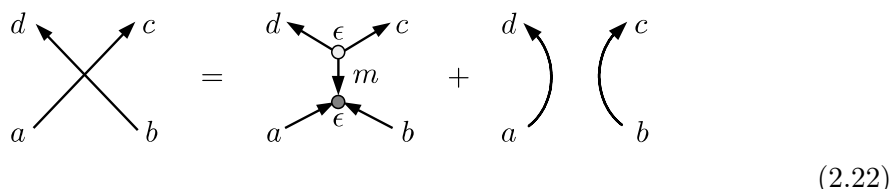
For general $N > 2$, the resolution of a self-intersection via skein relations therefore produces a network with two junctions. Let us consider again a figure-8 curve around two punctures:

$$\mathrm{tr}\mathbf{A}\mathbf{B}^{-1} = \mathbf{A}_a^d \mathbf{B}^{-1c}{}_b \delta_c^a \delta_d^b = \mathbf{A}_a^d \mathbf{B}^{-1c}{}_b \left(\frac{1}{(N-2)!} \epsilon^{abm_1 \cdots m_{N-2}} \epsilon_{cdm_1 \cdots m_{N-2}} + \delta_d^a \delta_c^b \right) \tag{2.23}$$

This relation can be represented graphically as in figure 4.

The natural appearance of junctions in the algebra $\mathcal{A}_{g,n}^N$ motivates us to adopt a set of generators for $\mathcal{A}_{g,n}^N$ which does not consist exclusively of trace functions, but also includes network functions.

2.5 Loop and network functions

The set of generators of $\mathcal{A}_{g,n}^N$ described in subsection 2.2 involves traces of large words of the holonomy matrices $\mathbf{A}_i$, $\mathbf{B}_i$, $\mathbf{M}_a$, which are generally associated with curves that have self-intersections. In this paper, we will mostly trade such self-intersecting curves for networks with junctions using the skein relations. Our generators are thus associated with simple loops (without self-intersections) and with networks.

Loops: each loop on $\mathcal{C}_{g,n}$ gives $N - 1$ trace functions A_i, $i = 1, \ldots N - 1$, which can be taken to be the coefficients of the characteristic polynomial of the associated holonomy matrix $\mathbf{A} \in SL(N, \mathbb{C})$:

$$\det(\mathbf{A} - \lambda \mathbf{I}) = (-\lambda)^N + (-\lambda)^{N-1} A_1 + (-\lambda)^{N-2} A_2 + \cdots - \lambda A_{N-1} + 1 \ . \tag{2.24}$$

The coefficients A_i are sums of all principal $i \times i$ minors of $\mathbf{A}$:

$$A_i = \sum_{n_1, \cdots, n_{N-i}} [\mathbf{A}]_{n_1 \cdots n_{N-i}} \ , \tag{2.25}$$

Figure 5. *Left*: loop functions are depicted as oriented simple closed curves labeled by integers $i = 1, \ldots, N - 1$. Reversing the orientation amounts to replacing i by $N - i$. *Right*: trivalent junctions with all outgoing edges (source) or all incoming edges (sink). Edges are labeled by integers i, j, k that sum to N.

where we denote the determinant of $\mathbf{A}$ with the rows and columns $n_1, \ldots, n_{N-i}$ removed by

$$[\mathbf{A}]_{n_1 \cdots n_{N-i}} = \frac{1}{i!} \epsilon_{n_1 \cdots n_{N-i} m_1 m_i} \mathbf{A}^{m_1}_{l_1} \cdots \mathbf{A}^{m_i}_{l_i} \epsilon^{n_1 \cdots n_{N-i} l_1 \cdots l_i} \ . \tag{2.26}$$

We can also write the loop functions A_i as traces of exterior powers of $\mathbf{A}$:

$$A_1 = \mathrm{tr}\mathbf{A} \ , \qquad A_2 = \frac{1}{2}[(\mathrm{tr}\mathbf{A})^2 - \mathrm{tr}(\mathbf{A}^2)], \quad \ldots, \quad A_i = \mathrm{tr}(\wedge^i \mathbf{A}) \ . \tag{2.27}$$

The loop function A_i corresponds to the ith fundamental antisymmetric representation $\wedge^i \square$ of $\mathrm{SL}(N, \mathbb{C})$. Note that if we replace $\mathbf{A}$ by its inverse $\mathbf{A}^{-1}$ in the expression for A_i we obtain the complex conjugate representation A_{N-i}. For example, the fundamental representation corresponds to $A_1 = \mathrm{tr}\mathbf{A}$, while the antifundamental representation corresponds to $A_{N-1} = \mathrm{tr}\mathbf{A}^{-1}$. We can thus represent loop functions graphically by an oriented loop labeled by an integer $i = 1, \ldots, \lfloor N/2 \rfloor$, where $\lfloor N/2 \rfloor$ is the integral part of $N/2$. Reversing the orientation corresponds to replacing $\mathbf{A}$ by $\mathbf{A}^{-1}$, the fundamental A_1 by the antifundamental A_{N-1}, and so on (see figure 5 left). For even N, the $(N/2)^{\mathrm{th}}$ representation is self-adjoint, and so the corresponding loop does not need an orientation.

Networks: we also construct functions associated with networks. By a *network*[5] we mean a closed directed graph whose edges carry antisymmetric representations and whose vertices carry invariant tensors.[6] The vertices, or junctions, are in principle N-valent but they can always be resolved into trivalent junctions, on which we therefore focus. The three edges that meet at a junction (either all outgoing or all incoming) are labeled by positive integers i, j, k satisfying $i + j + k = N$, which indicate that they carry respectively the ith, j^{th}, k^{th} antisymmetric representations (see figure 5 right). Junctions do not have labels since there is only one invariant tensor $\epsilon_{m_1 \cdots m_N}$ in $\wedge^i \square \otimes \wedge^j \square \otimes \wedge^k \square$. A network function is defined by contracting the holonomy matrices along the edges with the ϵ-tensors at the junctions. The resulting function is invariant under simultaneous conjugation of the holonomy matrices. For example, a network consisting of two junctions connected by three

---

[5]Closely related objects go under the names of spin networks, trace diagrams, tensor diagrams, birdtracks, webs, etc.

[6]We prefer this definition to the one given by Samuel Johnson in his *Dictionary of the English Language* (1755): "Network: any thing reticulated or decussated, at equal distances, with interstices between the intersections."
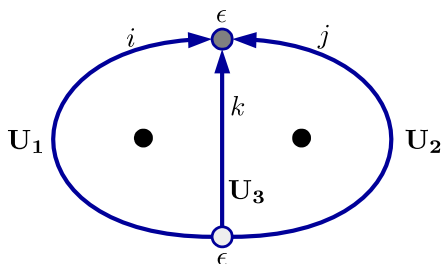
Figure 6. Network with two trivalent junctions and three edges surrounding two punctures. The edges carry the ith, j^{th}, and k^{th} antisymmetric representations of $\text{SL}(N, \mathbb{C})$, with $i+j+k = N$. The network function N_{ijk} is constructed by contracting i copies of the holonomy matrix $\mathbf{U_1}$, j copies of $\mathbf{U_2}$, and k copies of $\mathbf{U_3}$ with the two ϵ-tensors at the junctions.

oriented edges as in figure 6 gives $(N-1)(N-2)/2$ network functions N_{ijk} of the form

$$N_{ijk} = \frac{1}{i!j!k!}\epsilon_{m_1\cdots m_N}\mathbf{U_1}^{m_1}{}_{n_1}\cdots\mathbf{U_1}^{m_i}{}_{n_i}\mathbf{U_2}^{m_{i+1}}{}_{n_{i+1}}\cdots\mathbf{U_2}^{m_{i+j}}{}_{n_{i+j}}\mathbf{U_3}^{m_{i+j+1}}{}_{n_{i+j+1}}\cdots\mathbf{U_3}^{m_N}{}_{n_N}\epsilon^{n_1\cdots n_N}, \tag{2.28}$$

where $\mathbf{U_1}, \mathbf{U_2}, \mathbf{U_3}$ are the holonomy matrices (in the fundamental representation) along the three edges. If we reverse the orientation of the edges we obtain another set of $(N-1)(N-2)/2$ network functions, which we denote by $\bar{N}_{ijk}$.

From networks to self-intersecting curves: network functions can also be expressed in terms of the holonomy matrices $\mathbf{A}_i$, $\mathbf{B}_i$, $\mathbf{M}_a$ generating a representation of $\pi_1(\mathcal{C}_{g,n})$. In order to do this, let us recall that a flat $\text{SL}(N)$-connection can always be trivialized by gauge transformations in any simply-connected domain. Covering $\mathcal{C}_{g,n}$ by simply-connected domains one may describe the flat connections in terms of the constant transition functions from one domain to another. Equivalently, one may describe flat connections using branch-cuts, a collection of curves or arcs on $\mathcal{C}_{g,n}$ such that cutting along the branch-cuts produces a simply-connected domain. The holonomy $\text{Hol}(\gamma)$ will then receive contributions only when the curve γ crosses branch-cuts. $\text{Hol}(\gamma)$ can therefore be represented as the product of "jump"-matrices associated with the branch-cuts crossed by γ, taken in the order in which the different branch-cuts are crossed.

Considering the network N_{ijk} defined in (2.28), for example, we can use the branch-cuts depicted in figure 7. The "jump"-matrices associated with these branch-cuts coincide with the holonomy matrices $\mathbf{A}$ and $\mathbf{B}$ around the two punctures depicted in figure 7. The holonomy matrix associated with the middle arc labeled by the letter k is the identity, as no branch-cut is crossed. It follows that we can express N_{ijk} as

$$N_{ijk} = \frac{1}{i!j!k!}\epsilon_{m_1\cdots m_N}\mathbf{A}^{m_1}{}_{n_1}\cdots\mathbf{A}^{m_i}{}_{n_i}\mathbf{B}^{-1\,m_{i+1}}{}_{n_{i+1}}\cdots\mathbf{B}^{-1\,m_{i+j}}{}_{n_{i+j}}\delta^{m_{i+j+1}}_{n_{i+j+1}}\cdots\delta^{m_N}_{n_N}\epsilon^{n_1\cdots n_N},$$

$$= \frac{1}{i!j!}\delta^{n_1\cdots n_{i+j}}_{m_1\cdots m_{i+j}}\mathbf{A}^{m_1}{}_{n_1}\cdots\mathbf{A}^{m_i}{}_{n_i}\mathbf{B}^{-1\,m_{i+1}}{}_{n_{i+1}}\cdots\mathbf{B}^{-1\,m_{i+j}}{}_{n_{i+j}}$$

$$= \text{tr}\mathbf{A}^i\mathbf{B}^{-j} - \text{tr}\mathbf{A}^{i-1}\mathbf{B}^{-1}\mathbf{A}\mathbf{B}^{-j+1} + \cdots \tag{2.29}$$

We thus see that this point of view relates network functions to trace functions associated with self-intersecting curves as in subsection 2.2. As illustrated on the right of
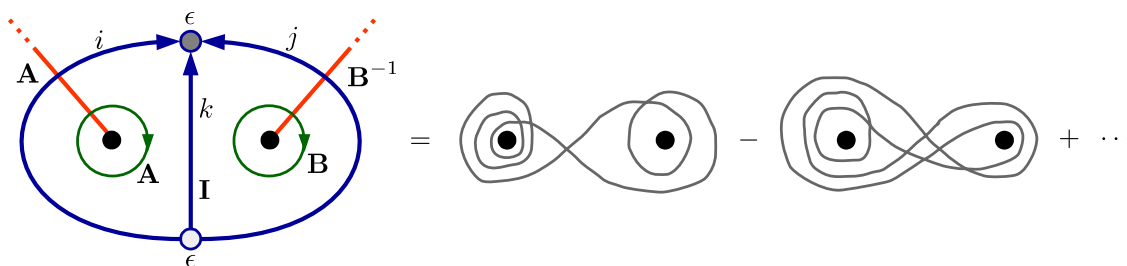
Figure 7. The branch-cuts (orange lines) encode the holonomies **A** and **B** around the punctures. The edges of the network N_{ijk} are associated with the holonomies of the branch-cuts that they cross: i times **A**, j times $\mathbf{B}^{-1}$, and k times the identity **I**. The right-hand side shows two of the self-intersecting curves that appear in the expansion of the network function in terms of traces.

figure 7, the corresponding trace functions are typically associated with very complicated curves with many self-intersections. This is one of the advantages of working with networks instead of self-intersecting curves. Different labelings of a network with a given topology account for a family of intricate curves. Notice that the relation (2.29) between network and trace functions can also be seen as a consequence of skein relations, given that it involves contractions of ϵ-tensors. We have shown a simple example in figure 4.

2.6 Commuting Hamiltonians

The moduli space $\bar{\mathcal{M}}_{g,n}^N$ with fixed conjugacy classes for the holonomies around the punctures exhibits the key features of an integrable Hamiltonian system. Firstly, $\bar{\mathcal{M}}_{g,n}^N$ is a symplectic manifold. Fixing the conjugacy classes of the holonomies around the punctures corresponds to restricting to a symplectic leaf of the Poisson manifold $\mathcal{M}_{g,n}^N$ viewed as a symplectic foliation.

We can moreover find a maximal set of Hamiltonians, that is a number of Poisson-commuting functions equal to half the dimension of the moduli space $\bar{\mathcal{M}}_{g,n}^N$. Goldman's formula (2.17) implies that trace functions associated with curves that do not intersect each other automatically Poisson-commute. In the case $N = 2$ we can simply consider the trace functions associated to a maximal number of mutually non-intersecting closed curves on $\mathcal{C}_{g,n}$. Cutting $\mathcal{C}_{g,n}$ along such a collection of curves defines a decomposition of $\mathcal{C}_{g,n}$ into $(2g - 2 + n)$ pairs of pants with $(3g - 3 + n)$. The traces of holonomies associated with these curves thus provides a maximal set of Poisson-commuting Hamiltonians:

$$\#\{\text{cutting loops}\} = 3g - 3 + n = \frac{1}{2}\dim \bar{\mathcal{M}}_{g,n}^2 \ . \tag{2.30}$$

However, for $N > 2$, the cutting curves alone do not suffice to get a maximal set of commuting Hamiltonians. We therefore supplement them by the two-junction networks (2.28) that can be put on each pair of pants (see figure 8). Each cutting curve provides $(N - 1)$ trace functions, and each pants network provides $(N - 1)(N - 2)/2$ network functions. They add up to give a number of functions which is precisely half the dimension (2.4) of the moduli space of flat connections with fixed holonomies around the punctures:

$$(3g - 3 + n)(N - 1) + (2g - 2 + n)\frac{(N - 1)(N - 2)}{2} = \frac{1}{2}\dim \bar{\mathcal{M}}_{g,n}^N \ . \tag{2.31}$$
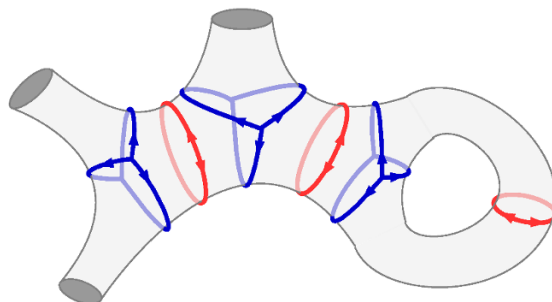
Figure 8. A maximal set of commuting Hamiltonians is provided by the functions associated with cutting curves (red) and with pants networks (blue) in a pair of pants decomposition of the surface $\mathcal{C}_{g,n}$.
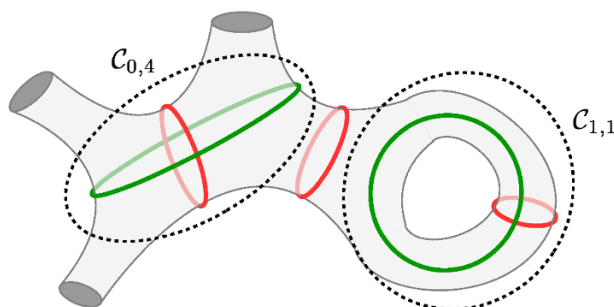
Figure 9. The neighborhood of a cutting loop (red) on $\mathcal{C}_{g,n}$ can look either like $\mathcal{C}_{0,4}$ or like $\mathcal{C}_{1,1}$. In each case we can find a natural conjugate loop (green).

The Poisson-commutativity of the cutting curves among themselves and with the networks is obvious from the fact that they do not intersect (Goldman's formula (2.17) applies to self-intersecting curves, and hence to networks as well). The same is true for pants networks on different pairs of pants. In contrast, it is not obvious that pants networks on the same pair of pants commute among themselves, since they intersect at least twice. We checked that they commute up to $N = 6$ (see section 3.1 for some sample computations).

2.7 Tinkertoys

In order to get a complete system of coordinates for $\bar{\mathcal{M}}_{g,n}^N$ we need to supplement the maximal set of commuting Hamiltonians described in the previous subsection by sufficiently many additional coordinate functions. A natural way to find additional variables that do not Poisson-commute with the pants networks N_{ijk} on $\mathcal{C}_{0,3}$ is to take the pants networks $\bar{N}_{ijk}$ with reverse orientation.

Simple additional coordinates that do not Poisson-commute with the trace functions associated to the cutting curves defining the pants decomposition can also be defined in a simple way. Each cutting curve is contained in a subsurface isomorphic either to a four-holed sphere or a one-holed torus embedded in $\mathcal{C}_{g,n}$, see figure 9 for an illustration. In the case of $\mathcal{C}_{0,4}$, natural additional coordinates are associated with curves surrounding another pair of holes than the cutting curve under consideration. In the case of $\mathcal{C}_{1,1}$ one may for

example consider an additional coordinate associated with the B-cycle if the cutting curve is the A-cycle, see figure 9.

Altogether, the cutting loops and their conjugate loops, together with the pants networks of both orientations provide a complete set of coordinates on $\bar{\mathcal{M}}_{g,n}^N$ that cover this space at least locally. We can therefore reduce the study of $\bar{\mathcal{M}}_{g,n}^N$ for a generic Riemann surface $\mathcal{C}_{g,n}$ to the study of pants networks on $\mathcal{C}_{0,3}$, and of pairs of conjugate loops on $\mathcal{C}_{0,4}$ and $\mathcal{C}_{1,1}$. This motivates us to focus on these three cases in the following subsections.

Note that the additional coordinates on $\bar{\mathcal{M}}_{g,n}^N$ that we introduced above are not *canonically* conjugate. However, it should be possible to define generalizations of the Fenchel-Nielsen coordinates, a set of Darboux coordinates for $\bar{\mathcal{M}}_{g,n}^N$ in terms of which one may parameterize the coordinate functions defined above. Such Darboux coordinates were shown in the case $N = 2$ to play a key role in the relation to integrable systems [39].

2.8 Skein quantization

Motivated by the applications to supersymmetric gauge theories, we will next discuss the quantization of the moduli space $\mathcal{M}_{g,n}^N$ of flat $\mathrm{SL}(N,\mathbb{C})$-connections on a Riemann surface $\mathcal{C}_{g,n}$. This means in particular to construct a family of noncommutative deformations $\mathcal{A}_{g,n}^N(q)$ of the algebra $\mathcal{A}_{g,n}^N$ of functions on $\mathcal{M}_{g,n}^N$ parameterized by one parameter $q \equiv \mathrm{e}^\hbar$. The loop and network functions get replaced by generators of the noncommutative algebra $\mathcal{A}_{g,n}^N(q)$. In the classical limit $q \to 1$ ($\hbar \to 0$), the product $\hat{A}\hat{B}$ of two operators reduces to the commutative product AB of the corresponding functions, while the commutator $[\hat{A}, \hat{B}] = \hat{A}\hat{B} - \hat{B}\hat{A}$ should reproduce the Poisson bracket $\{A, B\}$.

This problem has been extensively studied in the past, starting from [50], and motivated in particular by the relation to Chern-Simons theory[7] [51, 52]. Considering Chern-Simons theory on three-manifolds M_3 of the form $\mathcal{C}_{g,n} \times I$, with I an interval with coordinate t, one may note that parameterized closed curves on $\mathcal{C}_{g,n}$ naturally define knots in M_3. In the context of Chern-Simons theory it is natural to relate the ordering of the factors in a product of generators in $\mathcal{A}_{g,n}^N(q)$ to the ordering of observables according to the value of their "time"-coordinates t. Given two knots K_A and K_B one can define their formal product $K_A K_B$ to be the link composed of K_A in $\mathcal{C}_{g,n} \times [1/2, 1]$ and K_B in $\mathcal{C}_{g,n} \times [0, 1/2]$,

$$K_A K_B = \left\{ (x,t) \in \mathcal{C}_{g,n} \times [0,1] \, | \, (x, 2t-1) \in K_A \text{ for } t \geq \tfrac{1}{2} \, ; (x, 2t) \in K_B \text{ for } t \leq \tfrac{1}{2} \right\}. \quad (2.32)$$

This operation is depicted in figure 10. A natural set of relations to be imposed on the product in $\mathcal{A}_{g,n}^N(q)$ has been identified, severely constrained by the topological nature of Chern-Simons theory leading to the definition of isotopy invariants of knots and links.

The first constructions of quantum sl_N invariants were provided by Reshetikhin and Turaev [53] using the representation theory of the quantum group $\mathcal{U}_q(sl_N)$. It was later observed that the resulting algebra can be described without the use of quantum groups in terms of generators and relations. In the following we will briefly describe the work of

---

[7]A lot of the research in this direction was devoted to Chern-Simons theories with compact gauge groups like $\mathrm{SU}(N)$. However, the resulting algebras $\mathcal{A}_{g,n}^N(q)$ appearing in this context turn out to be independent of the real form of the corresponding complex group (here $\mathrm{SL}(N)$) under consideration.
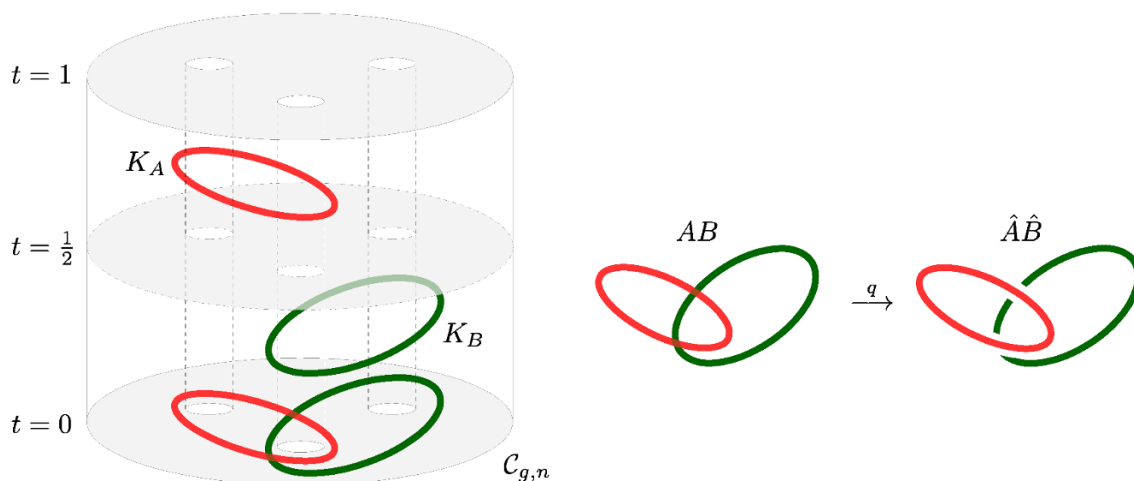
Figure 10. *Left*: product of two knots K_A and K_B in the 3-manifold $\mathcal{C}_{g,n} \times [0,1]$. *Right*: the corresponding loop operators that intersect classically are superposed at the quantum level.

Sikora [54] on link invariants in $\mathbb{R}^3$ which uses both points of view (see also [49] for SL(3), and [55] for similar formulations).

Sikora describes in [54] a construction of isotopy invariants of certain ribbon graphs called N-webs. The N-webs are composed of oriented ribbons emanating from, or ending in, N-valent vertices called sources or sinks, respectively (see [54] for a more formal definition). We will see that the N-webs are closely related to the networks considered in this paper. This construction can be understood as a special case of Reshetikhin and Turaev's constructions. It can be described using the projections of N-webs to $\mathbb{R}^2$ called N-web diagrams. The web-diagram can be decomposed into pieces of three types: (i) crossings, (ii) sinks or sources, and (iii) cups or caps of the form

With each of these pieces one associates intertwining maps between tensor products of fundamental representations $\square$ of $\mathcal{U}_q(sl_N)$. The maps associated with crossings, in particular, are in a basis $e_1, \ldots, e_N$ for $\mathbb{C}^N$ represented by

$$R(e_a \otimes e_b) = q^{\frac{1}{2N}} \begin{cases} e_b \otimes e_a & \text{for } a > b\,, \\ q^{-\frac{1}{2}} e_a \otimes e_b & \text{for } a = b\,, \\ e_b \otimes e_a + (q^{-\frac{1}{2}} - q^{\frac{1}{2}}) e_a \otimes e_b & \text{for } a < b\,, \end{cases} \qquad (2.33)$$

or by the inverse map R^{-1}, depending on which edge is on top of the other:

$$(2.34)$$

The maps associated with sinks are the unique (up to normalization) intertwining maps from the N-fold tensor product of the fundamental representation of $\mathcal{U}_q(sl_N)$ to the trivial representation, while the conjugate of this map is associated with the sources. In a similar way one associates to the caps the unique (up to normalization) intertwining maps from the tensor products of fundamental representations $\square$ with the anti-fundamental representations $\bar{\square}$ to the the trivial representation. The maps associated with the cups are the conjugate intertwining maps, respectively. Explicit formulae can be found in [54]. Using these building blocks one constructs the invariant associated with an N-web by composing the intertwining maps associated to the pieces in the natural way specified by the decomposition of the given N-web diagram into pieces.

The isotopy invariants of N-webs defined in this way satisfy various relations that can be used to calculate them explicitly. These relations relate invariants associated with N-web diagrams that are identical outside of suitable discs $\mathbb{D} \subset \mathbb{R}^2$. A typical example may be graphically represented as

$$ q^{\frac{1}{2N}} \diagup\!\!\!\!\!\diagdown \; - \; q^{-\frac{1}{2N}} \diagup\!\!\!\!\!\diagdown \; = \left(q^{\frac{1}{2}} - q^{-\frac{1}{2}} \right) \;\big)\; \big(\; \tag{2.35}$$

Such relations are quantum analogs of the skein relations discussed previously. Before entering into a more detailed description of the skein relations, let us note that the local nature of the skein relations will allow us to use the same relations as defining relations for the algebras $\mathcal{A}_{g,n}^N(q)$ we are interested in. This will be the basis for the approach used in the next section, as is illustrated in particular by figure 22 below. The three-dimensional isotopy invariance of the N-web invariants ensures that the resulting algebra has a three-dimensional interpretation via (2.32). It is easy to see that the relation (2.35) reproduces Goldman's bracket (2.17) in the limit $\hbar \to 0$.

We shall now turn to a more detailed description of the set of relations proposed in [54]. The first condition in [54] is the crossing condition (2.35).[8] Next, the quantum invariant for the union of two unlinked knots must be equal to the product of the quantum invariants for the knots. There are also conditions for the contraction of a trivial knot and for the Reidemeister move of type I:

$$ \bigcirc \; = \; (-1)^{N-1}[N] \qquad\qquad \text{\raisebox{-1ex}{$\circlearrowleft$}} = (-1)^{N-1} q^{\frac{N^2-1}{2N}} \big\uparrow \tag{2.36}$$

We have been using the notation $[n]$ defined as

$$ [n] \equiv \frac{q^{n/2} - q^{-n/2}}{q^{1/2} - q^{-1/2}} = q^{(n-1)/2} + q^{(n-3)/2} + \cdots + q^{-(n-1)/2} \; . \tag{2.37}$$

---

[8]We choose conventions that agree with the calculations in terms of Fock-Goncharov holonomies in section 4. They are related to the bracket used in [54] by the redefinition $q \to q^{-2}$, and then the renormalization of each junction by $\mathrm{i} q^{-N(N-1)/4}$ and of each edge carrying the ith antisymmetric representation by $1/[i]!$. We also introduce some signs in (2.36).

Finally, there is a relation between two nearby N-valent junctions (a source and a sink) and a sum of positive braids labeled by permutations σ (with lengths $l(\sigma)$):

$$
\cdots = -q^{-\frac{1}{4}N(N-1)} \sum_\sigma \left(-q^{\frac{N-1}{2N}}\right)^{l(\sigma)} \boxed{\sigma}
$$

(2.38)

It was shown in [54] that the relations above suffice to characterize the resulting invariant of N-webs uniquely.

Note that the edges do not carry labels in Sikora's formulation. For our goals it will be convenient to represent i parallel edges between two junctions by a single edge with label i. This will allow us to define the quantized counterparts of the networks introduced previously. A quantum network corresponding to the network shown in figure 6, for example, may be represented by an N-web obtained by splitting the N edges connecting one source and one sink into three groups of i, j, and k edges.

The relation (2.38) allows to derive skein relations for the resolution of all possible crossings in terms of N-web diagrams without crossings. Of particular interest is the following special case of the fundamental skein relation obtained by contracting $(N-2)$ pairs of edges from the upper and lower parts of (2.38):

$$
\times = q^{\frac{1}{2N}} \quad + \quad q^{\frac{1-N}{2N}} \;) \; (
$$

(2.39)

We indicate that the edge between the two junctions carries the label $N-2$ by drawing it thicker than the other edges associated with the fundamental representation. The fundamental skein relation with the other ordering at the crossing has q replaced by q^{-1}. A large set of useful relations can be derived from the relations stated above, including reduction moves of contractible bubbles (digons), squares, hexagons, etc. Such relations were worked out in [56–58]. We show some examples in figure 11.

Sikora's construction allows one to recover the construction of quantum sl_N invariants previously given by Murakami, Ohtsuki, and Yamada in [55] (a useful summary is given in [59]). This construction uses trivalent graphs with a "flow" built out of the following two types of vertices:

$$
i + j \qquad\qquad i \qquad j \\
i \qquad j \qquad\qquad i + j
$$

(2.40)

The edges connected at such vertices cary labels with values in $\{0, 1, \ldots, N-1\}$. An edge with label 0 can be removed, and an edge with label i is equivalent to an edge with label $N - i$ with opposite orientation, as depicted on the left of figure 5. The vertices (2.40) can be represented in terms of pairs of the sources and sinks used in Sikora's formulation, as explained in [54].
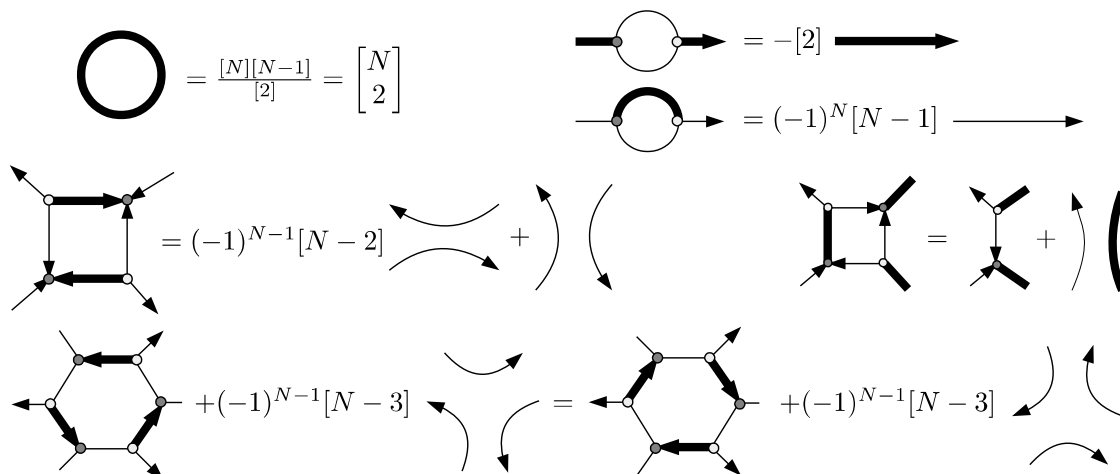
Figure 11. Reduction of contractible cycles. The square reduction on the right is valid for $N = 4$. Our conventions are that thin edges carry the fundamental representation, while thick edges carry the $(N-2)^{\text{th}}$ antisymmetric representation.

It is possible to derive an expression for a general skein relation resolving the crossing of lines labeled by arbitrary $i, j \in \{0, 1, \dots, N-1\}$ [55] (see [59] for the normalization):

$$(2.41)$$

with $m = \min\{i, j, N-i, N-j\}$. For the other ordering at the crossing, one should replace q by q^{-1}. When $i = j = 1$ this expression reproduces the fundamental skein relation (2.39). We will also need skein relations for $N = 4$ with $i = 2$ (thick line) and $j = 1$ or $j = 2$:

$$(2.42)$$

Let us finally note that the link invariants constructed in [55] also correspond to simple special cases of the Reshetikhin-Turaev construction. The label $i \in \{0, 1, \dots, N-1\}$ assigned to an edge of a colored N-web is identified with the label for one of the irreducible representation $M_i \equiv \wedge^i \square$ of the quantum group $\mathcal{U}_q(sl_N)$ that is obtained as the ith antisymmetric tensor power of the fundamental representation $\square$. The linear map $R_{ij} : M_j \otimes M_i \to M_i \otimes M_j$ appearing on the left hand side of (2.41) can be obtained from

the universal R-matrix $\mathcal{R}$ of $\mathcal{U}_q(sl_N)$ via

$$R_{ij} = P_{ij}(\pi_j \otimes \pi_i)(\mathcal{R}), \qquad (2.43)$$

with P_{ij} the permutation of tensor factors, $P_{ij} : M_j \otimes M_i \to M_i \otimes M_j$. The trivalent vertices in (2.40) are associated with the Clebsch-Gordan maps (with $k = i + j$):

$$C_{ij}^k : \; M_i \otimes M_j \to M_k, \qquad C_k^{ij} : \; M_k \to M_i \otimes M_j . \qquad (2.44)$$

In the case where $i + j = N$, one edge carries the trivial representation and can thus be removed. This gives cap and cup maps:

$$C_{i,N-i}^0 : \; M_i \otimes M_{N-i} \to \mathbb{C}, \qquad C_0^{N-j,j} : \; \mathbb{C} \to M_{N-j} \otimes M_j . \qquad (2.45)$$

Quantum invariants of a network are then obtained by composing the intertwining maps associated with the pieces of the network.

3 Quantization of tinkertoys

In this section we will describe the algebras obtained by using skein quantization in some simple examples associated with surface $\mathcal{C}_{g,n}$ with (g,n) being $(0,3)$, $(1,1)$ and $(0,4)$. As explained previously, it seems reasonable to regard the results as building blocks for the description of the algebras associated with more general surfaces $\mathcal{C}_{g,n}$.

3.1 Pants networks

As the prototypical illustration of the role of network operators, we consider flat $\mathrm{SL}(N, \mathbb{C})$-connections on a three-punctured sphere $\mathcal{C}_{0,3}$, also known as the pair of pants, or pants for short. As we mentioned in subsection 2.6, any Riemann surface $\mathcal{C}_{g,n}$ can be decomposed into pants by choosing a maximal set of simple loops that do not intersect. The pair of pants $\mathcal{C}_{0,3}$ is hence not merely the simplest example, but also the most essential one, from which any other surface can in principle be understood. The main novelties for the case $N > 2$ will be apparent in this example. Indeed, any simple loop on $\mathcal{C}_{0,3}$ can be deformed into a loop surrounding a puncture, so networks are the only relevant objects in this case. A particularly important network has two trivalent junctions and three edges, running between every pair of punctures; we call it the *pants network* (see figure 12). The number of possible pants network operators is given by the partition of N into three strictly positive integers $i + j + k = N$, which gives $\binom{N-1}{2} = (N-1)(N-2)/2$.

In terms of 4d $\mathcal{N} = 2$ gauge theories, $\mathcal{C}_{0,3}$ corresponds to the theory T_N studied by Gaiotto [2], which can be used as a fundamental building block for more general theories. T_N is a strongly coupled $\mathcal{N} = 2$ superconformal field theory with no known weakly-coupled Lagrangian description (except for T_2, which is free). It has $\mathrm{SU}(N)^3$ flavor symmetry and $\mathrm{SU}(2) \times \mathrm{U}(1)$ R-symmetry. It contains operators Q and $\tilde{Q}$ with scaling dimension $(N-1)$ that transform in the trifundamental representations $(\square, \square, \square)$ and $(\bar{\square}, \bar{\square}, \bar{\square})$ of $\mathrm{SU}(N)^3$.
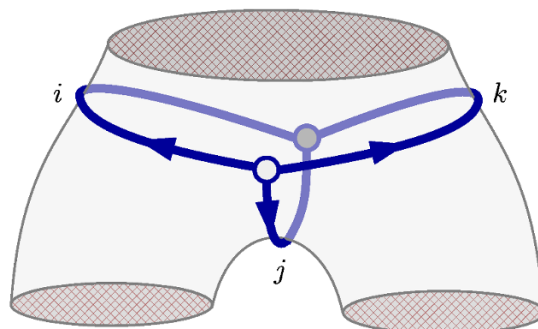
Figure 12. Pants network on a pair of pants $\mathcal{C}_{0,3}$.

There are also Higgs branch operators μ_1, μ_2, μ_3, which have scaling dimension 2 and transform in the adjoint of one SU(N). Finally, there are Coulomb branch operators $u_k^{(i)}$ with dimension k; the labels take the values $k = 3, \ldots, N$ and $i = 1, \ldots, k - 2$, so their number is $(N-1)(N-2)/2$. We see that this matches nicely the number of pants networks.

The fundamental group of the sphere $\mathcal{C}_{0,3}$ with three punctures A, B, C is represented by the loops $\gamma_A, \gamma_B, \gamma_C$ around each puncture satisfying one relation:

$$\pi_1(\mathcal{C}_{0,3}) = \langle \gamma_A, \gamma_B, \gamma_C \mid \gamma_A \gamma_B \gamma_C = \gamma_\circ \rangle, \tag{3.1}$$

where $\gamma_\circ$ denotes a contractible loop. The corresponding holonomy matrices $\mathbf{A}$, $\mathbf{B}$, $\mathbf{C}$ satisfy $\mathbf{ABC} = (-1)^{N-1}\mathbf{I}$ (the sign is chosen for consistency with (2.40) and (4.6)). The moduli space of flat SL($N, \mathbb{C}$)-connections has the dimension

$$\dim[\mathcal{M}_{0,3}^N] = N^2 - 1 . \tag{3.2}$$

The functions coming from the loops around the punctures, A_i, B_i, C_i, with $i = 1, \ldots, N-1$, and from the pants network with both orientations, N_a, $\bar{N}_a$, with $a = 1, \ldots, (N-1)(N-2)/2$, provide the correct number of coordinates on $\mathcal{M}_{0,3}^N$:

$$3(N-1) + 2\frac{(N-1)(N-2)}{2} = N^2 - 1 . \tag{3.3}$$

Fixing the eigenvalues of the holonomies around the punctures then gives $3(N-1)$ constraints and leaves us with only the pants networks:

$$\dim[\bar{\mathcal{M}}_{0,3}^N] = (N-2)(N-1) . \tag{3.4}$$

SL(3). The first non-trivial case is $N = 3$. We will show how to obtain a closed Poisson algebra involving the loops and pants network, together with an extra six-junction network. This gives 10 generators satisfying 2 polynomial relations, which can be quantized using quantum skein relations.

Loop and network functions: there are two loop functions for each holonomy matrix, namely the coefficients of the characteristic polynomial, which can be expressed in terms of traces as in (2.27): $A_1 = \mathrm{tr}\mathbf{A}$ and $A_2 = \mathrm{tr}\mathbf{A}^{-1}$ (and similarly for $\mathbf{B}$ and $\mathbf{C}$). The network
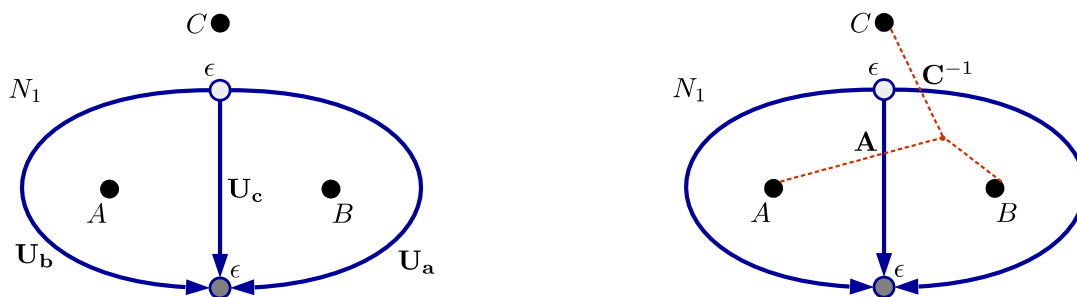
Figure 13. *Left*: construction of the network operator N_1 on $\mathcal{C}_{0,3}$ from the holonomy matrices $\mathbf{U_a}$, $\mathbf{U_b}$, $\mathbf{U_c}$ along its edges contracted with ϵ-tensors at the junctions. *Right*: the holonomy matrices $\mathbf{A}$, $\mathbf{B}$, $\mathbf{C}$ are associated with the branch-cuts (dashed) starting at the punctures A, B, C. Two edges of the network N_1 intersect the branch-cuts and are thus associated with $\mathbf{A}$ and $\mathbf{C^{-1}}$.
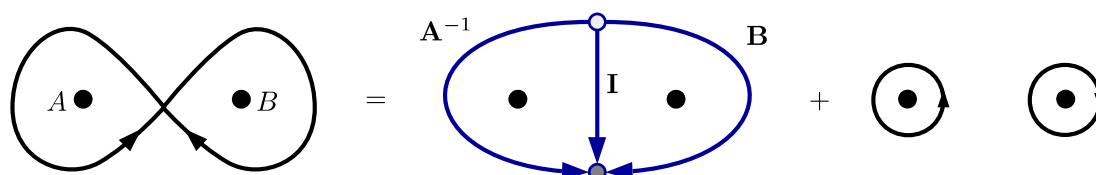
Figure 14. Applying the skein relation to a self-intersecting loop going around two punctures produces a network and pair of loops around the punctures.

function N_1 and its reverse $\bar{N}_1$ can be constructed as in (2.28) by fusing the three edges at the two trivalent junctions with ϵ-tensors (see figure 13 left):[9]

$$N_1 = -\epsilon_{mnp}\mathbf{U_a}_r^m \mathbf{U_b}_s^n \mathbf{U_c}_t^p \epsilon^{rst}\,,$$
$$\bar{N}_1 = -\epsilon_{mnp}(\mathbf{U_a^{-1}})_r^m (\mathbf{U_b^{-1}})_s^n (\mathbf{U_c^{-1}})_t^p \epsilon^{rst}\,. \tag{3.5}$$

Alternatively, we can construct the network functions as in (2.29) by associating holonomy matrices with the edges of the network according to which branch-cuts they cross (see figure 13 right). This gives the following expressions:

$$N_1 = -\epsilon_{mnp}\mathbf{A}_r^m \delta_s^n (\mathbf{C^{-1}})_t^p \epsilon^{rst} = \mathrm{tr}\mathbf{AC^{-1}} - A_1 C_2\,,$$
$$\bar{N}_1 = -\epsilon_{mnp}(\mathbf{A^{-1}})_r^m \delta_s^n \mathbf{C}_t^p \epsilon^{rst} = \mathrm{tr}\mathbf{A^{-1}C} - A_2 C_1\,. \tag{3.6}$$

The several possible choices for the position of the branch-cuts all lead to the same network function:

$$N_1 = \mathrm{tr}\mathbf{AC^{-1}} - A_1 C_2 = \mathrm{tr}\mathbf{BA^{-1}} - B_1 A_2 = \mathrm{tr}\mathbf{CB^{-1}} - C_1 B_2\,. \tag{3.7}$$

A term such as $\mathrm{tr}\mathbf{BA^{-1}}$ corresponds to a self-intersecting figure-8 loop going around the punctures B clockwise and A anticlockwise. Resolving the intersection with the skein relation in (2.22) produces the relation (3.7) (see figure 14).

---

[9]The overall sign is chosen for later convenience, so that N_1 will be expressed as a *positive* Laurent polynomial in the Fock-Goncharov coordinates, as in (4.24).
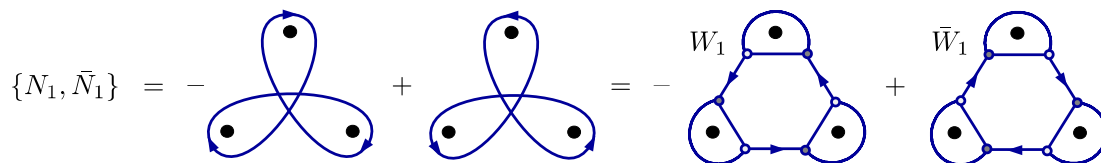
Figure 15. The Poisson bracket of the pants networks N_1 and $\bar{N}_1$ can be expressed in terms of Pochhammer curves or in terms of the 6-junction network W_1 and its reverse $\bar{W}_1$.

Closed Poisson algebra: we would like to find a set of generators including A_i, B_i, C_i and N_1, $\bar{N}_1$ that forms a closed Poisson algebra. The Poisson brackets can be obtained from Goldman's formula (2.17). Since the Poisson bracket is proportional to the intersection number, the loop functions A_i, B_i, C_i around the punctures obviously Poisson-commute with everything:

$$\{A_i, \bullet\} = \{B_i, \bullet\} = \{C_i, \bullet\} = 0 \ . \tag{3.8}$$

To apply Goldman's formula to the pants networks we use their expressions (3.6) in terms of trace functions. We get

$$\{N_1, \bar{N}_1\} = \{\mathrm{tr}\mathbf{A}\mathbf{C}^{-1}, \mathrm{tr}\mathbf{A}^{-1}\mathbf{C}\} = -\mathrm{tr}\mathbf{C}\mathbf{B}\mathbf{A} + \mathrm{tr}(\mathbf{C}\mathbf{B}\mathbf{A})^{-1} = -W_1 + \bar{W}_1 \,, \tag{3.9}$$

where the functions W_1 and $\bar{W}_1$ correspond to the six-junction networks shown in figure 15 and are related to the so-called Pochhammer curves $\mathrm{tr}\mathbf{C}\mathbf{B}\mathbf{A}$ and $\mathrm{tr}(\mathbf{C}\mathbf{B}\mathbf{A})^{-1}$ via the skein relation and reductions in (2.39) and figure 11 (with $q = 1$):

$$W_1 = \mathrm{tr}\mathbf{C}\mathbf{B}\mathbf{A} - A_1 A_2 - B_1 B_2 - C_1 C_2 \,,$$
$$\bar{W}_1 = \mathrm{tr}(\mathbf{C}\mathbf{B}\mathbf{A})^{-1} - A_1 A_2 - B_1 B_2 - C_1 C_2 \ . \tag{3.10}$$

If we want to obtain a closed Poisson algebra we thus need to add W_1 and $\bar{W}_1$ to the set of generators and compute their Poisson brackets. We find that they indeed close:[10]

$$
\begin{aligned}
\{N_1, W_1\} &= \mathrm{tr}\mathbf{B}^{-1}\mathbf{C}^2\mathbf{B}\mathbf{A} - \mathrm{tr}\mathbf{C}\mathbf{B}^{-1}\mathbf{C}\mathbf{B}\mathbf{A} + \mathrm{tr}\mathbf{A}^{-1}\mathbf{B}^{-1}\mathbf{A}\mathbf{C} - \mathrm{tr}\mathbf{C}\mathbf{B}^{-1} \\
&= -N_1 W_1 + 3\bar{N}_1^2 + 2\bar{N}_1(A_1 B_2 + B_1 C_2 + C_1 A_2) - 6N_1 + \Lambda \,, \\
\{N_1, \bar{W}_1\} &= -\mathrm{tr}\mathbf{C}\mathbf{B}^{-2}\mathbf{C}^{-1}\mathbf{A}^{-1} + \mathrm{tr}\mathbf{B}^{-1}\mathbf{C}\mathbf{B}^{-1}\mathbf{C}^{-1}\mathbf{A}^{-1} - \mathrm{tr}\mathbf{A}^{-1}\mathbf{B}^{-1}\mathbf{A}\mathbf{C} + \mathrm{tr}\mathbf{C}\mathbf{B}^{-1} \\
&= N_1 \bar{W}_1 - 3\bar{N}_1^2 - 2\bar{N}_1(A_1 B_2 + B_1 C_2 + C_1 A_2) + 6N_1 - \Lambda \,, \\
\{W_1, \bar{W}_1\} &= \mathrm{tr}(\mathbf{B}\mathbf{A}\mathbf{C})^{-1}\mathbf{A}\mathbf{C}\mathbf{B} - \mathrm{tr}(\mathbf{C}\mathbf{B}\mathbf{A})^{-1}\mathbf{A}\mathbf{C}\mathbf{B} + \mathrm{tr}(\mathbf{A}\mathbf{C}\mathbf{B})^{-1}\mathbf{C}\mathbf{B}\mathbf{A} \\
&\quad - \mathrm{tr}(\mathbf{B}\mathbf{A}\mathbf{C})^{-1}\mathbf{C}\mathbf{B}\mathbf{A} + \mathrm{tr}(\mathbf{C}\mathbf{B}\mathbf{A})^{-1}\mathbf{B}\mathbf{A}\mathbf{C} - \mathrm{tr}(\mathbf{A}\mathbf{C}\mathbf{B})^{-1}\mathbf{B}\mathbf{A}\mathbf{C} \\
&= 3(N_1^3 - \bar{N}_1^3) + 2N_1^2(A_2 B_1 + B_2 C_1 + C_2 A_1) \\
&\quad - 2\bar{N}_1^2(A_1 B_2 + B_1 C_2 + C_1 A_2) + N_1 \bar{\Lambda} - \bar{N}_1 \Lambda \,, \tag{3.11}
\end{aligned}
$$

---

[10]Because of the large number of self-intersections to resolve, it is tedious to get the expressions in terms of networks (second lines) from applying skein relations. However, they can be derived easily with Mathematica in the explicit representation of loop and network functions as Fock-Goncharov polynomials that we will present in section 4.
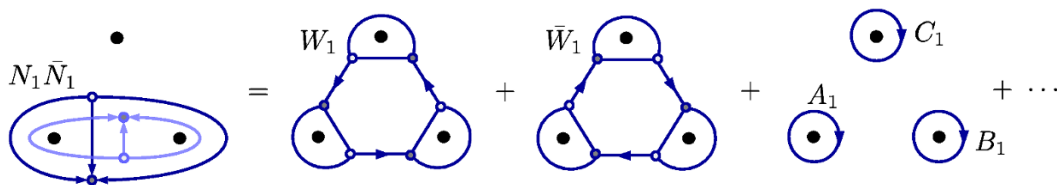
Figure 16. The product $N_1\bar{N}_1$ can be expressed in terms of the networks W_1 and $\bar{W}_1$ via the skein relation.

and the remaining Poisson brackets can be deduced by replacing every object by its reverse: $\mathbf{A} \to \mathbf{A}^{-1}$, $A_1 \to A_2$, $N_1 \to \bar{N}_1$, $W_1 \to \bar{W}_1$, and so on. Here we have defined

$$\Lambda \equiv A_1A_2B_2C_1 + B_1B_2C_2A_1 + C_1C_2A_2B_1 + A_1^2B_1 + B_1^2C_1 + C_1^2A_1$$
$$+A_2B_2^2 + B_2C_2^2 + C_2A_2^2 - 3(A_2B_1 + B_2C_1 + C_2A_1) \ . \tag{3.12}$$

In conclusion, we have obtained a closed Poisson algebra with the generators

$$A_i, B_i, C_i, N_1, \bar{N}_1, W_1, \bar{W}_1 \ . \tag{3.13}$$

Since the dimension of the moduli space $\mathcal{M}_{0,3}^3$ is 8, there must be 2 relations between these 10 generators.

Relations. A simple way to obtain a relation is to consider the product of N_1 and $\bar{N}_1$. We can draw these networks on $\mathcal{C}_{0,3}$ such that they have two intersections, which we resolve by applying the skein relation (see figure 16). The resulting networks can be simplified via the square reduction of figure 11 (with $q = 1$), and the polynomial relation is then $\mathcal{P}_1 = 0$ with

$$\mathcal{P}_1 = N_1\bar{N}_1 - \left(W_1 + \bar{W}_1 + A_1B_1C_1 + A_2B_2C_2 + A_1A_2 + B_1B_2 + C_1C_2 + 3\right) \ . \tag{3.14}$$

The second relation $\mathcal{P}_2 = 0$ comes from the product of W_1 and $\bar{W}_1$:[11]

$$\mathcal{P}_2 = (W_1 + 6)(\bar{W}_1 + 6) - \Big[N_1^3 + N_1^2(A_2B_1 + B_2C_1 + A_1C_2) + N_1\bar{\Lambda}$$
$$+A_1^3 + B_1^3 + C_1^3 + A_1^2A_2B_1C_1 + A_1B_1^2B_2C_1 + A_1B_1C_1^2C_2$$
$$+A_1^2B_1^2C_2 + A_2B_1^2C_1^2 + A_1^2B_2C_1^2 - 2(A_1^2B_2C_2 + A_2B_1^2C_2 + A_2B_2C_1^2) + \text{reverse}$$
$$+A_1A_2B_1B_2C_1C_2 + A_1A_2B_1B_2 + B_1B_2C_1C_2 + C_1C_2A_1A_2$$
$$-3(A_1B_1C_1 + A_2B_2C_2) - 9(A_1A_2 + B_1B_2 + C_1C_2) + 27\Big] \ , \tag{3.15}$$

Here "+reverse" means that all the previous terms should be added with reverse orientation.

We have therefore arrived at a description of the algebra $\mathcal{A}_{0,3}^3$ in terms of the 10 generators (3.13) satisfying the 2 relations $\mathcal{P}_1$ and $\mathcal{P}_2$:

$$\mathcal{A}_{0,3}^3 = \mathbb{C}\left[A_i, B_i, C_i, N_1, \bar{N}_1, W_1, \bar{W}_1\right]/\{\mathcal{P}_1, \mathcal{P}_2\} \ . \tag{3.16}$$

It is straightforward to relate our description involving networks to the description in terms of trace functions as in (2.15) and (2.16).

---

[11]This complicated expression is also more readily obtained in the explicit representation presented in section 4.
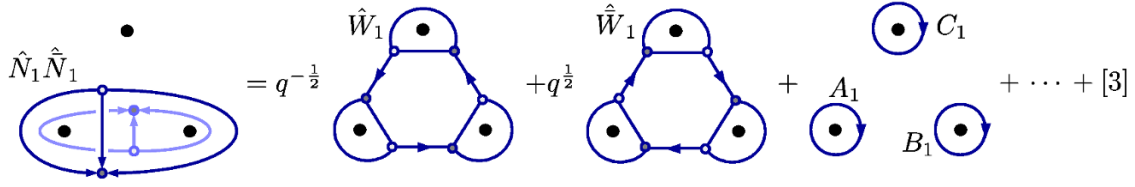
Figure 17. The quantum product of $\hat{N}_1\hat{\bar{N}}_1$ resolved via the quantum skein relation.

Remarkably, we can write the Poisson brackets in terms of derivatives of the polynomial relations (this can be compared with [48]):

$$\{N_1, \bar{N}_1\} = \frac{\partial \mathcal{P}_1}{\partial W_1}\frac{\partial \mathcal{P}_2}{\partial \bar{W}_1} - \frac{\partial \mathcal{P}_1}{\partial \bar{W}_1}\frac{\partial \mathcal{P}_2}{\partial W_1}, \qquad \{N_1, W_1\} = \frac{\partial \mathcal{P}_1}{\partial \bar{W}_1}\frac{\partial \mathcal{P}_2}{\partial \bar{N}_1} - \frac{\partial \mathcal{P}_1}{\partial \bar{N}_1}\frac{\partial \mathcal{P}_2}{\partial \bar{W}_1},$$

$$\{N_1, \bar{W}_1\} = \frac{\partial \mathcal{P}_1}{\partial \bar{N}_1}\frac{\partial \mathcal{P}_2}{\partial W_1} - \frac{\partial \mathcal{P}_1}{\partial W_1}\frac{\partial \mathcal{P}_2}{\partial \bar{N}_1}, \qquad \{W_1, \bar{W}_1\} = \frac{\partial \mathcal{P}_1}{\partial N_1}\frac{\partial \mathcal{P}_2}{\partial \bar{N}_1} - \frac{\partial \mathcal{P}_1}{\partial \bar{N}_1}\frac{\partial \mathcal{P}_2}{\partial N_1}. \qquad (3.17)$$

This implies that the Poisson structure of $\mathcal{M}_{0,3}^3$ is compatible with its structure as an algebraic variety.

Quantization: quantum versions of the polynomial relations $\mathcal{P}_1$ and $\mathcal{P}_2$, in which the network functions are replaced by noncommuting operators, can be obtained by applying the quantum skein relations in (2.39) and figure 11.

The quantum relation $\hat{\mathcal{P}}_1$ is obtained by superposing the operators $\hat{N}_1$ and $\hat{\bar{N}}_1$ and resolving their two intersections via the quantum skein relation (see figure 17):

$$\hat{N}_1\hat{\bar{N}}_1 = q^{-\frac{1}{2}}\hat{W}_1 + q^{\frac{1}{2}}\hat{\bar{W}}_1 + \hat{A}_1\hat{B}_1\hat{C}_1 + \hat{A}_2\hat{B}_2\hat{C}_2 + \hat{A}_1\hat{A}_2 + \hat{B}_1\hat{B}_2 + \hat{C}_1\hat{C}_2 + [3] . \quad(3.18)$$

The operator $\hat{N}_1$, which appears first in the product, is drawn on top of the second operator $\hat{\bar{N}}_1$. Note that the product $\hat{\bar{N}}_1\hat{N}_1$ with inverted order would give the same expression but with the replacement $q \to q^{-1}$.

The quantization of the second relation $\mathcal{P}_2$ gives

$$\begin{aligned}
\left(\hat{W}_1 + [6]\right)\left(\hat{\bar{W}}_1 + [6]\right) = {} & q^{\frac{3}{2}}\hat{N}_1^3 + \hat{q}N_1^2(\hat{A}_2\hat{B}_1 + \hat{B}_2\hat{C}_1 + \hat{A}_1\hat{C}_2) + q^{\frac{1}{2}}\hat{N}_1\hat{\bar{\Lambda}}' \\
& + \hat{A}_1^3 + \hat{B}_1^3 + \hat{C}_1^3 + \hat{A}_1^2\hat{A}_2\hat{B}_1\hat{C}_1 + \hat{A}_1\hat{B}_1^2\hat{B}_2\hat{C}_1 + \hat{A}_1\hat{B}_1\hat{C}_1^2\hat{C}_2 \\
& + \hat{A}_1^2\hat{B}_1^2\hat{C}_2 + \hat{A}_2\hat{B}_1^2\hat{C}_1^2 + \hat{A}_1^2\hat{B}_2\hat{C}_1^2 \\
& - (q + q^{-1})(\hat{A}_1^2\hat{B}_2\hat{C}_2 + \hat{A}_2\hat{B}_1^2\hat{C}_2 + \hat{A}_2\hat{B}_2\hat{C}_1^2) + \text{reverse} \\
& + \hat{A}_1\hat{A}_2\hat{B}_1\hat{B}_2\hat{C}_1\hat{C}_2 \\
& - (q - 3 + q^{-1})(\hat{A}_1\hat{A}_2\hat{B}_1\hat{B}_2 + \hat{B}_1\hat{B}_2\hat{C}_1\hat{C}_2 + \hat{C}_1\hat{C}_2\hat{A}_1\hat{A}_2) \\
& - (2q^2 + q - 3 + q^{-1} + 2q^{-2})(\hat{A}_1\hat{B}_1\hat{C}_1 + \hat{A}_2\hat{B}_2\hat{C}_2) \\
& - (2q^2 + q + 3 + q^{-1} + 2q^{-2})(\hat{A}_1\hat{A}_2 + \hat{B}_1\hat{B}_2 + \hat{C}_1\hat{C}_2) \\
& + q^5 + 2q^4 + q^3 + 3q^2 + 3q + 7 + 3q^{-1} + 3q^{-2} + q^{-3} + 2q^{-4} + q^{-5},
\end{aligned}$$
$$(3.19)$$

where now "+ reverse" also implies the replacement $q \to q^{-1}$, and in $\hat{\bar{\Lambda}}'$ we have replaced the coefficient of 3 by $2q + q^{-2}$.
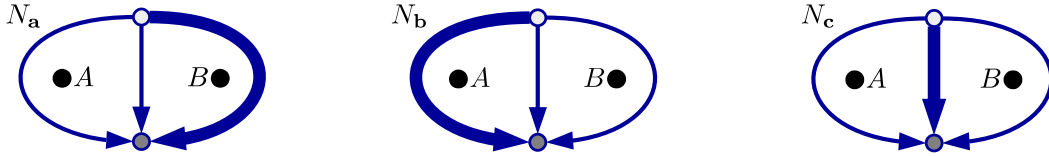
Figure 18. The pants networks $N_\mathbf{a}$, $N_\mathbf{b}$, $N_\mathbf{c}$ differ from one another by the choice of the edge (thick) that carries the second antisymmetric representation of SL(4).

We also find the following quantum commutators:

$$
\hat{N}_1\hat{\bar{N}}_1 - \hat{\bar{N}}_1\hat{N}_1 = (q^{\frac{1}{2}} - q^{-\frac{1}{2}})(\hat{\bar{W}}_1 - \hat{W}_1),
$$

$$
q^{\frac{1}{2}}\hat{N}_1\hat{W}_1 - q^{-\frac{1}{2}}\hat{W}_1\hat{N}_1 = (q^{\frac{3}{2}} - q^{-\frac{3}{2}})\hat{\bar{N}}_1^2 + (q - q^{-1})\hat{\bar{N}}_1(\hat{A}_1\hat{B}_2 + \hat{B}_1\hat{C}_2 + \hat{C}_1\hat{A}_2)
$$
$$
-(q^2 + q - q^{-1} - q^{-2})\hat{N}_1 + (q^{\frac{1}{2}} - q^{-\frac{1}{2}})\hat{\Lambda},
$$

$$
q^{-\frac{1}{2}}\hat{N}_1\hat{\bar{W}}_1 - q^{\frac{1}{2}}\hat{\bar{W}}_1\hat{N}_1 = (q^{-\frac{3}{2}} - q^{\frac{3}{2}})\hat{\bar{N}}_1^2 + (q^{-1} - q)\hat{\bar{N}}_1(\hat{A}_1\hat{B}_2 + \hat{B}_1\hat{C}_2 + \hat{C}_1\hat{A}_2)
$$
$$
-(q^{-2} + q^{-1} - q - q^2)\hat{N}_1 + (q^{-\frac{1}{2}} - q^{\frac{1}{2}})\hat{\Lambda},
$$

$$
\hat{W}_1\hat{\bar{W}}_1 - \hat{\bar{W}}_1\hat{W}_1 = (q^{\frac{3}{2}} - q^{-\frac{3}{2}})(\hat{N}_1^3 - \hat{\bar{N}}_1^3) + (q - q^{-1})\hat{N}_1^2(\hat{A}_2\hat{B}_1 + \hat{B}_2\hat{C}_1 + \hat{C}_2\hat{A}_1)
$$
$$
-(q - q^{-1})\hat{\bar{N}}_1^2(\hat{A}_1\hat{B}_2 + \hat{B}_1\hat{C}_2 + \hat{C}_1\hat{A}_2)
$$
$$
+(q^{\frac{1}{2}} - q^{-\frac{1}{2}})(\hat{N}_1\hat{\bar{\Lambda}} - \hat{\bar{N}}_1\hat{\Lambda}), \tag{3.20}
$$

where in $\hat{\Lambda}$ we have made the replacement $3 \to [3]$. These relations reduce at first order in $\hbar$ to the Poisson brackets (3.9) and (3.11). For example, with a little bit of rewriting we obtain

$$
[\hat{N}_1, \hat{W}_1] = (1 - q)\hat{W}_1\hat{N}_1 + (q - q^{-2})\hat{\bar{N}}_1^2 + (q^{\frac{1}{2}} - q^{-\frac{3}{2}})\hat{\bar{N}}_1(\hat{A}_1\hat{B}_2 + \hat{B}_1\hat{C}_2 + \hat{C}_1\hat{A}_2)
$$
$$
-(q^{\frac{3}{2}} + q^{\frac{1}{2}} - q^{-\frac{3}{2}} - q^{-\frac{5}{2}})\hat{N}_1 + (1 - q^{-1})\hat{\Lambda}
$$
$$
= \hbar\Big[-\hat{W}_1\hat{N}_1 + 3\hat{\bar{N}}_1^2 + 2\hat{\bar{N}}_1(\hat{A}_1\hat{B}_2 + \hat{B}_1\hat{C}_2 + \hat{C}_1\hat{A}_2) - 6\hat{N}_1 + \hat{\Lambda} \Big] + \mathcal{O}(\hbar^2)
$$
$$
= \hbar\{N_1, W_1\} + \mathcal{O}(\hbar^2). \tag{3.21}
$$

SL(4). We find a similar structure for SL(4) loop and network operators. The loop functions A_i around the puncture A are

$$
A_1 = \mathrm{tr}\mathbf{A}, \qquad A_2 = \frac{1}{2}\left[(\mathrm{tr}\mathbf{A})^2 - \mathrm{tr}(\mathbf{A}^2)\right], \qquad A_3 = \mathrm{tr}\mathbf{A}^{-1}. \tag{3.22}
$$

We can construct three pants networks $N_\mathbf{a}$, $N_\mathbf{b}$, $N_\mathbf{c}$, differing by the choice of the edge that carries the second antisymmetric representation of SL(4) (see figure 18):

$$
N_\mathbf{a} = -\frac{1}{2}\epsilon_{mnpq}\mathbf{U}_{\mathbf{a}\,r}^m\mathbf{U}_{\mathbf{a}\,s}^n\mathbf{U}_{\mathbf{b}\,t}^p\mathbf{U}_{\mathbf{c}\,u}^q\epsilon^{rstu} = \mathrm{tr}\mathbf{C}\mathbf{B}^{-1} - C_1B_3,
$$

$$
N_\mathbf{b} = -\frac{1}{2}\epsilon_{mnpq}\mathbf{U}_{\mathbf{a}\,r}^m\mathbf{U}_{\mathbf{b}\,s}^n\mathbf{U}_{\mathbf{b}\,t}^p\mathbf{U}_{\mathbf{c}\,u}^q\epsilon^{rstu} = \mathrm{tr}\mathbf{A}\mathbf{C}^{-1} - A_1C_3,
$$

$$
N_\mathbf{c} = -\frac{1}{2}\epsilon_{mnpq}\mathbf{U}_{\mathbf{a}\,r}^m\mathbf{U}_{\mathbf{b}\,s}^n\mathbf{U}_{\mathbf{c}\,t}^p\mathbf{U}_{\mathbf{c}\,u}^q\epsilon^{rstu} = \mathrm{tr}\mathbf{B}\mathbf{A}^{-1} - B_1A_3. \tag{3.23}
$$

Pants networks with the same orientation Poisson-commute with each other:

$$
\{N_\mathbf{a}, N_\mathbf{b}\} = \{N_\mathbf{b}, N_\mathbf{c}\} = \{N_\mathbf{c}, N_\mathbf{a}\} = 0, \tag{3.24}
$$
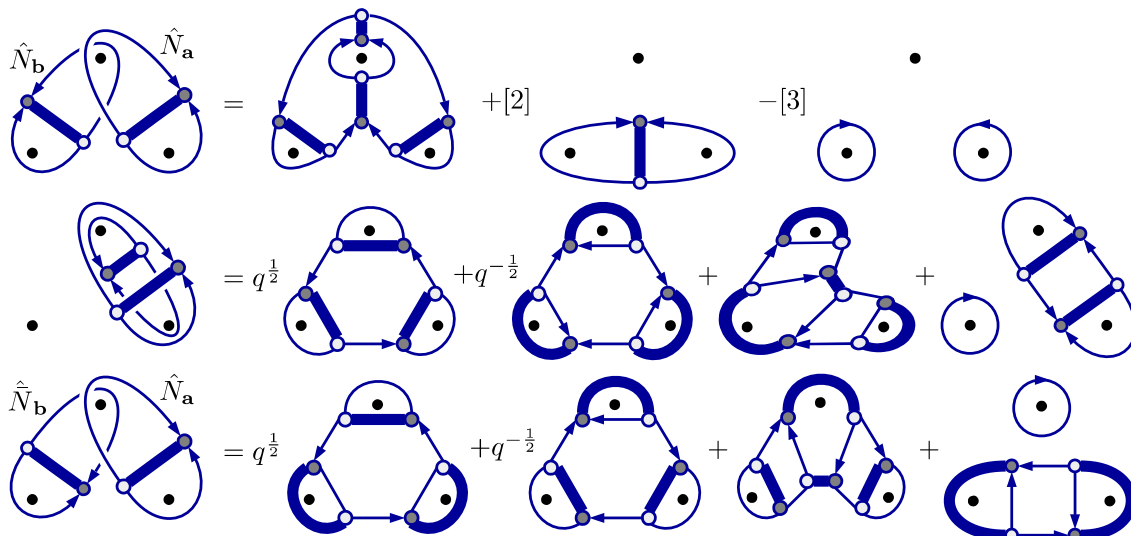
Figure 19. Product of pants networks: $\hat{N}_{\mathbf{a}}\hat{N}_{\mathbf{b}}$ (top), $\hat{N}_{\mathbf{a}}\hat{\bar{N}}_{\mathbf{a}}$ (middle), $\hat{N}_{\mathbf{a}}\hat{\bar{N}}_{\mathbf{b}}$ (bottom).

but they do not commute with their reverses:

$$\{N_{\mathbf{a}}, \bar{N}_{\mathbf{a}}\} = \{N_{\mathbf{b}}, \bar{N}_{\mathbf{b}}\} = \{N_{\mathbf{c}}, \bar{N}_{\mathbf{c}}\} = \mathrm{tr}\,\mathbf{CBA} - \mathrm{tr}\,(\mathbf{CBA})^{-1}\,,$$

$$\{N_{\mathbf{a}}, \bar{N}_{\mathbf{c}}\} = \mathrm{tr}\,\mathbf{CB}^{-1}\mathbf{AB}^{-1} - \mathrm{tr}\,\mathbf{CB}^{-2}\mathbf{A}\,,$$

$$\{N_{\mathbf{c}}, \bar{N}_{\mathbf{b}}\} = \mathrm{tr}\,\mathbf{BA}^{-1}\mathbf{CA}^{-1} - \mathrm{tr}\,\mathbf{BA}^{-2}\mathbf{C}\,,$$

$$\{N_{\mathbf{b}}, \bar{N}_{\mathbf{a}}\} = \mathrm{tr}\,\mathbf{AC}^{-1}\mathbf{BC}^{-1} - \mathrm{tr}\,\mathbf{AC}^{-2}\mathbf{B}\,. \tag{3.25}$$

As in the SL(3) case, to obtain a closed Poisson algebra we would need to add the functions appearing in the Poisson brackets of the pants networks to the set of generators, compute their Poisson brackets, and so on. Repeating this procedure until the Poisson algebra closes would lead to a large number of generators, satisfying many polynomial relations. Ultimately, it should be possible to choose the set of 15 *independent* generators of $\mathcal{A}_{0,3}^4$ to be given by the loop functions around the punctures and by the pants networks:

$$A_i, B_i, C_i, N_{\mathbf{a}}, \bar{N}_{\mathbf{a}}, N_{\mathbf{b}}, \bar{N}_{\mathbf{b}}, N_{\mathbf{c}}, \bar{N}_{\mathbf{c}}\,. \tag{3.26}$$

This can be compared with the 15 generators of the ring of invariants of two matrices given in [60].

Many quantum relations can be easily obtained by applying quantum skein relations to products of pants networks. We show a few examples in figure 19.

3.2 One-punctured torus

Our next simple example is the torus with one full puncture, denoted by $\mathcal{C}_{1,1}$ (see figure 20). The corresponding 4d gauge theory is the so-called $\mathcal{N} = 2^*$ SU(N) gauge theory, which can be obtained from the $\mathcal{N} = 4$ theory by giving a mass to an adjoint hypermultiplet.

The fundamental group of $\mathcal{C}_{1,1}$ consists of three loops, the A-cycle γ_A (meridian), the B-cycle γ_B (longitude), and the loop γ_M around the puncture, subject to one relation:

$$\pi_1(\mathcal{C}_{1,1}) = \langle \gamma_A, \gamma_B, \gamma_M \mid \gamma_A \gamma_B \gamma_A^{-1} \gamma_B^{-1} = \gamma_M \rangle\,. \tag{3.27}$$
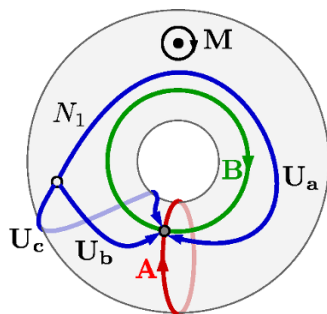
Figure 20. One-punctured torus $\mathcal{C}_{1,1}$. The A- and B-cycles are shown, together with a network operator N_1, consisting of three edges and two junctions.

The holonomy matrices by $\mathbf{A}$, $\mathbf{B}$, and $\mathbf{M}$ satisfy $\mathbf{ABA}^{-1}\mathbf{B}^{-1} = \mathbf{M}$. We can also combine the matrices $\mathbf{A}$ and $\mathbf{B}$ into matrices $\mathbf{C} \equiv (\mathbf{AB})^{-1}$ and $\mathbf{C}' \equiv \mathbf{AB}^{-1}$ associated with the curves $\gamma_C = (\gamma_A \gamma_B)^{-1}$ and $\gamma_{C'} = \gamma_A \gamma_B^{-1}$, respectively. Each of these holonomy matrices gives $(N-1)$ loop functions.

We also consider a particular two-junction network N_1 with two junctions whose edges go around the A- and B-cycles (in contrast to the case of $\mathcal{C}_{0,3}$, there are many two-junction networks that we can consider on $\mathcal{C}_{1,1}$). The network N_1 and its reverse $\bar{N}_1$ each contributes $(N-1)(N-2)/2$ operators. Together, the operators coming from $\mathbf{A}$, $\mathbf{B}$, $\mathbf{C}$ and from the networks N_1, $\bar{N}_1$ add up to the dimension (2.3) of the moduli space of flat SL(N)-connections on $\mathcal{C}_{1,1}$:

$$3(N-1) + 2\frac{(N-1)(N-2)}{2} = N^2 - 1 = \dim[\mathcal{M}_{1,1}^N] \,. \tag{3.28}$$

SL(2). We start by briefly reviewing the well-studied case of flat SL$(2, \mathbb{C})$-connections on the one-punctured torus $\mathcal{C}_{1,1}$ [22] (see also [25, 39, 61]). The Poisson bracket of the A-cycle function $A_1 = \text{tr}\mathbf{A}$ and the B-cycle function $B_1 = \text{tr}\mathbf{B}$ is (by Goldman's formula (2.17)):

$$\{A_1, B_1\} = \text{tr}\mathbf{AB} - \frac{1}{2}A_1 B_1 = -\text{tr}\mathbf{AB}^{-1} + \frac{1}{2}A_1 B_1 \,. \tag{3.29}$$

The extra traces $C_1 = \text{tr}\mathbf{AB}$ and $C_1' = \text{tr}\mathbf{AB}^{-1}$ correspond to curves that go once around the A-cycle and once around the B-cycle (in different directions). Applying the skein relation to products of loop functions gives

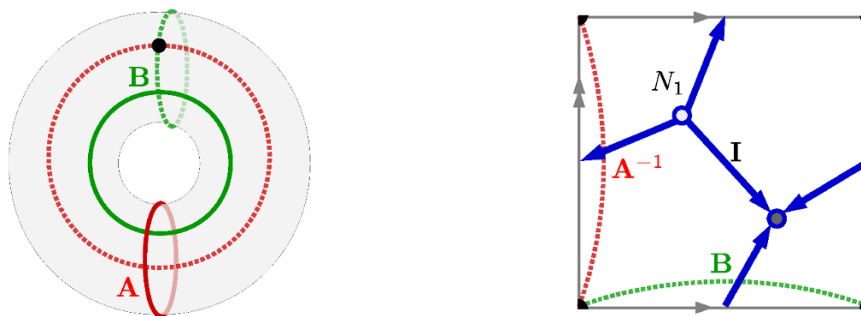$$A_1 B_1 = C_1 + C_1', \qquad C_1 C_1' = A_1^2 + B_1^2 + M_1 - 2 \,, \tag{3.30}$$

which can be combined to obtain the relation $\mathcal{P}_1 = 0$ with

$$\mathcal{P}_1 = A_1 B_1 C_1 - (A_1^2 + B_1^2 + C_1^2 + M_1 - 2) \,. \tag{3.31}$$

The Poisson bracket between the generators A_1, B_1, C_1 can be written as

$$\{A_1, B_1\} = -\frac{1}{2}\frac{\partial \mathcal{P}_1}{C_1} \,, \tag{3.32}$$

Figure 21. *Left*: covering of $\mathcal{C}_{1,1}$ with two branch-cuts (dashed lines). Each branch-cut is associated with a holonomy matrix **A** or **B**. *Right*: $\mathcal{C}_{1,1}$ described as a square with opposite sides identified, and with the puncture at the corners. The holonomy matrices associated with the three edges of the network N_1 are determined by the branch-cuts that they cross.

and cyclic permutations of A_1, B_1, C_1.

To obtain quantum relations, we apply the quantum skein relation:

$$\hat{A}_1 \hat{B}_1 = q^{\frac{1}{4}} \hat{C}_1 + q^{-\frac{1}{4}} \hat{C}_1' \, . \tag{3.33}$$

Inverting the order in the product amounts to exchanging $q \leftrightarrow q^{-1}$, so we can obtain the q-deformed commutation relation

$$q^{\frac{1}{4}} \hat{A}_1 \hat{B}_1 - q^{-\frac{1}{4}} \hat{B}_1 \hat{A}_1 = \left(q^{\frac{1}{2}} - q^{-\frac{1}{2}} \right) \hat{C}_1 \, . \tag{3.34}$$

Note that this relation can be written as a quantum commutator

$$[\hat{A}_1, \hat{B}_1] = (q^{-\frac{1}{2}} - 1) \hat{B}_1 \hat{A}_1 + (q^{\frac{1}{4}} - q^{-\frac{3}{4}}) \hat{C}_1 \, , \tag{3.35}$$

which reproduces the Poisson bracket (3.29) at first order in $\hbar$. Similarly, the quantum skein relation leads to the quantization of the cubic relation (3.31):

$$\hat{\mathcal{P}}_1 = q^{\frac{1}{4}} \hat{A}_1 \hat{B}_1 \hat{C}_1 - \left(q^{\frac{1}{2}} \hat{A}_1^2 + q^{-\frac{1}{2}} \hat{B}_1^2 + q^{\frac{1}{2}} \hat{C}_1^2 + M_1 - [2] \right) \, . \tag{3.36}$$

SL(3). We now have the loop functions $A_1 = \text{tr}\mathbf{A}$ and $A_2 = \text{tr}\mathbf{A}^{-1}$ and similarly for B_i, M_i, C_i, and C_i'. There are many different two-junction networks that can be put on $\mathcal{C}_{1,1}$. A natural choice is the network that goes once around the A-cycle and once around the B-cycle. The associated network function N_1 and its reverse $\bar{N}_1$ can be expressed as

$$\begin{aligned}
N_1 &= \epsilon_{mnp} \mathbf{U}_{\mathbf{a}\,r}^m \mathbf{U}_{\mathbf{b}\,s}^n \mathbf{U}_{\mathbf{c}\,t}^p \epsilon^{rst} \, , \\
\bar{N}_1 &= \epsilon_{mnp} (\mathbf{U}_{\mathbf{a}}^{-1})_r^m (\mathbf{U}_{\mathbf{b}}^{-1})_s^n (\mathbf{U}_{\mathbf{c}}^{-1})_t^p \epsilon^{rst} \, .
\end{aligned} \tag{3.37}$$

As explained in section (2.5), the network functions N_1 and $\bar{N}_1$ can also be obtained from the transition functions in a covering of $\mathcal{C}_{1,1}$. We can for example cover $\mathcal{C}_{1,1}$ with one patch that overlaps itself along two branch-cuts that go around the A- and B-cycles and intersect at the puncture (see figure 21). The network N_1 has one edge that crosses the branch-cut
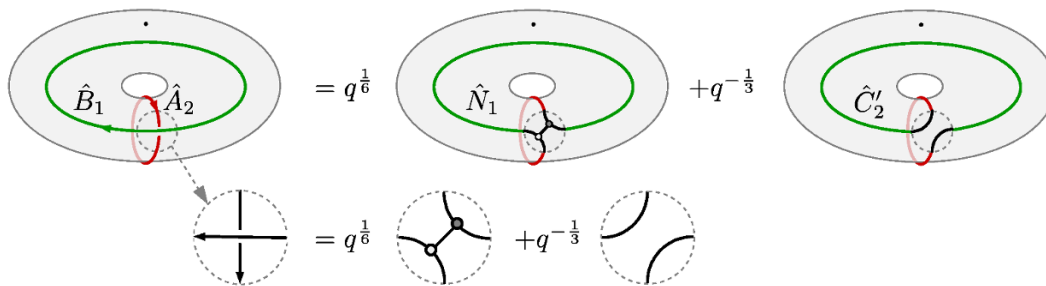
Figure 22. Relations between loop and network operators arise from the skein relation.
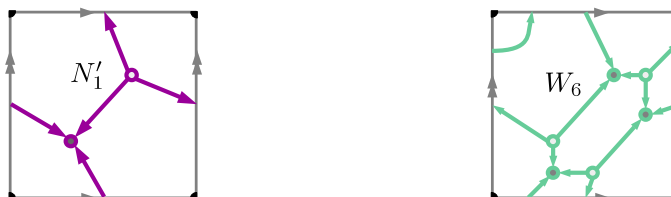
Figure 23. *Left*: flipped network N_1'. *Right*: network W_6 appearing in the product $N_1 \bar{N}_1$.

associated with **A** (with reverse orientation), one that crosses the branch-cut associated with **B**, and one that does not cross any branch-cut. This gives the following expressions

$$N_1 = \epsilon_{mnp}(\mathbf{A}^{-1})^m{}_r \mathbf{B}^n{}_s \delta^p{}_t \epsilon^{rst} = A_2 B_1 - C_2' \,,$$
$$\bar{N}_1 = \epsilon_{mnp} \mathbf{A}^m{}_r (\mathbf{B}^{-1})^n{}_s \delta^p{}_t \epsilon^{rst} = A_1 B_2 - C_1' \,, \tag{3.38}$$

with $C_1' = \mathrm{tr}\,\mathbf{A}\mathbf{B}^{-1}$ and $C_2' = \mathrm{tr}\,\mathbf{A}^{-1}\mathbf{B}$. Such relations between networks and products of intersecting loops can of course also be understood as arising from the skein relation (2.22) (see figure 22):

$$A_2 B_1 = N_1 + C_2' \,, \qquad\qquad A_1 B_2 = \bar{N}_1 + C_1' \,. \tag{3.39}$$

The quantization of relations such as (3.39) can be obtained by applying quantum skein relations to resolve the intersection of the A- and B-cycles:

$$\hat{A}_2 \hat{B}_1 = q^{\frac{1}{6}} \hat{N}_1 + q^{-\frac{1}{3}} \hat{C}_2' \,, \qquad\qquad \hat{A}_1 \hat{B}_1 = q^{-\frac{1}{6}} \hat{N}_1' + q^{\frac{1}{3}} \hat{C}_2 \,,$$
$$\hat{A}_1 \hat{B}_2 = q^{\frac{1}{6}} \hat{\bar{N}}_1 + q^{-\frac{1}{3}} \hat{C}_1' \,, \qquad\qquad \hat{A}_2 \hat{B}_2 = q^{-\frac{1}{6}} \hat{\bar{N}}_1' + q^{\frac{1}{3}} \hat{C}_1 \,. \tag{3.40}$$

Here the operator $\hat{N}_1'$ corresponds to the flipped network shown on the left of figure 23.

Changing the ordering in the product of two operators simply inverts q, so we can deduce expressions for commutators, whose leading terms in $\hbar$ correspond to the Poisson brackets. For example we obtain

$$[\hat{A}_2, \hat{B}_1] = (q^{\frac{1}{6}} - q^{-\frac{1}{6}})\hat{N}_1 + (q^{-\frac{1}{3}} - q^{\frac{1}{3}})\hat{C}_2' \quad \rightarrow \quad \{A_2, B_1\} = \frac{1}{3}(N_1 - 2C_2') \,. \tag{3.41}$$

We can also apply the quantum skein relation to the product of $\hat{N}_1$ and $\hat{\bar{N}}_1$:

$$\hat{N}_1 \hat{\bar{N}}_1 = q^{-\frac{1}{2}} \hat{W}_6 + q^{\frac{1}{2}} \hat{\bar{W}}_6 + \hat{A}_1 \hat{A}_2 + \hat{B}_1 \hat{B}_2 + \hat{C}_1 \hat{C}_2 + \hat{M}_1 + \hat{M}_2 + [3] \,, \tag{3.42}$$

where W_6 is a network with six junctions shown on the right of figure 23. The same network W_6 also appears in the product

$$\hat{\bar{N}}_1' \hat{C}_2 = \hat{W}_6 + q^{\frac{1}{2}} \hat{A}_1 \hat{A}_2 + q^{-\frac{1}{2}} \hat{B}_1 \hat{B}_2 \ . \tag{3.43}$$

More complicated relations are impractical to derive in this way, but can be computed in the explicit representation of the loop and network operators in terms of Fock-Goncharov polynomials, as we will discuss in section 4. We have for example the classical relation (also given in [45, 62])

$$\begin{aligned}
A_1 A_2 B_1 B_2 C_1 C_2 = \ &\Big[N_1^3 + N_1^2 (A_2 B_1 + B_2 C_1 + C_2 A_1) \tag{3.44}\\
&+ N_1 (A_1 A_2 B_1 C_2 + A_1^2 C_1 + A_2^2 B_2 - 3 A_1 B_2 + \text{cyclic}) \\
&- (A_1 B_2^2 C_2^2 - 2 A_1^2 B_2 C_2 + A_1^3 + \text{cyclic}) + \text{reverse} \Big] \\
&- N_1 \bar{N}_1 (A_1 A_2 + \text{cyclic}) - (A_1 A_2 B_1 B_2 + \text{cyclic}) \\
&+ 3 (A_1 B_1 C_1 + A_2 B_2 C_2) + M_1 M_2 + 6 (M_1 + M_2) + 9 \ .
\end{aligned}$$

Here "+cyclic" means adding the terms obtained by cyclic permutation of A, B, C, and "+reverse" the terms obtained by reversing the orientation, $A_1 \leftrightarrow A_2$, $N_1 \leftrightarrow \bar{N}_1$, and so on. Recall that at the classical level the algebraic structures of $\mathcal{M}_{0,3}^N$ and $\mathcal{M}_{1,1}^N$ are the same, so that the relation (3.44) is the counterpart of the relation (3.15) for the 3-punctured sphere. The Poisson structures on $\mathcal{M}_{0,3}^N$ and $\mathcal{M}_{1,1}^N$ can also be related via a symplectic quotient, as explained in [63].

In conclusion, we can describe the algebra $\mathcal{A}_{1,1}^3$ in terms of the 10 generators A_i, B_i, M_i, C_i, N_1, $\bar{N}_1$ satisfying the relations (3.42) and (3.44). Classically, these generators form a closed Poisson algebra (as noted in [62]):

$$\begin{aligned}
\{A_1, B_1\} &= C_2 - \frac{1}{3} A_1 B_1 \ , & \{A_2, B_1\} &= N_1 - \frac{2}{3} A_2 B_1 \ , \\
\{B_1, C_1\} &= A_2 - \frac{1}{3} B_1 C_1 \ , & \{B_2, C_1\} &= N_1 - \frac{2}{3} B_2 C_1 \ , \\
\{C_1, A_1\} &= B_2 - \frac{1}{3} C_1 A_1 \ , & \{C_2, A_1\} &= N_1 - \frac{2}{3} C_2 A_1 \ , \\
\{A_1, N_1\} &= -\frac{1}{3} A_1 N_1 + A_2 C_2 - B_1 \ , & \{A_1, \bar{N}_1\} &= \frac{1}{3} A_1 \bar{N}_1 - A_2 B_2 + C_1 \ , \\
\{B_1, N_1\} &= -\frac{1}{3} B_1 N_1 + A_2 B_2 - C_1 \ , & \{B_1, \bar{N}_1\} &= \frac{1}{3} B_1 \bar{N}_1 - B_2 C_2 + A_1 \ , \\
\{C_1, N_1\} &= -\frac{1}{3} C_1 N_1 + B_2 C_2 - A_1 \ , & \{C_1, \bar{N}_1\} &= \frac{1}{3} C_1 \bar{N}_1 - A_2 C_2 + B_1 \ , \\
\{N_1, \bar{N}_1\} &= A_1 B_1 C_1 - A_2 B_2 C_2 \ . &&
\end{aligned} \tag{3.45}$$

The remaining Poisson brackets can be obtained by reversing the orientation. In addition, the functions M_i associated with the curve around the puncture are central elements of the Poisson algebra, $\{M_i, \bullet\} = 0$.

Fixing the values of the central elements M_i leaves us with a 6-dimensional moduli space $\bar{\mathcal{M}}_{1,1}^3$ which is symplectic. A natural maximal set of commuting Hamiltonians consists
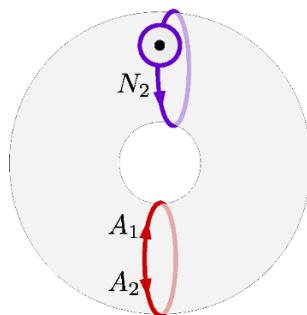
Figure 24. A maximal set of commutting Hamiltonians on $\bar{\mathcal{M}}^3_{1,1}$ is provided by the A-cycle functions A_i and the pants network N_2.
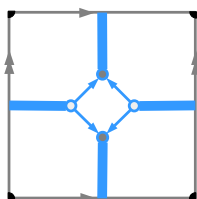
Figure 25. Network N_4 that appears in the product $A_2 B_2$ (thick lines carry $\wedge^2 \square$)).

of the A-cycle functions A_i together with a network N_2 that surrounds the puncture and has one edge along the A-cycle (see figure 24):

$$N_2 = -\epsilon_{mnp} \mathbf{A}^m_{\ r} \mathbf{M}^n_{\ s} \delta^p_{\ t} \epsilon^{rst} = \mathrm{tr} \mathbf{A} \mathbf{M} - A_1 M_1 \ . \tag{3.46}$$

This network is the pants network in the pants decomposition obtained by cutting $\mathcal{C}_{1,1}$ along the A-cycle. It is related to the network N_1 defined above via

$$N_2 = -N_1 C_1 - \bar{N}_1 B_1 + A_2 B_1 C_1 + B_2 C_2 - A_2^2 + A_1 \ . \tag{3.47}$$

The A-cycle functions A_i and the pants network N_2 Poisson-commute, as is obvious from the fact that they do not intersect:

$$\{A_1, A_2\} = \{A_1, P_1\} = \{A_2, P_1\} = 0 \ . \tag{3.48}$$

SL(4). The A-cycle functions are $A_1 = \mathrm{tr} \mathbf{A}$, $A_2 = \frac{1}{2} \left[(\mathrm{tr} \mathbf{A})^2 - \mathrm{tr}(\mathbf{A}^2) \right]$, $A_3 = \mathrm{tr} \mathbf{A}^{-1}$. We define three networks which are going once around the A-cycle and once around the B-cycle, and differ by the choice of the branch that is doubled:

$$\begin{aligned} N_a &= \tfrac{1}{2} \epsilon_{mnpq} \mathbf{U}^m_{\mathbf{a}\,r} \mathbf{U}^n_{\mathbf{a}\,s} \mathbf{U}^p_{\mathbf{b}\,t} \mathbf{U}^q_{\mathbf{c}\,u} \epsilon^{rstu} \ , \\ N_{\mathbf{b}} &= \tfrac{1}{2} \epsilon_{mnpq} \mathbf{U}^m_{\mathbf{a}\,r} \mathbf{U}^n_{\mathbf{b}\,s} \mathbf{U}^p_{\mathbf{b}\,t} \mathbf{U}^q_{\mathbf{c}\,u} \epsilon^{rstu} \ , \\ N_{\mathbf{c}} &= \tfrac{1}{2} \epsilon_{mnpq} \mathbf{U}^m_{\mathbf{a}\,r} \mathbf{U}^n_{\mathbf{b}\,s} \mathbf{U}^p_{\mathbf{c}\,t} \mathbf{U}^q_{\mathbf{c}\,u} \epsilon^{rstu} \ . \end{aligned} \tag{3.49}$$
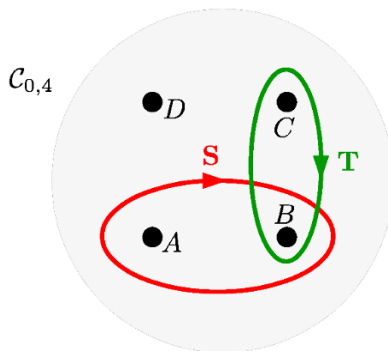
Figure 26. Sphere $\mathcal{C}_{0,4}$ with 4 punctures A, B, C, D. The holonomy matrices **S** and **T** are associated with loops surrounding pairs of punctures.

Quantum relations between the loop and network operators can be obtained by applying quantum skein relations:

$$
\begin{aligned}
\hat{A}_1 \hat{B}_3 &= q^{-\frac{1}{8}} \hat{\bar{N}}_{\mathbf{b}} + q^{\frac{3}{8}} \hat{C}'_1, & \hat{A}_1 \hat{B}_1 &= q^{\frac{1}{8}} \hat{N}'_{\mathbf{b}} + q^{-\frac{3}{8}} \hat{C}_3, \\
\hat{A}_3 \hat{B}_1 &= q^{-\frac{1}{8}} \hat{N}_{\mathbf{b}} + q^{\frac{3}{8}} \hat{C}'_3, & \hat{A}_3 \hat{B}_3 &= q^{\frac{1}{8}} \hat{\bar{N}}'_{\mathbf{b}} + q^{-\frac{3}{8}} \hat{C}_1, \\
\hat{A}_1 \hat{B}_2 &= q^{-\frac{1}{4}} \hat{\bar{N}}_{\mathbf{a}} + q^{\frac{1}{4}} \hat{N}'_{\mathbf{a}}, & \hat{A}_2 \hat{B}_1 &= q^{-1/4} \hat{N}_{\mathbf{c}} + q^{\frac{1}{4}} \hat{N}'_{\mathbf{c}}, \\
\hat{A}_3 \hat{B}_2 &= q^{-\frac{1}{4}} \hat{N}_{\mathbf{a}} + q^{\frac{1}{4}} \hat{\bar{N}}'_{\mathbf{a}}, & \hat{A}_2 \hat{B}_3 &= q^{-1/4} \hat{\bar{N}}_{\mathbf{c}} + q^{\frac{1}{4}} \hat{\bar{N}}'_{\mathbf{c}}, \\
\hat{A}_2 \hat{B}_2 &= q^{\frac{1}{2}} \hat{C}'_2 + q^{-\frac{1}{2}} \hat{C}_2 + \hat{N}_4.
\end{aligned}
\tag{3.50}
$$

Here the networks with a prime are flipped, and N_4 is the four-junction network shown in figure 25.

3.3 Four-punctured sphere

The next example (with $\chi = -2$) is the sphere $\mathcal{C}_{0,4}$ with four full punctures, denoted by A, B, C, D. Its fundamental group can be expressed in terms of the loops $\gamma_A, \gamma_B, \gamma_C, \gamma_D$ surrounding the punctures clockwise, subject to one relation:

$$
\pi_1(\mathcal{C}_{0,4}) = \langle \gamma_A, \gamma_B, \gamma_C, \gamma_D \mid \gamma_A \gamma_B \gamma_C \gamma_D = \gamma_\circ \rangle.
\tag{3.51}
$$

We associate the holonomy matrices $\mathbf{A}, \mathbf{B}, \mathbf{C}, \mathbf{D}$ to these loops, satisfying $\mathbf{ABCD} = (-1)^{N-1}\mathbf{I}$. In addition, we consider the loops γ_S and γ_T surrounding pairs of punctures: $\mathbf{S} \equiv \mathbf{AB}$ and $\mathbf{T} \equiv \mathbf{BC}$ (see figure 26). We also define the two networks N_{AB}, N_{CD} (and their inverses $\bar{N}_{AB}, \bar{N}_{CD}$) around punctures A, B, and C, D, respectively, which are adapted to the pants decomposition determined by the curve γ_S. Each of the holonomy matrices $\mathbf{A}, \mathbf{B}, \mathbf{C}, \mathbf{D}, \mathbf{S}, \mathbf{T}$ gives $(N-1)$ functions, while each of the four networks $N_{AB}, N_{CD}, \bar{N}_{AB}, \bar{N}_{CD}$ gives $(N-1)(N-2)/2$ functions. This gives the following number of functions:

$$
6(N-1) + 4\frac{(N-1)(N-2)}{2} = 2(N^2-1) = \dim[\mathcal{M}^N_{0,4}].
\tag{3.52}
$$

Fixing the conjugacy classes of $\mathbf{A}, \mathbf{B}, \mathbf{C}, \mathbf{D}$ gives $4(N-1)$ constraints.

SL(2). The generators $A_1, B_1, C_1, D_1, S_1, T_1$ do not form a closed Poisson algebra on their own. Indeed, applying the quantum skein relation gives

$$\hat{S}_1\hat{T}_1 = q^{-\frac{1}{2}}\hat{U}_1 + q^{\frac{1}{2}}\hat{U}_1' + \hat{A}_1\hat{C}_1 + \hat{B}_1\hat{D}_1 \,, \tag{3.53}$$

with $U_1 \equiv \text{tr}\mathbf{BD}$ and $U_1' \equiv \text{tr}\mathbf{AC}$ (up to an overall sign for later convenience). The leading order in $\hbar$ gives the Poisson bracket

$$\{S_1, T_1\} = -U_1 + U_1' \,. \tag{3.54}$$

We can eliminate U_1' via the relation (3.53), but then we must include U_1 in the set of generators in order to obtain a closed Poisson algebra. The closure of the Poison algebra with the 7 generators $A_1, B_1, C_1, D_1, S_1, T_1, U_1$ is implied by the following q-deformed commutators:

$$\begin{aligned}
q^{-\frac{1}{2}}\hat{S}_1\hat{T}_1 - q^{\frac{1}{2}}\hat{T}_1\hat{S}_1 &= (q^{-1} - q)\hat{U}_1 - (q^{\frac{1}{2}} - q^{-\frac{1}{2}})(\hat{A}_1\hat{C}_1 + \hat{B}_1\hat{D}_1)\,, \\
q^{-\frac{1}{2}}\hat{T}_1\hat{U}_1 - q^{\frac{1}{2}}\hat{U}_1\hat{T}_1 &= (q^{-1} - q)\hat{S}_1 - (q^{\frac{1}{2}} - q^{-\frac{1}{2}})(\hat{A}_1\hat{B}_1 + \hat{C}_1\hat{D}_1)\,, \\
q^{-\frac{1}{2}}\hat{U}_1\hat{S}_1 - q^{\frac{1}{2}}\hat{S}_1\hat{U}_1 &= (q^{-1} - q)\hat{T}_1 - (q^{\frac{1}{2}} - q^{-\frac{1}{2}})(\hat{B}_1\hat{C}_1 + \hat{A}_1\hat{D}_1)\,.
\end{aligned} \tag{3.55}$$

Since $\dim[\mathcal{M}_{0,4}^2] = 6$, there must be one relation between the 7 generators. It is provided by the product of U_1 and U_1':

$$\begin{aligned}
\hat{U}_1\hat{U}_1' &= q\hat{S}_1^2 + q^{-1}\hat{T}_1^2 + q^{\frac{1}{2}}\hat{S}_1(\hat{A}_1\hat{B}_1 + \hat{C}_1\hat{D}_1) + q^{-\frac{1}{2}}\hat{T}_1(\hat{B}_1\hat{C}_1 + \hat{A}_1\hat{D}_1) \\
&\quad + \hat{A}_1\hat{B}_1\hat{C}_1\hat{D}_1 + \hat{A}_1^2 + \hat{B}_1^2 + \hat{C}_1^2 + \hat{D}_1^2 - [2]^2 \,.
\end{aligned} \tag{3.56}$$

Eliminating U_1' with the relation (3.53) we obtain the familiar cubic relation (see for example [25])

$$\begin{aligned}
\hat{\mathcal{P}}_1 &= q^{-\frac{1}{2}}\hat{S}_1\hat{T}_1\hat{U}_1 - q^{-1}\hat{S}_1^2 - q\hat{T}_1^2 - q^{-1}\hat{U}_1^2 \\
&\quad - q^{-\frac{1}{2}}\hat{S}_1(\hat{A}_1\hat{B}_1 + \hat{C}_1\hat{D}_1) - q^{\frac{1}{2}}\hat{T}_1(\hat{B}_1\hat{C}_1 + \hat{A}_1\hat{D}_1) - q^{-\frac{1}{2}}\hat{U}_1(\hat{A}_1\hat{C}_1 + \hat{B}_1\hat{D}_1) \\
&\quad - \hat{A}_1\hat{B}_1\hat{C}_1\hat{D}_1 - \hat{A}_1^2 - \hat{B}_1^2 - \hat{C}_1^2 - \hat{D}_1^2 + [2]^2 \,.
\end{aligned} \tag{3.57}$$

Note that the same relation holds with U_1 replaced by U_1' and q by q^{-1}. We thus have a presentation of the algebra $\mathcal{A}_{0,4}^2$ in terms of 7 generators satisfying the cubic relation $\mathcal{P}_1$:

$$\mathcal{A}_{0,4}^2 = \mathbb{C}\left[A_1, B_1, C_1, D_1, S_1, T_1, U_1\right]/\mathcal{P}_1 \,. \tag{3.58}$$

The Poisson brackets can be expressed as derivatives of $\mathcal{P}_1$, for example

$$\{S_1, T_1\} = \frac{\partial \mathcal{P}_1}{\partial U_1} = S_1 T_1 - 2U_1 - (A_1 C_1 + B_1 D_1) \,. \tag{3.59}$$

SL(3). For Riemann surfaces with $\dim[\pi_1(\mathcal{C}_{g,n})] = 3$ such as $\mathcal{C}_{0,4}$, the SL(3) character variety has dimension 16, and is generated by a minimal number of 45 trace functions, see [60, 64]. This implies the existence of 29 relations between the generators. Choices for the 16 *independent* generators were given in [65]. In terms our description, we can take the following loop and pants network functions:

$$A_i, B_i, C_i, S_i, T_i, U_i', N_{AB}, \bar{N}_{AB}, N_{AC}, \bar{N}_{AC} \,, \tag{3.60}$$
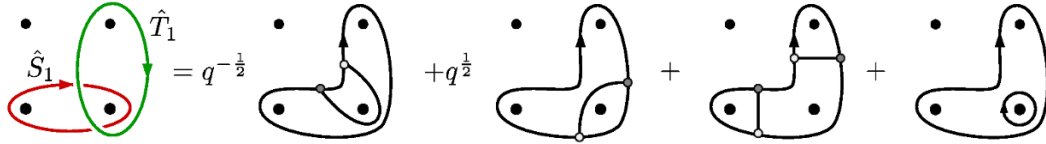
Figure 27. The product $\hat{S}_1 \hat{T}_1$ generates networks via skein relations.
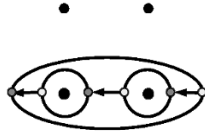
Figure 28. The six-junction network N_6 that appears in the product $N_{AB} \bar{N}_{AB}$.

with

$$N_{AB} = \mathrm{tr}\mathbf{AB}^{-1} - A_1 B_2 , \qquad N_{AC} = \mathrm{tr}\mathbf{AC}^{-1} - A_1 C_2 . \tag{3.61}$$

We can then apply quantum skein relations to products of generators to obtain relations. For example we get (see figure 27)

$$\hat{S}_1 \hat{T}_1 = q^{-\frac{1}{2}} \hat{N}_{BD} + q^{\frac{1}{2}} \hat{N}'_{BD} + \hat{N}_{ABC} + \hat{B}_1 \hat{D}_2 , \tag{3.62}$$

with

$$N_{BD} = \mathrm{tr}\mathbf{BD}^{-1} - B_1 D_2 , \qquad N'_{BD} = \mathrm{tr}\mathbf{AB}^{-1}\mathbf{C} - B_2 U'_1 ,$$
$$N_{ABC} = \mathrm{tr}\mathbf{CB}^{-1}\mathbf{A} - A_1 \bar{N}_{BC} - C_1 N_{AB} - A_1 B_2 C_1 . \tag{3.63}$$

We also find

$$\begin{aligned}
\hat{N}_{AB} \hat{\bar{N}}_{AB} = {}& q^{-\frac{1}{2}} \hat{N}_6 + q^{\frac{1}{2}} \hat{\bar{N}}_6 \\
& + \hat{S}_1 \hat{A}_2 \hat{B}_2 + \hat{S}_2 \hat{A}_1 \hat{B}_1 + \hat{S}_1 \hat{S}_2 + \hat{A}_1 \hat{A}_2 + \hat{B}_1 \hat{B}_2 + [3] ,
\end{aligned} \tag{3.64}$$

with (see figure 28)

$$N_6 = \mathrm{tr}\mathbf{ABA}^{-1}\mathbf{B}^{-1} - S_1 S_2 - A_1 A_2 - B_1 B_2 . \tag{3.65}$$

4 Fock-Goncharov holonomies

We now give an explicit representation of the algebra $\mathcal{A}_{g,n}^N$ in terms of polynomials in the coordinates defined by Fock and Goncharov in their seminal work on higher Teichmüller theory [30]. The holonomy matrices constructed with their methods have some nice positivity properties, which imply that all loop and network functions are given by Laurent polynomials with positive integral coefficients. Relations between generators can then be easily obtained (with the help of Mathematica for higher rank). Thanks to the natural quantization of the Fock-Goncharov coordinates, these relations can be quantized uniquely.

Figure 29. *Left*: ideal triangulation of the three-punctured sphere $\mathcal{C}_{0,3}$ into two triangles. *Right*: N-triangulation of an ideal triangle into N^2 small black and white triangles (here for $N = 4$). The Poisson structure ε is encoded in the arrows circulating clockwise around the small black triangles.

In all examples we have studied perfect agreement is found with the results of skein quantization presented in the previous section. The most non-trivial part of the quantization concerns the positive integral coefficients in the loop and network polynomials. We will see that they get quantized to positive integral Laurent polynomials in $q^{1/2}$ — as expected from their interpretation as the framed protected spin characters of Gaiotto, Moore, and Neitzke [22]. We give many examples up to $N = 4$ for the surfaces $\mathcal{C}_{0,3}$, $\mathcal{C}_{1,1}$, and $\mathcal{C}_{0,4}$.

4.1 Fock-Goncharov coordinates

Fock and Goncharov defined useful systems of coordinates for $\mathcal{M}_{g,n}^N$ associated with triangulations of $\mathcal{C}_{g,n}$. Provided that $\mathcal{C}_{g,n}$ is a hyperbolic surface with at least one puncture, it can be decomposed into triangles with vertices at the punctures. There are -2χ triangles and -3χ edges in this ideal triangulation. Each ideal triangle can then be further decomposed into N^2 small triangles, which produces a so-called N-triangulation (see figure 29). The Fock-Goncharov coordinates x_α, with $\alpha = 1, \ldots, d$, are associated with the vertices of these small triangles (excluding the punctures of $\mathcal{C}_{g,n}$). There are $(N-1)$ coordinates on each edge, and $\binom{N-1}{2}$ coordinates inside each face, which add up to $d \equiv \dim[\mathcal{M}_{g,n}^N]$ (see appendix A for more details).

The Poisson structure on $\mathcal{M}_{g,n}^N$ can be neatly encoded in a system of oriented arrows on the edges of the small triangles of the N-triangulation (see figure 29 right). The Poisson bracket between two Fock-Goncharov coordinates is given by

$$\{x_\alpha, x_\beta\} = \varepsilon_{\alpha\beta} x_\alpha x_\beta \,, \tag{4.1}$$

with

$$\varepsilon_{\alpha\beta} = \#(\text{arrows from } x_\alpha \text{ to } x_\beta) - \#(\text{arrows from } x_\beta \text{ to } x_\alpha) \quad \in \{0, \pm 1, \pm 2\} \,. \tag{4.2}$$

A monomial $x_1^{\mathsf{a}_1} \cdots x_d^{\mathsf{a}_d}$ can be encoded in a vector of exponents $\mathbf{a} = (\mathsf{a}_1, \ldots, \mathsf{a}_d)$, called tropical a-coordinates.[12] The Poisson bracket between two monomials $x_{\mathbf{a}} \equiv \prod_\alpha x_\alpha^{\mathsf{a}_\alpha}$ and

---

[12]The a_i are coordinates for the tropicalization of the $\mathcal{A}$-space defined by Fock and Goncharov, which is dual to the $\mathcal{X}$-space parameterized by the x_i. The $\mathcal{A}$-space is isomorphic to the space of laminations on $\mathcal{C}_{g,n}$.
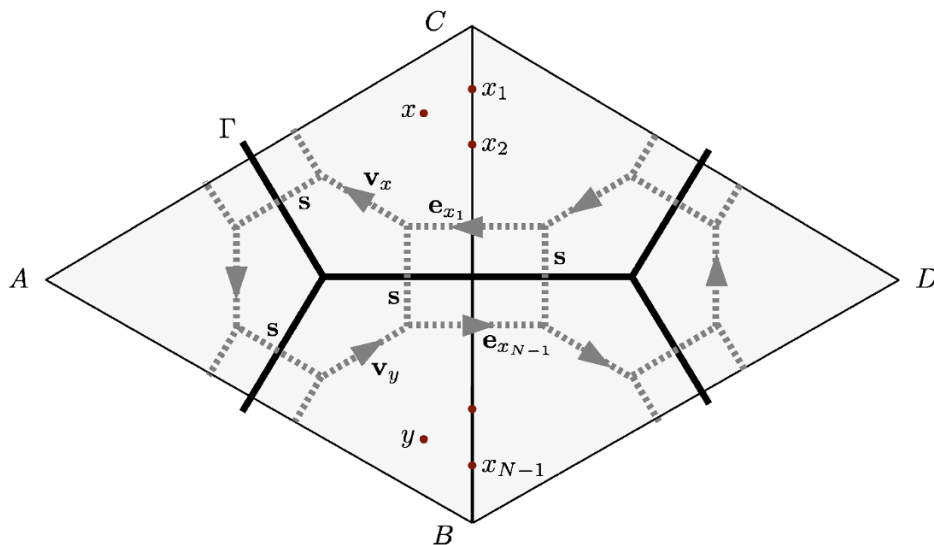
Figure 30. Two triangles in a triangulation and the corresponding dual graph Γ (black). The fat dual graph (dashed) is decomposed into rectangles and hexagons, and its segments are associated with matrices $\mathbf{e}$, $\mathbf{s}$, $\mathbf{v}$.

$x_{\mathbf{b}} \equiv \prod_\alpha x_\alpha^{\mathbf{b}_\alpha}$ is given by

$$\{x_{\mathbf{a}}, x_{\mathbf{b}}\} = \sum_{\alpha,\beta} (\mathbf{a}_\alpha \varepsilon_{\alpha\beta} \mathbf{b}_\beta) x_{\mathbf{a}} x_{\mathbf{b}} = (\mathbf{a}^{\mathrm{t}} \varepsilon \mathbf{b}) x_{\mathbf{a}} x_{\mathbf{b}} = -\sum_\alpha (\mathsf{x}_\alpha \mathbf{b}_\alpha) x_{\mathbf{a}} x_{\mathbf{b}} \ . \tag{4.3}$$

In the last expression, the combinations $\mathsf{x}_\alpha \equiv \sum_\beta \varepsilon_{\alpha\beta} \mathbf{a}_\beta$ are the tropical x-coordinates of the monomial $x_{\mathbf{a}}$. Clearly, monomials with $\mathsf{x}_\alpha = 0$ for all α are central elements of the Poisson algebra (we will see below that they correspond to traces of holonomies around the punctures). The moduli space $\mathcal{M}_{g,n}^N$ is a symplectic fibration over the space of central monomials.

4.2 Holonomies

Fock and Goncharov constructed holonomies on the triangulated surface $\mathcal{C}_{g,n}$ using the snake matrices reviewed in appendix A. The general procedure to obtain the holonomy for a curve γ is to choose a curve homotopic to γ on the graph Γ that is dual to the triangulation and multiply the matrices assigned to the corresponding edges and vertices of the dual graph.

More precisely, the dual graph Γ must be fattened and decomposed into rectangles along its edges and hexagons around its vertices (see figure 30). There are three types of segments in the decomposed fat graph: the segments e crossing an edge of the triangulation, the segments s intersecting the dual graph, and the segments v around the vertices of the dual graph. The segments e and v are oriented clockwise around the punctures, while the segments s are not oriented. The matrices $\mathbf{e}, \mathbf{s}, \mathbf{v} \in \mathrm{SL}(N, \mathbb{C})$ assigned to the segments e, s, v of the decomposed fat graph are the snake matrices defined in appendix A (normalized to have unit determinant):

$$\mathbf{e}_{x_1} = H_1(x_1) H_2(x_2) \cdots H_{N-1}(x_{N-1}) \,, \qquad \mathbf{s} = S \,, \qquad \mathbf{v}_x = \mathcal{F} \,. \tag{4.4}$$

Here the matrix $\mathbf{e}_{x_1}$ depends on the $(N-1)$ coordinates $x_1, \ldots, x_{N-1}$ along the relevant edge in the triangulation (for conciseness we only indicate the coordinate that is closest to the puncture around which it rotates). Similarly, the matrix $\mathbf{v}_x$ depends on all the coordinates inside the relevant face in the triangulation. For example, for $N = 3$ we have

$$\mathbf{e}_{x_1} = \begin{pmatrix} 1 & 0 & 0 \\ 0 & x_1 & 0 \\ 0 & 0 & x_1 x_2 \end{pmatrix}, \qquad \mathbf{s} = \begin{pmatrix} 0 & 0 & 1 \\ 0 & -1 & 0 \\ 1 & 0 & 0 \end{pmatrix}, \qquad \mathbf{v}_x = \begin{pmatrix} 1 & 0 & 0 \\ 1 & 1 & 0 \\ 1 & 1+x & x \end{pmatrix}. \qquad (4.5)$$

The holonomy for a path on the fat graph with successive segments $(s_1, s_2, \cdots, s_m)$, where $s_i \in \{e, s, v\}$, is given by the product of the corresponding matrices: $\mathbf{s_m} \cdots \mathbf{s_2 s_1}$. The holonomy around a rectangle or an hexagon is (projectively) equal to the identity:

$$\mathbf{eses} = \mathbf{vsvsvs} = (-1)^{N-1}\mathbf{I} . \qquad (4.6)$$

Note that this sign is consistent with our conventions for the contraction of a fundamental loop in (2.39) (in the classical case $q = 1$).

The holonomy for any curve γ on the surface $\mathcal{C}_{g,n}$ is obtained by choosing a curve homotopic to γ on the fat graph and multiplying the corresponding matrices (the properties (4.6) ensure that the choice of curve on the graph is irrelevant). Fock and Goncharov showed that the resulting holonomy matrix is conjugate to a matrix whose minors are given by Laurent polynomials with positive integral coefficients (in any coordinate system, that is for any triangulation).[13] It follows that the loop functions A_i that we defined in (2.25) as sums of principal minors (invariant under conjugation) will also be given by positive integral Laurent polynomials in the variables $x_\alpha^{1/N}$. We will moreover observe in explicit examples below that the network functions (2.28) also turn out to be positive integral Laurent polynomials, but we did not find an easy derivation of this property from the positivity of the minors.

A loop or network function L will always contain a highest term with unit coefficient, that is a monomial $x_\mathbf{a} = \prod_\alpha x_\alpha^{\mathbf{a}_\alpha}$ such that any other monomial $x_\mathbf{b} = \prod_\alpha x_\alpha^{\mathbf{b}_\alpha}$ has $\mathbf{b}_\alpha \leq \mathbf{a}_\alpha$ for all α:

$$L = x_1^{\mathbf{a}_1} x_2^{\mathbf{a}_2} \cdots x_d^{\mathbf{a}_d} + \cdots \qquad (4.7)$$

In contrast, other monomials in L have integral coefficients $\overline{\Omega}$ that can be larger than 1:

$$L = x_\mathbf{a} + \overline{\Omega}_\mathbf{b} x_\mathbf{b} + \overline{\Omega}_\mathbf{c} x_\mathbf{c} + \cdots . \qquad (4.8)$$

The product of two loop or network functions L and L' can be expanded as

$$LL' = \sum_{L''} c(L, L'; L'') L'' . \qquad (4.9)$$

For SL(2), Fock and Goncharov proved the positivity of the coefficients $c(L, L'; L'')$ by applying the skein relation shown in figure 3 to the intersections between the loops associated

---

[13]In the case of a holonomy for a loop running around a puncture, the resulting matrix is moreover conjugate to a triangular matrix.

with L and L' and by reducing contractible loops as in (2.36).[14] Note that the positivity of the SL(N) skein relation (2.22) immediately implies that a product of loop or network functions can be written as a finite sum with positive coefficient. However, reduction moves such as those shown in figure 11 can spoil this positivity since they involve negative signs.

4.3 Quantization

The Fock-Goncharov coordinates admit a natural quantization. The algebra $\mathcal{A}_{g,n}^N$ of functions on $\mathcal{M}_{g,n}^N$ can be q-deformed into a noncommutative algebra $\mathcal{A}_{g,n}^N(q)$ by promoting the coordinates x_α to operators $\hat{x}_\alpha$ satisfying the relations

$$\hat{x}_\alpha \hat{x}_\beta = q^{\varepsilon_{\alpha\beta}} \hat{x}_\beta \hat{x}_\alpha \ . \tag{4.10}$$

It is convenient to work with logarithmic coordinates X_α, defined via $x_\alpha = \exp X_\alpha$, and the corresponding operators $\hat{X}_\alpha$, which satisfy the commutation relation (recall $q = \exp\hbar$)

$$[\hat{X}_\alpha, \hat{X}_\beta] = \hbar\{X_\alpha, X_\beta\} = \hbar\varepsilon_{\alpha\beta} \ . \tag{4.11}$$

A monomial in the Fock-Goncharov coordinates can be quantized by first expressing it as an exponential of a sum of logarithmic coordinates, and then promoting them to operators (as in [61] for example):

$$x_{\mathbf{a}} = \prod_{\alpha=1}^n x_\alpha^{\mathsf{a}_\alpha} = \exp\sum_\alpha \mathsf{a}_\alpha X_\alpha \quad \xrightarrow{q} \quad \hat{x}_{\mathbf{a}} = \exp\sum_\alpha \mathsf{a}_\alpha \hat{X}_\alpha = q^{-\frac{1}{2}\sum_{\alpha<\beta} \mathsf{a}_\alpha \varepsilon_{\alpha\beta} \mathsf{a}_\beta} \prod_\alpha \hat{x}_\alpha^{\mathsf{a}_\alpha} \ , \tag{4.12}$$

where in the last step we used the Baker-Campbell-Hausdorff formula. Similarly, the quantum product of two monomials is given by

$$\hat{x}_{\mathbf{a}} * \hat{x}_{\mathbf{b}} = \exp\sum_\alpha \mathsf{a}_\alpha \hat{X}_\alpha * \exp\sum_\beta \mathsf{b}_\beta \hat{X}_\beta = e^{\frac{1}{2}\sum_{\alpha,\beta}[\mathsf{a}_\alpha \hat{X}_\alpha, \mathsf{b}_\beta \hat{X}_\beta]} \exp\sum_\alpha (\mathsf{a}_\alpha + \mathsf{b}_\alpha)\hat{X}_\alpha$$

$$= q^{\frac{1}{2}\mathbf{a}^{\mathrm{t}}\varepsilon\mathbf{b}} \hat{x}_{\mathbf{a}+\mathbf{b}} \ . \tag{4.13}$$

The loop and network functions that we want to quantize are positive integral Laurent polynomials in the Fock-Goncharov coordinates. The monomials $x_{\mathbf{a}}$ that they involve can simply be quantized as in (4.12). It is much less obvious to determine how to quantize the positive integral coefficients $\overline{\Omega}$ of the monomials. Fock and Goncharov conjectured that these quantum coefficients are positive Laurent polynomials in $q^{1/2}$. They also conjectured that the highest term, which has a unit coefficient classically, has a unit coefficient in the quantum operator too. We will make the assumption that all the unit coefficients in a loop or network polynomial remain unit coefficients in the quantized operator (as expected from the interpretation of these coefficients as protected spin characters in [22]). What remains to find is how the non-unit coefficients $\overline{\Omega}$ get quantized:

$$L = x_{\mathbf{a}} + \overline{\Omega}_{\mathbf{b}} x_{\mathbf{b}} + \cdots \quad \xrightarrow{q} \quad \hat{L} = \hat{x}_{\mathbf{a}} + \overline{\Omega}_{\mathbf{b}}^q \hat{x}_{\mathbf{b}} + \cdots \ . \tag{4.14}$$

---

[14]More precisely, their proof does not apply to the loop functions A_i that we are using, but to their slightly different "canonical maps" $\mathbf{I} = \mathrm{tr}(\mathbf{A}^i)$ from the space of integral $\mathcal{A}$-laminations to the space of positive Laurent polynomials.
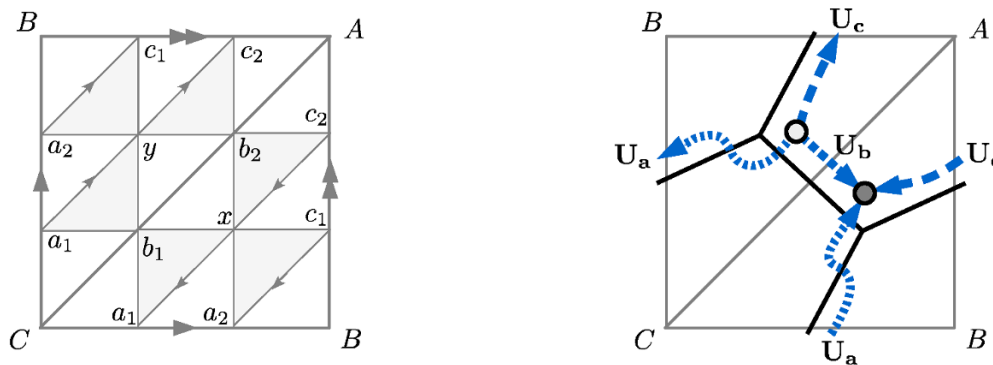
Figure 31. *Left*: 3-triangulation of the sphere $\mathcal{C}_{0,3}$ with three punctures labeled by A, B, C. The edges carry two coordinates each, a_i, b_i, c_i and the faces one each, x, y. *Right*: the dual graph, and the branches $\mathbf{U_a}, \mathbf{U_b}, \mathbf{U_c}$ projected on the fat graph. The white junction indicates the base point for the loops in $\pi_1(\mathcal{C}_{0,3})$.

Our strategy is to demand that the classical loop and network functions, which satisfy some relations of the form (4.9) (such as (3.14) and (3.15) for $\mathcal{C}_{0,3}$), get quantized into operators satisfying quantized versions of these relations. This requirement turns out to be powerful enough to determine uniquely the coefficients in expansions of the loop and network generators into monomials of quantised Fock-Goncharov-coordinates. We will illustrate this quantization procedure in many examples in the following subsections.

We first need to determine how the quantized relations look like. The classical relations are typically of the form (4.9) and get quantized to

$$\hat{L} * \hat{L}' = \sum_{\hat{L}''} c^q(\hat{L}, \hat{L}'; \hat{L}'') \hat{L}'', \tag{4.15}$$

where the $c^q(\hat{L}, \hat{L}'; \hat{L}'')$ are some functions of q. On the left-hand side, the quantum product $\hat{L}\hat{L}'$ generates some powers of q as in (4.13). Focusing on the monomials in $\hat{L}$, $\hat{L}'$, and $\hat{L}''$ with unit coefficients, we can then read off the quantum coefficients $c^q(\hat{L}, \hat{L}'; \hat{L}'')$. We will see that they are integral Laurent polynomials in $q^{1/2N}$. The resulting quantum relations agree with the ones that we could obtain from skein quantization, such as (3.18).

We can then determine the quantum coefficients $\overline{\Omega}^q$ by comparing coefficients of monomials with the same exponents on both sides of the quantum relations. We will find that the $\overline{\Omega}^q$ are always finite positive integral Laurent polynomials in $q^{1/2}$ which are invariant under $q \leftrightarrow q^{-1}$. This is in agreement with the positivity conjectures made in [22] for the protected spin characters.

4.4 Pants networks

We come back to the basic example of flat $\mathrm{SL}(N, \mathbb{C})$-connections on the pair of pants $\mathcal{C}_{0,3}$. The abstract structure of the algebra of loop and network operators was discussed in subsection 3.1.

– 41 –

SL(3). A 3-triangulation of the pair of pants $\mathcal{C}_{0,3}$ is shown in figure 31 left. We denote the Fock-Goncharov coordinates on the edges of the triangles by a_i, b_i, c_i, with $i = 1, 2$, and on the faces by x, y.

Loop functions: the dual graph consists of three edges $\mathbf{U_a}, \mathbf{U_b}, \mathbf{U_c}$, which we can project on segments of the fat graph to obtain the following holonomy matrices:

$$\mathbf{U_a} = \mathbf{s v}_x^{-1} \mathbf{s e}_{a_2} \mathbf{s v}_y^{-1} \mathbf{s}, \qquad \mathbf{U_b} = \mathbf{e}_{b_2}^{-1}, \qquad \mathbf{U_c} = \mathbf{v}_x \mathbf{e}_{c_2} \mathbf{v}_y. \tag{4.16}$$

The holonomy matrices for the three clockwise loops around the punctures can then be expressed as

$$\mathbf{A} = \mathbf{U_b}^{-1}\mathbf{U_c}, \qquad \mathbf{B} = \mathbf{U_c}^{-1}\mathbf{U_a}, \qquad \mathbf{C} = \mathbf{U_a}^{-1}\mathbf{U_b}, \tag{4.17}$$

so that they satisfy the relation $\mathbf{ABC} = \mathbf{I}$ from $\pi_1(\mathcal{C}_{0,3})$. The eigenvalues of these matrices correspond (up to normalizations) to products of coordinates along parallel loops around the punctures in the 3-triangulation (see figure 32 left):

$$
\begin{array}{llll}
\mathbf{A}: & (1, \alpha_1, \alpha_1\alpha_2), & \alpha_1 = b_2 c_2, & \alpha_2 = b_1 c_1 xy, \\
\mathbf{B}: & (1, \beta_1, \beta_1\beta_2), & \beta_1 = c_1 a_2, & \beta_2 = c_2 a_1 xy, \\
\mathbf{C}: & (1, \gamma_1, \gamma_1\gamma_2), & \gamma_1 = a_1 b_1, & \gamma_2 = a_2 b_2 xy.
\end{array} \tag{4.18}
$$

Defining the loop functions $A_1 = \mathrm{tr}\mathbf{A}$ and $A_2 = \mathrm{tr}\mathbf{A}^{-1}$, we can write the compact expression

$$A_i = \prod_j \alpha_j^{-\kappa_{ij}^{-1}} (1 + \alpha_i + \alpha_1\alpha_2), \tag{4.19}$$

where the normalization factor is determined by the Cartan matrix κ of SL(3):

$$\kappa = \begin{pmatrix} 2 & -1 \\ -1 & 2 \end{pmatrix}, \qquad \kappa^{-1} = \frac{1}{3}\begin{pmatrix} 2 & 1 \\ 1 & 2 \end{pmatrix}. \tag{4.20}$$

This simple interpretation of the loop functions comes from the fact that for a path around a puncture the Fock-Goncharov holonomy matrix can be written as a triangular matrix:

$$\mathbf{A} = \prod_j \alpha_j^{-\kappa_{1j}^{-1}} \begin{pmatrix} 1 & 0 & 0 \\ b_2 + \alpha_1 & \alpha_1 & 0 \\ b_1 b_2(1 + c_2 + c_2 x + c_1 c_2 x) & b_1\alpha_1(1 + x + c_1 x + c_1 xy) & \alpha_1\alpha_2 \end{pmatrix}. \tag{4.21}$$

The normalization factor ensures that $\det \mathbf{A} = 1$. Note that the tropical x-coordinates all vanish for A_i, B_i, C_i, which implies that they are central elements of the Poisson algebra (recall (4.3)).

Network functions: we construct the network function N_1 and its reverse $\bar{N}_1$ by fusing the three edges at the two trivalent junctions with ϵ-tensors (see (3.5), or alternatively (3.6)):

$$
\begin{aligned}
N_1 &= -\epsilon_{mnp}\mathbf{U}_{\mathbf{a}\,r}^m \mathbf{U}_{\mathbf{b}\,s}^n \mathbf{U}_{\mathbf{c}\,t}^p \epsilon^{rst}, \\
\bar{N}_1 &= -\epsilon_{mnp}(\mathbf{U_a}^{-1})_r^m (\mathbf{U_b}^{-1})_s^n (\mathbf{U_c}^{-1})_t^p \epsilon^{rst}.
\end{aligned} \tag{4.22}
$$
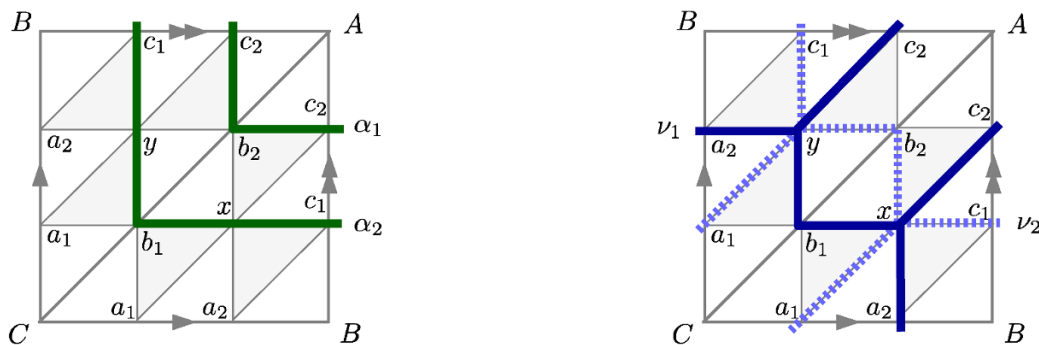
Figure 32. *Left*: paths homotopic to the loop around the puncture A on the 3-triangulation of $C_{0,3}$, which correspond to the monomials $\alpha_1 = b_2 c_2$ and $\alpha_2 = b_1 c_1 xy$. *Right*: paths homotopic to the network N_1, corresponding to $\nu_1 = a_2 b_1 c_2 xy$ (dark) and $\nu_2 = a_1 b_2 c_1 xy$ (dashed).

This gives polynomials with 25 terms each. Three of these terms stand out: the highest term, the lowest term, and the middle term (which also happens to be the only term with a non-unit coefficient). They can be written in terms of monomials ν_1 and ν_2 that have a geometric interpretation as paths homotopic to the network on the 3-triangulation (see figure 32 right):

$$N_1 \ni \prod_i \nu_i^{-\kappa_{1i}^{-1}} \left(1 + 2\nu_1 + \nu_1\nu_2\right), \qquad \nu_1 = a_2 b_1 c_2 xy,$$

$$\bar{N}_1 \ni \prod_i \nu_i^{-\kappa_{2i}^{-1}} \left(1 + 2\nu_2 + \nu_1\nu_2\right), \qquad \nu_2 = a_1 b_2 c_1 xy. \tag{4.23}$$

The full expression for N_1 is

$$\begin{aligned}
N_1 = \prod_i \nu_i^{-\kappa_{1i}^{-1}} \Big(&1 + y + a_2 y + b_1 y + c_2 y + a_2 b_1 y + a_2 c_2 y + b_1 c_2 y + a_2 b_1 c_2 y + a_2 b_1 xy \\
&+ a_2 c_2 xy + b_1 c_2 xy + 2\nu_1 + a_1 a_2 b_1 c_2 xy + a_2 b_1 b_2 c_2 xy + a_2 b_1 c_1 c_2 xy \\
&+ a_2 b_1 c_2 x^2 y + a_1 a_2 b_1 c_2 x^2 y + a_2 b_1 b_2 c_2 x^2 y + a_1 a_2 b_1 b_2 c_2 x^2 y + a_2 b_1 c_1 c_2 x^2 y \\
&+ a_1 a_2 b_1 c_1 c_2 x^2 y + a_2 b_1 b_2 c_1 c_2 x^2 y + a_1 a_2 b_1 b_2 c_1 c_2 x^2 y + \nu_1\nu_2 \Big). \tag{4.24}
\end{aligned}$$

This is consistent with the expression obtained in [62] from products of trace functions (see also [66]). The tropical a-coordinates of N_1 (the exponents of its highest term) and its tropical x-coordinates are given by

$$\mathbf{a}(N_1) = \frac{1}{3}(2,1,1,2,2,1,3,3), \qquad \mathbf{x}(N_1) = (0,0,0,0,0,0,1,-1). \tag{4.25}$$

Poisson brackets: the Poisson bracket for the pants networks is computed by using (4.3). The Poisson tensor (4.2) can be read off from the 3-triangulation in figure 31, and is given

in the basis $\{a_1, a_2, b_1, b_2, c_1, c_2, x, y\}$ by

$$\varepsilon = \begin{pmatrix} 0 & 0 & 0 & 0 & 0 & 0 & -1 & 1 \\ 0 & 0 & 0 & 0 & 0 & 0 & 1 & -1 \\ 0 & 0 & 0 & 0 & 0 & 0 & 1 & -1 \\ 0 & 0 & 0 & 0 & 0 & 0 & -1 & 1 \\ 0 & 0 & 0 & 0 & 0 & 0 & -1 & 1 \\ 0 & 0 & 0 & 0 & 0 & 0 & 1 & -1 \\ 1 & -1 & -1 & 1 & 1 & -1 & 0 & 0 \\ -1 & 1 & 1 & -1 & -1 & 1 & 0 & 0 \end{pmatrix} \tag{4.26}$$

This gives the Poisson bracket (3.9)

$$\{N_1, \bar{N}_1\} = -W_1 + \bar{W}_1 \; . \tag{4.27}$$

The network functions W_1 and $\bar{W}_1$ have 187 terms each, with the following highest, lowest, and middle terms:

$$W_1 \ni \prod_j \sigma_j^{-\kappa_{1j}^{-1}} (1 + 8\sigma_1 + \sigma_1\sigma_2) \;, \qquad \sigma_1 = a_1 a_2 b_1 b_2 c_1 c_2 y^3 \;,$$

$$\bar{W}_1 \ni \prod_j \sigma_j^{-\kappa_{2j}^{-1}} (1 + 8\sigma_2 + \sigma_1\sigma_2) \;, \qquad \sigma_2 = a_1 a_2 b_1 b_2 c_1 c_2 x^3 \;. \tag{4.28}$$

All the Poisson brackets (3.11) between the generators $N_1, \bar{N}_1, W_1, \bar{W}_1$ can be easily computed in this way.

Classical relations: it is easy to obtain the polynomial relations between the generators $A_i, B_i, C_i, N_1, \bar{N}_1, W_1, \bar{W}_1$. One useful method is to start with a product, say $N_1\bar{N}_1$, and to look for a combination of generators with the same highest term, in this case $A_1 B_1 C_1$, in order to cancel it. Then we find that the highest terms in $N_1\bar{N}_1 - A_1 B_1 C_1$ can be cancelled by W_1 and $\bar{W}_1$. Repeating this procedure a few more times leads to the relation $\mathcal{P}_1$ given in (3.14). After implementing this algorithm in Mathematica we can obtain relatively complicated relations such as $\mathcal{P}_2$ given in (3.15). In contrast, it would be very laborious to derive this relation purely from applying skein relations, because it would require the resolution of many intersections in the products $W_1\bar{W}_1$, N_1^3, and N_1^2. Of course, the fact that $\mathcal{P}_2$ is a combination of several product expansions of the form (4.9) implies that its coefficients can appear somewhat unnatural (this comment applies even more for the quantized relation (3.19)).

Quantization of the relations: we now want to obtain quantum versions of the polynomial relations $\mathcal{P}_1$ and $\mathcal{P}_2$, in which the network functions are replaced by noncommuting operators. Each term in the classical relations can acquire at the quantum level a coefficient that is an arbitrary function of the quantization parameter $q = e^{\hbar}$ and that reduces to the classical integral coefficient in the limit $q \to 1$.

The quantum product of polynomials in the Fock-Goncharov coordinates can be obtained by applying the product (4.13) to each pair of monomials. For example, the quantum

product $\hat{N}_1\hat{\bar{N}}_1$ will produce a certain power of q for each pair of monomials coming from $\hat{N}_1$ and $\hat{\bar{N}}_1$. Let us consider first the highest terms $x_{\mathbf{a}}$ and $x_{\bar{\mathbf{a}}}$ in N_1 and $\bar{N}_1$ with tropical a-coordinates

$$\mathbf{a} = \frac{1}{3}(2,1,1,2,2,1,3,3), \qquad \bar{\mathbf{a}} = \frac{1}{3}(1,2,2,1,1,2,3,3) . \tag{4.29}$$

These two monomials Poisson-commute, $\{x_{\mathbf{a}}, x_{\bar{\mathbf{a}}}\} = 0$, which implies that their quantum product does not produce any power of q:

$$\hat{x}_{\mathbf{a}}\hat{x}_{\bar{\mathbf{a}}} = \hat{x}_{\mathbf{a}+\bar{\mathbf{a}}} . \tag{4.30}$$

This implies that the corresponding term in $\hat{\mathcal{P}}_1$ with tropical a-coordinate

$$\mathbf{a} + \bar{\mathbf{a}} = (1,1,1,1,1,1,2,2) \tag{4.31}$$

must have the same coefficient as $\hat{N}_1\hat{\bar{N}}_1$. This term turns out to be the highest term in $\hat{A}_1\hat{B}_1\hat{C}_1$, and so, by an overall rescaling, we can set the coefficients of $\hat{N}_1\hat{\bar{N}}_1$ and $\hat{A}_1\hat{B}_1\hat{C}_1$ to one in the quantum relation $\hat{\mathcal{P}}_1$. The next highest terms in the relation have tropical a-coordinates $(1,1,1,1,1,1,2,1)$ and $(1,1,1,1,1,1,1,2)$. They correspond respectively to the highest terms of the operators $\hat{W}_1$ and $\hat{\bar{W}}_1$, as well as to two products of monomials in $\hat{N}_1\hat{\bar{N}}_1$ with coefficients $q^{-1/2}$ and $q^{1/2}$. This fixes the quantum coefficients of $\hat{W}_1$ and $\hat{\bar{W}}_1$ in $\hat{\mathcal{P}}_1$.

Repeating this procedure for the next highest terms in the relation allows us to determine all the quantum coefficients, except for the constant term 3 in $\mathcal{P}_1$. We find that it should quantize as $Q_2\bar{Q}_2 - 1$, where Q_2 and $\bar{Q}_2$ are the quantizations of the coefficients of 2 that appear in the expansion of the network operators $\hat{N}_1$ and $\hat{\bar{N}}_1$ (recall (4.23)). We will show momentarily that $Q_2 = \bar{Q}_2 = [2]$ and thus the 3 should quantize as $[2]^2 - 1 = [3]$. The quantum relation $\hat{\mathcal{P}}_1$ finally takes the form

$$\hat{N}_1\hat{\bar{N}}_1 = q^{-\frac{1}{2}}\hat{W}_1 + q^{\frac{1}{2}}\hat{\bar{W}}_1 + \hat{A}_1\hat{B}_1\hat{C}_1 + \hat{A}_2\hat{B}_2\hat{C}_2 + \hat{A}_1\hat{A}_2 + \hat{B}_1\hat{B}_2 + \hat{C}_1\hat{C}_2 + [3] . \tag{4.32}$$

Pleasingly, this quantum relation agrees exactly with the result (3.18) that we obtained in section 3.1 by applying the quantum skein relation.

Applying the same procedure (with the help of Mathematica) to the second relation $\mathcal{P}_2$ leads to the quantum relation given in (3.19).

Quantization of the generators: having quantized the relations, we would now like to quantize the generators themselves, as described in subsection 4.3. The generators are polynomials in the Fock-Goncharov coordinates with integer coefficients. The unit coefficients should not be affected by the quantization, but we need to find how to quantize the non-integral coefficients that appear in front of some monomials. We will see how the quantum relation (3.18) can be used to determine these quantum coefficients uniquely.

There is only one term in the expansion for N_1 with a non-unit coefficient, namely the middle term with the factor of 2 in (4.23). In the quantum operator $\hat{N}_1$, this coefficient of 2 will be replaced by a function Q_2 of q. We can determine Q_2 by finding a term in the quantum relation that is linear in it. For example, the monomial $1/a_1$ appears in $\hat{N}_1\hat{\bar{N}}_1$

with the coefficient Q_2, and also in $\hat{W}_1$ and $\hat{\bar{W}}_1$ with unit coefficient. Since W_1 and $\bar{W}_1$ appear in the quantum relation (3.18) with factors of $q^{1/2}$ and $q^{-1/2}$, we deduce that the coefficient of 2 in N_1 simply becomes a quantum $[2]$ in $\hat{N}_1$:

$$2 \in N_1 \quad \overset{q}{\to} \quad Q_2 = q^{\frac{1}{2}} + q^{-\frac{1}{2}} \equiv [2] \in \hat{N}_1 \,. \tag{4.33}$$

The coefficient of 2 in $\bar{N}_1$ similarly quantizes to $\bar{Q}_2 = [2]$. So we have (up to normalization)

$$\begin{aligned} N_1 \ni 1 + 2\nu_1 + \nu_1\nu_2 \qquad &\overset{q}{\to} \qquad \hat{N}_1 \ni 1 + [2]\hat{\nu}_1 + \hat{\nu}_1\hat{\nu}_2 \,, \\ \bar{N}_1 \ni 1 + 2\nu_2 + \nu_1\nu_2 \qquad &\overset{q}{\to} \qquad \hat{N}_1 \ni 1 + [2]\hat{\nu}_2 + \hat{\nu}_1\hat{\nu}_2 \,. \end{aligned} \tag{4.34}$$

Among the 187 monomials in the network W_1, 24 have a coefficient 2, 4 a 3, 12 a 4, 6 a 5, 2 a 6, and 1 an 8. Let us focus on the monomial $8y/x$ in W_1. In the classical relation $\mathcal{P}_1$ given in (3.14), the coefficient of 8 is cancelled by 8 pairs of monomials in $N_1\bar{N}_1$, $x_{\mathbf{a}_i}$ from N_1 and $x_{\bar{\mathbf{a}}_i}$ from $\hat{\bar{N}}_1$, whose products give y/x. For example we have

$$\mathbf{a}_1 = -\frac{1}{3}(1,2,2,1,1,2,3,0) \,, \qquad \bar{\mathbf{a}}_1 = \frac{1}{3}(1,2,2,1,1,2,0,3) \tag{4.35}$$

satisfying $\mathbf{a}_1 + \bar{\mathbf{a}}_1 = (0,0,0,0,0,0,-1,1)$. In the quantum relation, however, the quantum product of the corresponding monomials in $\hat{N}_1\hat{\bar{N}}_1$ produces some power of q as in (4.13):

$$\hat{x}_{\mathbf{a}_1}\hat{x}_{\bar{\mathbf{a}}_1} = q^{\frac{1}{2}\mathbf{a}_1^{\mathsf{t}}\varepsilon\bar{\mathbf{a}}_1}\hat{x}_{\mathbf{a}_1+\bar{\mathbf{a}}_1} = q\hat{x}_{\mathbf{a}_1+\bar{\mathbf{a}}_1} \,. \tag{4.36}$$

Summing over the contributions of all such pairs $(\mathbf{a}_i, \bar{\mathbf{a}}_i)$, we obtain the expression for the quantization of the term $8y/x$ in $\hat{W}_1$ (recall there is a factor of $q^{-1/2}$ in front of $\hat{W}_1$ in the quantum relation (3.18)):

$$8 \in W_1 \quad \overset{q}{\to} \quad q^{\frac{1}{2}}\sum_{i=1}^{8} q^{\frac{1}{2}\mathbf{a}_i^{\mathsf{t}}\varepsilon\bar{\mathbf{a}}_i} = q^{\frac{3}{2}} + 3q^{\frac{1}{2}} + 3q^{-\frac{1}{2}} + q^{-\frac{3}{2}} = [2]^3 \in \hat{W}_1 \,. \tag{4.37}$$

The quantization of all the non-unit coefficients in the network operators $\hat{W}_1$ and $\hat{\bar{W}}_1$ can be determined in the same way. We find

$$\begin{aligned} 2 &\to q^{\frac{1}{2}} + q^{-\frac{1}{2}} = [2] \,, & 8 &\to q^{\frac{3}{2}} + 3q^{\frac{1}{2}} + 3q^{-\frac{1}{2}} + q^{-\frac{3}{2}} = [2]^3 \,, \\ 3 &\to q + 1 + q^{-1} = [3] \,, & 4 &\to q + 2 + q^{-1} = [3] + 1 = [2]^2 \,, \\ 5 &\to q + 3 + q^{-1} = [3] + 2 \,, & 6 &\to q + 4 + q^{-1} = [3] + 3 \,. \end{aligned} \tag{4.38}$$

We see that all the quantized coefficients in the loop and network operators are positive integral Laurent polynomials in $q^{1/2}$, and are also invariant under $q \to q^{-1}$.

This provides further evidence for the positivity conjectures of Gaiotto, Moore, and Neitzke [22] about the framed protected spin characters (1.6), which should take the form

$$\overline{\underline{\Omega}}(L,\gamma;q) = \mathrm{tr}_{\mathcal{H}_L^{\mathrm{BPS}}} q^{J_3} \,, \tag{4.39}$$

with J_3 a generator of so(3).
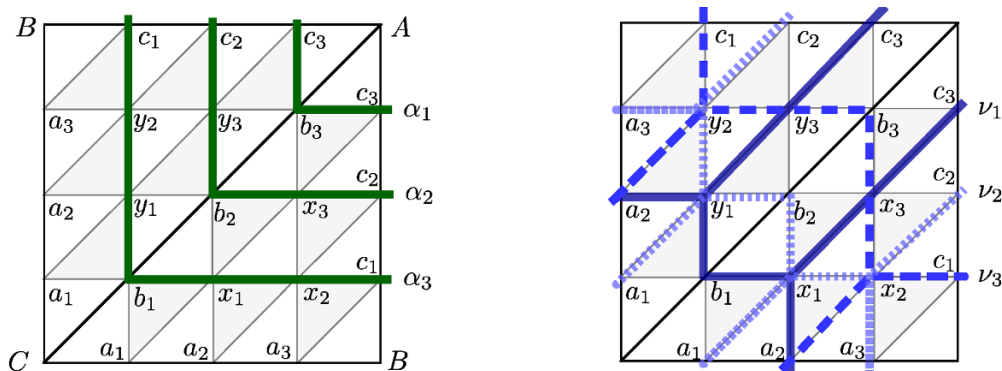
Figure 33. 4-triangulation of $\mathcal{C}_{0,3}$. *Left*: the green lines represent the eigenvalues α_i of the holonomy matrix $\mathbf{A}$ around the puncture A. *Right*: paths corresponding to ν_1 (continuous), ν_2 (fine dashed), and ν_3 (dashed) appearing in N_1.

SL(4). We find a similar structure for SL(4) loop and network operators. For example, the holonomy matrix $\mathbf{A}$ around the puncture A has the following eigenvalues (see figure 33):

$$\mathbf{A}: \qquad \prod_i \alpha_i^{-\kappa_{1i}^{-1}} \left(1, \alpha_1, \alpha_1\alpha_2, \alpha_1\alpha_2\alpha_3\right),$$

$$\alpha_1 = b_3 c_3, \quad \alpha_2 = b_2 c_2 x_3 y_3, \quad \alpha_3 = b_1 c_1 x_1 x_2 y_1 y_2, \tag{4.40}$$

with the SL(4) Cartan matrix

$$\kappa = \begin{pmatrix} 2 & -1 & 0 \\ -1 & 2 & -1 \\ 0 & -1 & 2 \end{pmatrix}, \qquad \kappa^{-1} = \frac{1}{4}\begin{pmatrix} 3 & 2 & 1 \\ 2 & 4 & 2 \\ 1 & 2 & 3 \end{pmatrix}. \tag{4.41}$$

The loop functions A_i can be expressed in terms of the α_i:

$$A_1 = \mathrm{tr}\mathbf{A} = \prod_i \alpha_i^{-\kappa_{1i}^{-1}}\left(1 + \alpha_1 + \alpha_1\alpha_2 + \alpha_1\alpha_2\alpha_3\right),$$

$$A_2 = \frac{1}{2}\left[(\mathrm{tr}\mathbf{A})^2 - \mathrm{tr}(\mathbf{A}^2)\right] = \prod_i \alpha_i^{-\kappa_{2i}^{-1}}\left(1 + \alpha_2 + \alpha_1\alpha_2 + \alpha_2\alpha_3 + \alpha_1\alpha_2\alpha_3 + \alpha_1\alpha_2^2\alpha_3\right),$$

$$A_3 = \mathrm{tr}\mathbf{A}^{-1} = \prod_i \alpha_i^{-\kappa_{3i}^{-1}}\left(1 + \alpha_3 + \alpha_2\alpha_3 + \alpha_1\alpha_2\alpha_3\right). \tag{4.42}$$

We can construct three pants networks $N_\mathbf{a}$, $N_\mathbf{b}$, $N_\mathbf{c}$ (and their reverses), differing by the choice of the edge that carries the second antisymmetric representation of SL(4) (recall figure 18):

$$N_\mathbf{a} = -\frac{1}{2}\epsilon_{mnpq}\mathbf{U}_{\mathbf{a}\,r}^m \mathbf{U}_{\mathbf{a}\,s}^n \mathbf{U}_{\mathbf{b}\,t}^p \mathbf{U}_{\mathbf{c}\,u}^q \epsilon^{rstu} = \mathrm{tr}\mathbf{CB}^{-1} - C_1 B_3,$$

$$N_\mathbf{b} = -\frac{1}{2}\epsilon_{mnpq}\mathbf{U}_{\mathbf{a}\,r}^m \mathbf{U}_{\mathbf{b}\,s}^n \mathbf{U}_{\mathbf{b}\,t}^p \mathbf{U}_{\mathbf{c}\,u}^q \epsilon^{rstu} = \mathrm{tr}\mathbf{AC}^{-1} - A_1 C_3,$$

$$N_\mathbf{c} = -\frac{1}{2}\epsilon_{mnpq}\mathbf{U}_{\mathbf{a}\,r}^m \mathbf{U}_{\mathbf{b}\,s}^n \mathbf{U}_{\mathbf{c}\,t}^p \mathbf{U}_{\mathbf{c}\,u}^q \epsilon^{rstu} = \mathrm{tr}\mathbf{BA}^{-1} - B_1 A_3. \tag{4.43}$$

These pants network functions contain 176 terms each, all with unit coefficient apart from 12 that have a coefficient of 2. Some of the terms have an interpretation as paths homotopic to the network (see figure 33), and we can write for example

$$N_{\mathbf{a}} \ni \prod_i \nu_i^{-\kappa_{1i}^{-1}} \left(1 + 2\nu_1 + 2\nu_1\nu_2 + \nu_1\nu_2\nu_3\right), \tag{4.44}$$

$$\bar{N}_{\mathbf{a}} \ni \prod_i \nu_i^{-\kappa_{3i}^{-1}} \left(1 + 2\nu_3 + 2\nu_2\nu_3 + \nu_1\nu_2\nu_3\right), \tag{4.45}$$

with $\nu_1 = a_2 b_1 c_3 x_1 x_3 y_1 y_3$, $\nu_2 = a_1 a_3 b_2 c_2 x_1 x_2 y_1 y_2$, and $\nu_3 = a_2 b_3 c_1 x_2 x_3 y_2 y_3$.

Quantum relations can be obtained by using the quantum skein relations for $\mathcal{U}_q(sl_4)$ (see figure 19). The quantization of the network operators can then be obtained from these relations. In particular, the 12 coefficients of 2 appearing in each pants operator get quantized to $[2] = q^{1/2} + q^{-1/2}$, much in the same way as for SL(3). A more elaborate illustration is provided by the network that appears with a factor of $q^{1/2}$ in the relation for $\hat{N}_a \hat{\bar{N}}_b$ (see figure 19). This network operator contains 2344 terms with a coefficient of 2, 184 with a 3, 815 with a 4, 123 with a 5, 91 with a 6, 115 with an 8, 6 with a 9, 14 with a 10, 8 with a 12, and 4 with a 16. Every coefficient gets quantized in a unique way. Note however that coefficients that are the same classically can quantize in different ways:

$$
\begin{aligned}
2 &\to q^{\frac{1}{2}} + q^{-\frac{1}{2}} & \text{or} & & 2\,, \\
3 &\to q + 1 + q^{-1} & \text{or} & & 3\,, \\
4 &\to q + 2 + q^{-1} & \text{or} & & 2q^{\frac{1}{2}} + 2q^{-\frac{1}{2}}\,, \\
5 &\to q + 3 + q^{-1}\,, \\
6 &\to q^{\frac{3}{2}} + 2q^{\frac{1}{2}} + 2q^{-\frac{1}{2}} + q^{-\frac{3}{2}} & \text{or} & & 3q^{\frac{1}{2}} + 3q^{-\frac{1}{2}} & \text{or} & & q + 4 + q^{-1}\,, \\
8 &\to 2q + 4 + 2q^{-1} & \text{or} & & q^{\frac{3}{2}} + 3q^{\frac{1}{2}} + 3q^{-\frac{1}{2}} + q^{-\frac{3}{2}}\,, \\
9 &\to 2q + 5 + 2q^{-1}\,, \\
10 &\to q^{\frac{3}{2}} + 4q^{\frac{1}{2}} + 4q^{-\frac{1}{2}} + q^{-\frac{3}{2}}\,, \\
12 &\to q^2 + 3q + 4 + 3q^{-1} + q^{-2} & \text{or} & & 2q^{\frac{3}{2}} + 4q^{\frac{1}{2}} + 4q^{-\frac{1}{2}} + 2q^{-\frac{3}{2}}\,, \\
16 &\to q^2 + 4q + 6 + 4q^{-1} + q^{-2} & \text{or} & & 2q^{\frac{3}{2}} + 6q^{\frac{1}{2}} + 6q^{-\frac{1}{2}} + 2q^{-\frac{3}{2}}\,, \tag{4.46}
\end{aligned}
$$

4.5 One-punctured torus

SL(2). We start by briefly reviewing the well-studied case of flat $SL(2, \mathbb{C})$-connections on the one-punctured torus $\mathcal{C}_{1,1}$ [22] (see also [61]). A triangulation of $\mathcal{C}_{1,1}$ and its dual graph are shown on the right of figure 34. The three edges of the dual graph can be used to express all the loop and network functions. After projecting the edges on the fat graph, we can express the corresponding holonomy matrices as products of (normalized) snake matrices:

$$\mathbf{U_a} = \mathbf{s}\mathbf{v}^{-1}\mathbf{s}\mathbf{e}_a\mathbf{v}_y\,, \qquad \mathbf{U_b} = \mathbf{e}_b^{-1}\,, \qquad \mathbf{U_c} = \mathbf{v}\mathbf{e}_c\mathbf{s}\mathbf{v}^{-1}\mathbf{s}\,. \tag{4.47}$$

The holonomy matrices for the A- and B-cycles, and for the clockwise closed loop around the puncture (all based at the black junction in figure 20) are expressed as

$$\mathbf{A} = \mathbf{U_b}\mathbf{U_c^{-1}}\,, \qquad \mathbf{B} = \mathbf{U_a}\mathbf{U_b^{-1}}\,, \qquad \mathbf{M} = \mathbf{U_b}\mathbf{U_c^{-1}}\mathbf{U_a}\mathbf{U_b^{-1}}\mathbf{U_c}\mathbf{U_a^{-1}}\,. \tag{4.48}$$
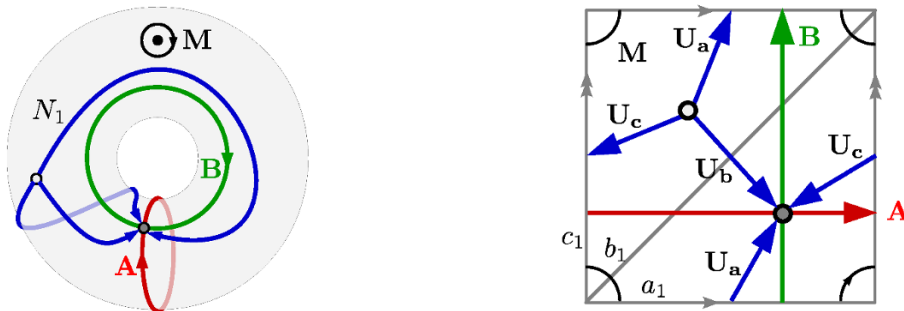
Figure 34. *Left*: one-punctured torus $\mathcal{C}_{1,1}$. The A- and B-cycles are shown, together with a network operator N_1. *Right*: a triangulation of $\mathcal{C}_{1,1}$ into two triangles. The dual graph consists of the edges $\mathbf{U}_a$, $\mathbf{U}_b$, $\mathbf{U}_c$, and corresponds to the network N_1.

In terms of the Fock-Goncharov coordinates a, b, c on the edges of the triangulation, these loop functions are given by

$$A_1 = \sqrt{bc} + \sqrt{\frac{b}{c}} + \frac{1}{\sqrt{bc}}, \quad B_1 = \sqrt{ab} + \sqrt{\frac{a}{b}} + \frac{1}{\sqrt{ab}}, \quad M_1 = abc + \frac{1}{abc}. \quad (4.49)$$

These results were already derived by Gaiotto, Moore, and Neitzke [22], who emphasized that they were unexpected from classical reasoning. Indeed, the vev of a Wilson line operator in a representation $\mathcal{R}$ of the gauge group would naively correspond in the IR theory (where the gauge group is broken to its Cartan subgroup) to a sum of vevs of Wilson lines labeled by the weights of $\mathcal{R}$. In the case of A_1 in (4.49), these IR Wilson lines correspond to the terms $\sqrt{bc}$ and $1/\sqrt{bc}$. However, extra contributions, such as $\sqrt{b/c}$, come as a surprise. They were attributed to interesting bound states in [22].

The Poisson bracket of A_1 and B_1 can be obtained by direct calculation from (4.1) and agrees with (3.29):

$$\{A_1, B_1\} = \text{tr}\mathbf{AB} - \frac{1}{2}A_1 B_1 = -\text{tr}\mathbf{AB}^{-1} + \frac{1}{2}A_1 B_1. \quad (4.50)$$

The traces $C_1 = \text{tr}\mathbf{AB}$ and $C_1' = \text{tr}\mathbf{AB}^{-1}$ correspond to curves that go once around the A-cycle and once around the B-cycle (in different directions) and take the form

$$C_1 = \sqrt{ca} + \sqrt{\frac{c}{a}} + \frac{1}{\sqrt{ca}}, \qquad C_1' = \sqrt{\frac{a}{c}}\left(bc + b + 2 + \frac{1}{b} + \frac{1}{ab}\right). \quad (4.51)$$

As explained in subsection 4.3, in order to quantize the generators we first write them in terms of logarithmic coordinates A, B, C defined via $a = \mathrm{e}^A$, $b = \mathrm{e}^B$, $c = \mathrm{e}^C$, and then promote these coordinates to operators $\hat{A}, \hat{B}, \hat{C}$ satisfying the commutation relations

$$[\hat{A}, \hat{B}] = [\hat{B}, \hat{C}] = [\hat{C}, \hat{A}] = 2\hbar. \quad (4.52)$$

For example, the quantized A-cycle operator is given by

$$\hat{A}_1 = \mathrm{e}^{-\frac{1}{2}(\hat{B}+\hat{C})} + \mathrm{e}^{\frac{1}{2}(\hat{B}-\hat{C})} + \mathrm{e}^{\frac{1}{2}(\hat{B}+\hat{C})}. \quad (4.53)$$
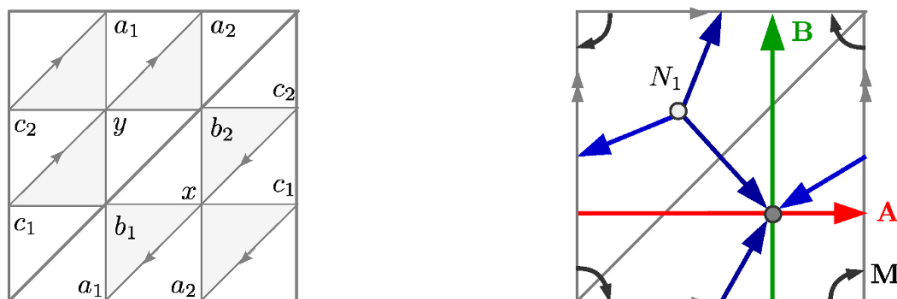
Figure 35. *Left*: 3-triangulation of $\mathcal{C}_{1,1}$. The edges carry two coordinates each, a_i, b_i, c_i, and the faces one each, x, y. *Right*: the A-cycle (red), the B-cycle (green), the loop around the puncture (black), and the network N_1 corresponding to the dual graph (blue).

We can explicitly check that the quantum relation (3.36) is satisfied by using the quantum product (4.13).

A key point is that the loop function C_1' contains a coefficient of 2 in (4.51), and it is not clear a priori how to quantize it. However, the quantum relation (3.33) imposes that this 2 in C_1' be replaced by the quantum integer $[2] = q^{1/2} + q^{-1/2}$ in $\hat{C}_1'$.

SL(3). A 3-triangulation of $\mathcal{C}_{1,1}$ is shown in figure 35. There are now two Fock-Goncharov coordinates for each edge, a_i, b_i, c_i, with $i = 1, 2$, and one for each triangle, x, y. We express the holonomy matrices corresponding to the three branches of the dual graph as

$$\mathbf{U_a} = \mathbf{sv}_x^{-1}\mathbf{se}_{a_2}\mathbf{v}_y\,, \qquad \mathbf{U_b} = \mathbf{e}_{b_2}^{-1}\,, \qquad \mathbf{U_c} = \mathbf{v}_x\mathbf{e}_{c_2}\mathbf{sv}_y^{-1}\mathbf{s}\,. \tag{4.54}$$

These three branches can be used to construct all the loop and network functions, exactly as in (4.48) for the SL(2) case.

The loop functions $M_1 = \mathrm{tr}\mathbf{M}$ and $M_2 = \mathrm{tr}\mathbf{M}^{-1}$ can be expressed compactly as

$$M_i = \prod_j \mu_j^{-\kappa_{ij}^{-1}}\left(1 + \mu_i + \mu_1\mu_2\right), \tag{4.55}$$

where $\mu_1 = a_1a_2b_1b_2c_1c_2$ and $\mu_2 = a_1a_2b_1b_2c_1c_2x^3y^3$ correspond to products of coordinates along paths surrounding the puncture. The A-cycle functions $A_1 = \mathrm{tr}\mathbf{A}$ and $A_2 = \mathrm{tr}\mathbf{A}^{-1}$ similarly involve the monomials $\alpha_1 = b_1c_1x$ and $\alpha_2 = b_2c_2y$, which are products of coordinates along paths homotopic to the A-cycle (see figure 36):

$$A_1 = \prod_j \alpha_j^{-\kappa_{1j}^{-1}}\left[1 + b_1 + b_1x + b_1b_2x + \alpha_1(1 + b_2 + b_2y + \alpha_2)\right],$$

$$A_2 = \prod_j \alpha_j^{-\kappa_{2j}^{-1}}\left[1 + b_2 + b_2y + b_1b_2y + \alpha_2(1 + b_1 + b_1x + \alpha_1)\right]. \tag{4.56}$$

Interestingly, the tropical x-coordinates of the terms in A_i involving only the α_i (namely the highest, middle, and lowest terms) reproduce the weight systems of the fundamental and
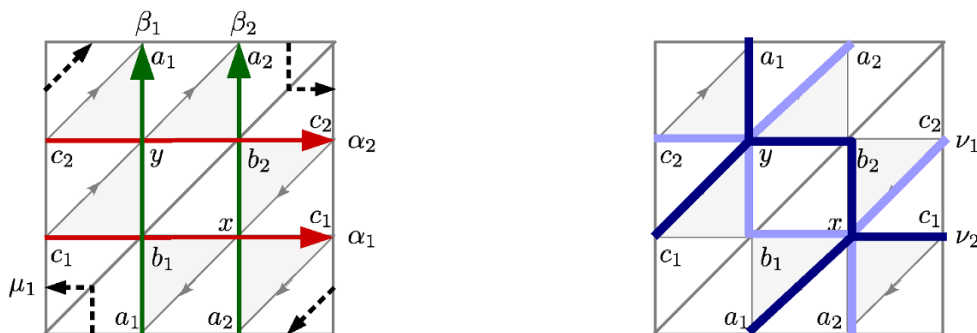
Figure 36. *Left*: paths corresponding to the monomials $\alpha_1 = b_1 c_1 x$, $\alpha_2 = b_2 c_2 y$, $\beta_1 = a_1 b_1 x$, $\beta_2 = a_2 b_2 y$, and $\mu_1 = a_1 a_2 b_1 b_2 c_1 c_2$. *Right*: paths corresponding to $\nu_1 = a_2 b_1 c_2 xy$ and $\nu_2 = a_1 b_2 c_1 xy$.

anti-fundamental representations. More specifically, the tropical x-coordinates $(\mathsf{b}_1, \mathsf{b}_2)$ are

$$A_1 \ni \prod_j \alpha_j^{-\kappa_{1j}^{-1}} \begin{cases} \alpha_1\alpha_2 : & (0,1) \\ \alpha_1 & : & (1,-1) \\ 1 & : & (-1,0), \end{cases} \qquad A_2 \ni \prod_j \alpha_j^{-\kappa_{2j}^{-1}} \begin{cases} \alpha_1\alpha_2 : & (1,0) \\ \alpha_2 & : & (-1,1) \\ 1 & : & (0,-1). \end{cases} \qquad (4.57)$$

The B-cycle functions B_i have similar expressions, involving the monomials $\beta_1 = a_1 b_1 x$ and $\beta_2 = a_2 b_2 y$. The Poisson bracket between β_i and α_j can be neatly expressed in terms of the Cartan matrix κ (as in [67]):

$$\{\beta_i, \alpha_j\} = \kappa_{ij}\beta_i\alpha_j, \qquad \{\beta_i, \beta_j\} = \{\alpha_i, \alpha_j\} = 0. \qquad (4.58)$$

The network function N_1 and its reverse $\bar{N}_1$ defined as

$$N_1 = \epsilon_{mnp}\mathbf{U}_{\mathbf{a}\,r}^m \mathbf{U}_{\mathbf{b}\,s}^n \mathbf{U}_{\mathbf{c}\,t}^p \epsilon^{rst},$$
$$\bar{N}_1 = \epsilon_{mnp}(\mathbf{U}_{\mathbf{a}}^{-1})_r^m (\mathbf{U}_{\mathbf{b}}^{-1})_s^n (\mathbf{U}_{\mathbf{c}}^{-1})_t^p \epsilon^{rst} \qquad (4.59)$$

contain 28 terms each, only one of which has a non-unit coefficient of 2. The full expression for N_1 is precisely the same as the expression (4.24) for the pants network function on $\mathcal{C}_{0,3}$, apart from three extra terms:

$$N_1(\mathcal{C}_{1,1}) = N_1(\mathcal{C}_{0,3}) + \prod_j \nu_j^{-\kappa_{1j}^{-1}} (a_2 b_1 b_2 xy + b_1 c_1 c_2 xy + c_2 a_1 a_2 xy). \qquad (4.60)$$

The loop functions $C'_1 = \mathrm{tr}\mathbf{A}\mathbf{B}^{-1}$ and $C'_2 = \mathrm{tr}\mathbf{A}^{-1}\mathbf{B}$ are polynomials with 27 terms, 8 of which have a coefficient of 2.

The quantization of relations such as (3.39) can be obtained by using the quantum product:

$$\hat{A}_2\hat{B}_1 = q^{\frac{1}{6}}\hat{N}_1 + q^{-\frac{1}{3}}\hat{C}'_2, \qquad \hat{A}_1\hat{B}_1 = q^{-\frac{1}{6}}\hat{N}'_1 + q^{\frac{1}{3}}\hat{C}_2,$$
$$\hat{A}_1\hat{B}_2 = q^{\frac{1}{6}}\hat{\bar{N}}_1 + q^{-\frac{1}{3}}\hat{C}'_1, \qquad \hat{A}_2\hat{B}_2 = q^{-\frac{1}{6}}\hat{\bar{N}}'_1 + q^{\frac{1}{3}}\hat{C}_1. \qquad (4.61)$$

Here the network operator $\hat{N}'_1$ corresponds to the flipped dual graph (see figure 23). This agrees with the relations (3.40) obtained by applying the quantum skein relation.
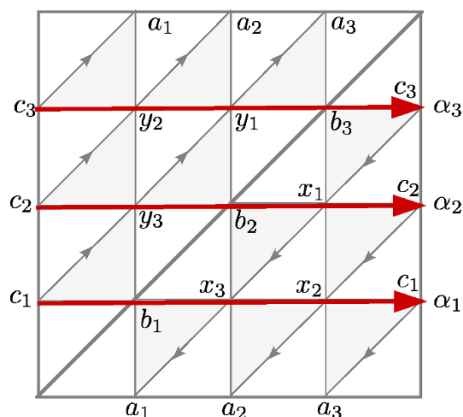
Figure 37. 4-triangulation of $\mathcal{C}_{1,1}$. The edges carry three coordinates each, a_i, b_i, c_i, and the faces three each, x_i and y_i. The paths corresponding to the monomials $\alpha_1 = b_1c_1x_2x_3$, $\alpha_2 = b_2c_2x_1y_3$, and $\alpha_3 = b_3c_3y_1y_2$ appearing in the loop functions A_i are indicated.

In order for these quantum relations to hold, the coefficients of 2 appearing in the classical functions N_1, C_i', and N_1' must be replaced by the quantum integer $[2] = q^{1/2} + q^{-1/2}$ in the operators $\hat{N}_1$, $\hat{C}_i'$, and $\hat{N}_1'$.

We can also reproduce the quantum relations (3.42):

$$\hat{N}_1\hat{\bar{N}}_1 = q^{-\frac{1}{2}}\hat{W}_6 + q^{\frac{1}{2}}\hat{\bar{W}}_6 + \hat{A}_1\hat{A}_2 + \hat{B}_1\hat{B}_2 + \hat{C}_1\hat{C}_2 + \hat{M}_1 + \hat{M}_2 + [3]\,, \qquad (4.62)$$

where W_6 is a network with six junctions shown in figure 23. The same network W_6 also appears in the product

$$\hat{\bar{N}}_1'\hat{C}_2 = \hat{W}_6 + q^{\frac{1}{2}}\hat{A}_1\hat{A}_2 + q^{-\frac{1}{2}}\hat{B}_1\hat{B}_2\,. \qquad (4.63)$$

We can further compute the classical relation (also obtained in [45] and [62])

$$\begin{aligned}
A_1A_2B_1B_2C_1C_2 = &\left[N_1^3 + N_1^2(A_2B_1 + B_2C_1 + C_2A_1)\right. & (4.64) \\
&\quad + N_1(A_1A_2B_1C_2 + A_1^2C_1 + A_2^2B_2 - 3A_1B_2 + \text{cyclic}) \\
&\quad \left. - (A_1B_2^2C_2^2 - 2A_1^2B_2C_2 + A_1^3 + \text{cyclic}) + \text{reverse}\right] \\
&- N_1\bar{N}_1(A_1A_2 + \text{cyclic}) - (A_1A_2B_1B_2 + \text{cyclic}) \\
&+ 3(A_1B_1C_1 + A_2B_2C_2) + M_1M_2 + 6(M_1 + M_2) + 9\,.
\end{aligned}$$

Here "+cyclic" means adding the terms obtained by cyclic permutation of A, B, C, and "+reverse" the terms obtained by reversing the orientation, $A_1 \leftrightarrow A_2$, $N_1 \leftrightarrow \bar{N}_1$ and so on. We also managed to quantize the relation (4.64) but the result is not very enlightening so we omit it (in a basis where each monomial is ordered alphabetically, we need to add terms that vanish in the classical limit $q \to 1$).

SL(4). The 4-triangulation of $\mathcal{C}_{1,1}$ has 15 coordinates, 3 for each edge, a_i, b_i, c_i, and 3 for each face, $\{x_i, y_i\}$, with $i = 1, 2, 3$ (see figure 37). The A-cycle functions A_1 and A_3 have

21 terms each, while A_2 has 56 terms, some of which can be expressed as

$$A_1 \ni \prod_i \alpha_i^{-\kappa_{1i}^{-1}} \left(1 + \alpha_1 + \alpha_1\alpha_2 + \alpha_1\alpha_2\alpha_3\right),$$

$$A_2 \ni \prod_i \alpha_i^{-\kappa_{2i}^{-1}} \left(1 + \alpha_2 + \alpha_1\alpha_2 + \alpha_2\alpha_3 + \alpha_1\alpha_2\alpha_3 + \alpha_1\alpha_2^2\alpha_3\right), \qquad (4.65)$$

$$A_3 \ni \prod_i \alpha_i^{-\kappa_{3i}^{-1}} \left(1 + \alpha_3 + \alpha_2\alpha_3 + \alpha_1\alpha_2\alpha_3\right),$$

with $\alpha_1 = b_1 c_1 x_2 x_3$, $\alpha_2 = b_2 c_2 x_1 y_3$, and $\alpha_3 = b_3 c_3 y_1 y_2$. The tropical x-coordinates $\{b_1, b_2, b_3\}$ of these terms in A_1 and A_3 reproduce the weight systems of the fundamental and anti-fundamental representations (similarly to (4.57)), while those in A_2 form the weight system of the second antisymmetric representation:

$$A_2 \ni \prod_i \alpha_i^{-\kappa_{2i}^{-1}} \begin{cases} \alpha_1\alpha_2^2\alpha_3 & : & (0,1,0) \\ \alpha_1\alpha_2\alpha_3 & : & (1,-1,1) \\ \alpha_1\alpha_2, \alpha_2\alpha_3 & : & (-1,0,1),(1,0,-1) \\ \alpha_2 & : & (-1,1,-1) \\ 1 & : & (0,-1,0) \ . \end{cases} \qquad (4.66)$$

We define three networks homotopic to the dual graph, differing by the choice of the branch that is doubled (their expansions contain 223 monomials each):

$$N_a = \frac{1}{2}\epsilon_{mnpq}\mathbf{U}_{\mathbf{a}\,r}^m \mathbf{U}_{\mathbf{a}\,s}^n \mathbf{U}_{\mathbf{b}\,t}^p \mathbf{U}_{\mathbf{c}\,u}^q \epsilon^{rstu},$$

$$N_b = \frac{1}{2}\epsilon_{mnpq}\mathbf{U}_{\mathbf{a}\,r}^m \mathbf{U}_{\mathbf{b}\,s}^n \mathbf{U}_{\mathbf{b}\,t}^p \mathbf{U}_{\mathbf{c}\,u}^q \epsilon^{rstu},$$

$$N_c = \frac{1}{2}\epsilon_{mnpq}\mathbf{U}_{\mathbf{a}\,r}^m \mathbf{U}_{\mathbf{b}\,s}^n \mathbf{U}_{\mathbf{c}\,t}^p \mathbf{U}_{\mathbf{c}\,u}^q \epsilon^{rstu} \ . \qquad (4.67)$$

The quantum relations in (3.50) allow to uniquely determine how all the integral coefficients of 2, 4, and 8 appearing in the Fock-Goncharov expansions of the network functions get quantized:

$$2 \rightarrow [2] = q^{\frac{1}{2}} + q^{-\frac{1}{2}}, \qquad\qquad 4 \rightarrow [2]^2 = q + 2 + q^{-1},$$

$$8 \rightarrow [2]^3 = q^{\frac{3}{2}} + 3q^{\frac{1}{2}} + 3q^{-\frac{1}{2}} + q^{-\frac{3}{2}} \ . \qquad (4.68)$$

4.6 Four-punctured sphere

Another example is a sphere $\mathcal{C}_{0,4}$ with four full punctures, A, B, C, D. It can be triangulated into four triangles, as shown in figure 38.

SL(2). The loop around the punctures give the following trace functions:

$$A_1 = \sqrt{acf} + \frac{1}{\sqrt{acf}}, \qquad\qquad B_1 = \sqrt{bce} + \frac{1}{\sqrt{bce}},$$

$$C_1 = \sqrt{def} + \frac{1}{\sqrt{def}}, \qquad\qquad D_1 = \sqrt{abd} + \frac{1}{\sqrt{abd}} \ . \qquad (4.69)$$
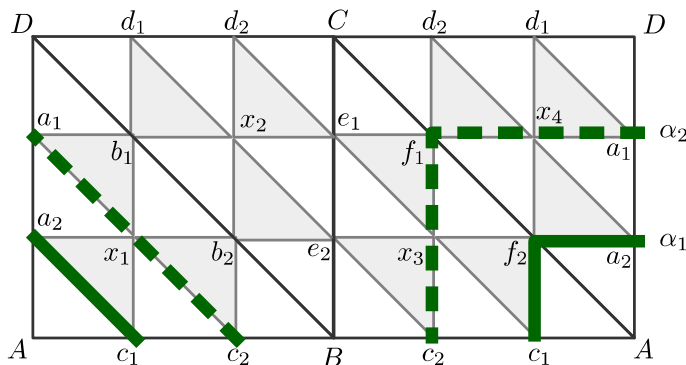
Figure 38. 3-triangulation of $\mathcal{C}_{0,4}$. The edges on the left and on the right are glued together. The paths corresponding to the monomials $\alpha_1 = a_2 c_1 f_2$ and $\alpha_2 = a_1 c_2 f_1 x_1 x_3 x_4$ are indicated.

We also consider loops surrounding pairs of punctures, $\mathbf{S = AB}$, $\mathbf{T = BC}$, and $\mathbf{U = BD}$ (see [22]):

$$
\begin{aligned}
S_1 &= \frac{1}{\sqrt{abef}}(1 + a + e + ae + abe + aef + abef)\,, \\
T_1 &= \frac{1}{\sqrt{bcdf}}(1 + b + f + bf + bcf + bdf + bcdf)\,, \\
U_1 &= \frac{1}{\sqrt{acde}}(1 + c + d + cd + acd + cde + acde)\,.
\end{aligned}
\tag{4.70}
$$

These polynomials do not contain any non-unit coefficients, so their quantization is straightforward. In particular, we can reproduce the quantum relation $\hat{\mathcal{P}}_1$ (3.57).

The loop function associated with the holonomy $\mathbf{U' = AC}$ does however contain coefficients of 2 and 4:

$$
\begin{aligned}
U_1' = \frac{1}{\sqrt{ab}\sqrt{c}\sqrt{d}\sqrt{ef}}\big(&ab^2cdef^2 + ab^2cef^2 + ab^2cef + ab^2def^2 + ab^2def + ab^2ef^2 \\
&+ 2ab^2ef + ab^2e + abcef^2 + abcef + abdef^2 + abdef + 2abef^2 \\
&+ 4abef + 2abe + abf + ab + aef^2 \\
&+ 2aef + ae + af + a + bef + be + ef + e + 1\big)\,.
\end{aligned}
\tag{4.71}
$$

The quantization of these non-unit coefficients can be determined by demanding that the quantum relation (3.53) holds. We find that we must make the following replacements:

$$
2 \to q^{\frac{1}{2}} + q^{-\frac{1}{2}}\,, \qquad\qquad 4 \to q + 2 + q^{-1}\,.
\tag{4.72}
$$

SL(3). A 3-triangulation of $\mathcal{C}_{0,4}$ is shown in figure 38. Each holonomy matrix gives two loop functions, for example

$$
A_i = \prod_j \alpha_j^{-\kappa_{ij}^{-1}}(1 + \alpha_i + \alpha_1\alpha_2)\,, \qquad\qquad \alpha_1 = a_2 c_1 f_2\,, \quad \alpha_2 = a_1 c_2 f_1 x_1 x_3 x_4\,.
\tag{4.73}
$$

The monomials α_i are products of coordinates along paths surrounding the puncture on the 3-triangulation (see figure 38). The operators coming from $\mathbf{S}, \mathbf{T}, \mathbf{U}$ have 48 terms each. The operators S_i contain the terms

$$S_i \ni \prod_j \sigma_j^{-\kappa_{ij}^{-1}}(1 + \sigma_i + \sigma_1\sigma_2), \qquad \sigma_1 = a_2 b_2 e_2 f_2 x_1 x_3, \quad \sigma_2 = a_1 b_1 e_1 f_1 x_2 x_4 . \quad (4.74)$$

We can reproduce the quantum relations (3.62) and (3.64), provided that we quantize the non-unit integer coefficients appearing in the network operators as follows:

$$
\begin{aligned}
&2 \to q^{\frac{1}{2}} + q^{-\frac{1}{2}}, && 3 \to q + 1 + q^{-1}, && 4 \to q + 2 + q^{-1}, \\
&5 \to q + 3 + q^{-1}, && 6 \to q + 4 + q^{-1} \quad \text{or} \quad q^{\frac{3}{2}} + 2q^{\frac{1}{2}} + 2q^{-\frac{1}{2}} + q^{-\frac{3}{2}}, && (4.75) \\
&7 \to q + 5 + q^{-1}, && 8 \to q^{\frac{3}{2}} + 3q^{\frac{1}{2}} + 3q^{-\frac{1}{2}} + q^{-\frac{3}{2}}, && 10 \to q^{\frac{3}{2}} + 4q^{\frac{1}{2}} + 4q^{-\frac{1}{2}} + q^{-\frac{3}{2}} .
\end{aligned}
$$

Note that among the 21 coefficients of 6 appearing in N_6, 13 are quantized to $q + 4 + q^{-1}$ and 8 to $q^{3/2} + 2q^{1/2} + 2q^{-1/2} + q^{-3/2}$.

5   Relation to conformal field theory

We will now explain how the quantized algebras $\mathcal{A}_{g,n}^N(q)$ of functions on $\mathcal{M}_{g,n}^N$ arise naturally in conformal field theory. We first review several aspects of sl(N) Toda field theory.[15] We then define Verlinde network operators, which are natural generalizations of Verlinde loop operators. We show that their algebra is equivalent to the quantum skein algebra described in section 2.8. Our arguments are based on the fact that the braid matrix is twist-equivalent to the R-matrix of the quantum group $\mathcal{U}_q(sl_N)$ defining the skein algebra.

5.1   Toda field theory and W_N-algebra

The Lagrangian for sl(N) Toda field theory has the form

$$\mathcal{L} = \frac{1}{8\pi}(\partial_a \phi, \partial^a \phi) + \mu \sum_{i=1}^{N-1} e^{b(e_i, \phi)}, \qquad (5.1)$$

where $\phi = (\phi_1, \ldots, \phi_{N-1})$ is a two-dimensional scalar field and $(\cdot, \cdot)$ denotes the scalar product in $\mathbb{R}^{N-1}$. The vectors e_i are the simple roots of the Lie algebra sl(N). Our conventions on the Lie algebra sl(N) are summarized in appendix B.1. The parameters are the dimensionless coupling constant b and the scale parameter μ.

The example of Liouville theory corresponding to the case $N = 2$ [69, 70] suggests that we should to be able to construct the Toda field $\phi(z, \bar{z})$ using chiral free fields $\varphi_j(z)$, $j = 1, \ldots, N - 1$ with mode expansion

$$\varphi_j(z) = q_j - i p_j \ln z + \sum_{n \neq 0} \frac{i}{n} a_n^j z^{-n}, \qquad (5.2)$$

---

[15]A somewhat different approach leading to important results is described in [68] and references therein.

where the modes satisfy

$$[a_n^i, a_m^j] = n\delta_{ij}\delta_{n+m}\,, \qquad a_n^{i\dagger} = a_{-n}^i\,, \qquad [p_j, q_k] = -\mathrm{i}\delta_{jk}\,. \tag{5.3}$$

In order to build the non-chiral fields $\phi_i(z, \bar{z})$ out of the chiral free fields $\varphi_j(z)$ one must of course supplement them with a similar collection of anti-chiral fields $\bar{\varphi}_j(\bar{z})$.

The chiral algebra of Toda conformal field theory is a W_N-algebra. It is an associative algebra generated by holomorphic currents $W^j(z)$ of spin $j = 2, \ldots, N$ (see [71] for a review). These can be constructed in the free-field representation via the Miura transformations

$$\prod_{i=0}^{N-1} :(Q\partial + (h_{N-i}, \partial\varphi)): = \sum_{k=0}^{N} W^{N-k}(z)(Q\partial)^k\,, \tag{5.4}$$

where : : denotes Wick ordering, $Q \equiv b + b^{-1}$, and $W^0(z) = 1$, $W^1(z) = 0$. The currents $W^k(z)$, $k = 2, \ldots, N$, have mode expansions

$$W^k(z) = \sum_{n=-\infty}^{\infty} W_n^k z^{-n-k}\,. \tag{5.5}$$

The modes $L_n \equiv W_n^2$ of the stress energy tensor $T(z) \equiv W^2(z) = (Q\rho, \partial^2\varphi) - \frac{1}{2}(\partial\varphi, \partial\varphi)$ generate a Virasoro subalgebra

$$[L_n, L_m] = (n - m)L_{n+m} + \frac{c}{12}(n^3 - n)\delta_{n+m}\,. \tag{5.6}$$

The modes of the currents $W^k(z)$ satisfy nonlinear commutation relations which contain a quadratic term. The W_N-algebra is therefore not a Lie algebra.

Irreducible representations $\mathcal{V}_\alpha$ of the W_N-algebra are labeled by an $(N-1)$-component vector α in the Cartan subalgebra of A_{N-1}. The representations $\mathcal{V}_\alpha$ are generated from highest-weight vectors v_α which are annihilated by the positive modes of $W^k(z)$, and eigenvectors of W_0^k with eigenvalues determined by α. The representation space of $\mathcal{V}_\alpha$ is generated by acting on v_α with the modes W_{-n}^k for $n > 0$, as usual.

It will be useful to distinguish three types of representations. A distinguished role will be played by the representations which have $\alpha = -b\omega_i - b^{-1}\omega_j$, where ω_i and ω_j are weights of finite-dimensional representations of sl(N). Such representations are called *fully degenerate* to reflect the fact that the vectors in these representations satisfy the maximal possible number of inequivalent relations of the form $\mathcal{P}_l(W_{-n}^k)v_\alpha = 0$ for certain polynomials $\mathcal{P}_l$. For generic α one has no such relations in the representations $\mathcal{V}_\alpha$, which are then called *fully non-degenerate*. There are various intermediate cases, called *semi-degenerate*, in which there do exist relations of the form $\mathcal{P}_l(W_{-n}^k)v_\alpha = 0$, but the number of inequivalent relations of this type is smaller than in fully degenerate representations. This happens for example if $\alpha = \kappa\omega_1$, with $\kappa \in \mathbb{C}$.

5.2 Conformal blocks

Conformal blocks can be introduced elegantly as certain invariants in the tensor product of representations of W_N-algebras associated with Riemann surfaces $\mathcal{C}_{g,n}$. The definition will

be spelled out explicitly only for the case $g = 0$, more general cases are discussed in [72]. We shall associate a highest-weight representation $\mathcal{V}_r \equiv \mathcal{V}_{\alpha_r}$ of the W_N-algebra with the rth puncture P_r of $\mathcal{C}_{g,n}$ for $r = 1, \ldots, n$. Let t_r be local coordinates around P_r such that $t_r(P_r) = 0$. Conformal blocks can be defined as linear functionals

$$\mathcal{F}_{0,n} : \otimes_{r=1}^{n} \mathcal{V}_r \to \mathbb{C} \tag{5.7}$$

satisfying an invariance condition of the form

$$\mathcal{F}_{0,n}\big(W^k[\eta_k] \cdot v\big) = 0, \qquad v \in \otimes_{r=1}^{n} \mathcal{V}_r, \tag{5.8}$$

where $W^k[\eta_k]$ is defined for meromorphic $(1-k)$-differentials $\eta_k(t)$ on $\mathcal{C}_{0,n}$ by expanding

$$\eta_k(t) = \sum_{n \in \mathbb{Z}} \eta_{k,n}^{(r)} \, t_r^{n-(1-k)}, \tag{5.9}$$

and setting

$$W^k[\eta_k] = \sum_{r=1}^{n} \sum_{n \in \mathbb{Z}} \eta_{k,n}^{(r)} \left[\text{id} \otimes \cdots \otimes \underset{r^{\text{th}}}{W_n^k} \otimes \cdots \otimes \text{id} \right]. \tag{5.10}$$

The conditions (5.8) generalize the conformal Ward identities [73]. The value of a conformal block on vectors $\otimes_{r=1}^{n} w_r$ can be interpreted as a generalized correlation function of n chiral vertex operators $V_{\alpha_r}(w_r|P_r)$. If $w_r = v_{\alpha_r}$ is the highest-weight state in the representation $\mathcal{V}_{\alpha_r}$, one calls $V_{\alpha_r}(P_r) \equiv V_{\alpha_r}(v_{\alpha_r}|P_r)$ a primary field, otherwise a descendant.

Space of conformal blocks: the invariance conditions (5.8) represent an infinite system of linear equations defining a subspace of the dual vector space to $\otimes_{i=1}^{n} \mathcal{V}_i$. The vector space defined in this way is called the space of conformal blocks $\text{CB}(\mathcal{V}_{[n]}, \mathcal{C}_{0,n})$ associated with the Riemann surface $\mathcal{C}_{0,n}$ with representations $\mathcal{V}_i$ at the punctures. This space is infinite-dimensional, in general. We now want to get a first idea about the "size" of this space.

In the case $N = 2$, the conformal block for $\mathcal{C}_{0,3}$ is known to be defined uniquely up to normalization by the invariance property (5.8). Using this same equation one may express all values $\mathcal{F}_{0,4}(w_4 \otimes w_3 \otimes w_2 \otimes w_1)$ associated with $\mathcal{C}_{0,4}$ in terms of

$$\mathcal{F}_{0,4}(v_{\alpha_4} \otimes v_{\alpha_3} \otimes L_{-1}^k v_{\alpha_2} \otimes v_{\alpha_1}) \equiv F_k, \qquad F_k \in \mathbb{C}, \qquad k \in \mathbb{Z}_{>0}. \tag{5.11}$$

One therefore finds that the space of conformal blocks associated with $\mathcal{C}_{0,4}$ is infinite-dimensional and isomorphic as a vector space to the space of formal power series in one variable. This space is far too big to be interesting for physical applications, as stressed in [25, 74]. Only if the growth of the complex numbers F_k ensures convergence of series like $F(z) = \sum_k \frac{1}{k!} F_k z^k$, can one integrate the canonical connection on spaces of conformal blocks defined by the energy-momentum tensor at least locally. Further conditions like existence of an analytic continuation of $F(z)$ to the Teichmüller space $\mathcal{T}_{0,4}$, and reasonable growth at the boundaries of $\mathcal{T}_{0,4}$ characterize the subspaces of $\text{CB}(\mathcal{V}_{[4]}, \mathcal{C}_{0,4})$ of potential physical interest.

In the case $N = 3$, one generically finds an infinite-dimensional space of conformal blocks already for the three-punctured sphere. Using the invariance property (5.8), it is possible to express the values of the conformal blocks associated with $\mathcal{C}_{0,3}$ in terms of [75]

$$\mathcal{F}_{0,3}(v_{\alpha_3} \otimes (W^3_{-1})^k v_{\alpha_2} \otimes v_{\alpha_1}) \in \mathbb{C} \ . \tag{5.12}$$

Therefore, similarly to (5.11), the space of conformal blocks associated with $\mathcal{C}_{0,3}$ is infinite-dimensional. It can also be identified with the space of formal Taylor series in one variable. In analogy to the case $N = 2$, $n = 4$ mentioned above we may expect that the physically relevant subspaces of $\mathrm{CB}(\mathcal{V}_{[3]}, \mathcal{C}_{0,3})$ may have a representation as spaces of analytic functions in one variable.

At general rank $(N - 1)$, the number of extra variables required to get similar representations for the spaces of conformal blocks associated with $\mathcal{C}_{0,3}$ is equal to half of the dimension[16] of the moduli space of flat connections $(N - 1)(N - 2)/2$. One way to understand this is by considering, as in [76, 77], the difference between the number of basic 3-point functions and the number of constraints from the Ward identities (5.8) and corresponding to generators of the W_N-algebra. There are $N(N - 1)/2$ descendant operators constructed by acting with the modes $(W^k_{-l})^n$ on a highest-weight state, for $l = 1, 2, \ldots, k - 1$ and $k = 2, 3, \ldots, N$, which lead to $3N(N - 1)/2$ basic 3-point functions after taking into account the three primaries. Subtracting $N^2 - 1$ constraints corresponding to generators W^k_l, for $l = -k + 1, -k + 2, \ldots, k - 1$ and $k = 2, \ldots, N$, gives precisely the number $(N - 1)(N - 2)/2$ of unconstrained positive integers parameterizing the conformal block associated with $\mathcal{C}_{0,3}$.

Gluing construction: given a possibly disconnected Riemann surface with two marked points P^i_0, $i = 1, 2$, surrounded by parameterized discs one can construct a new Riemann surface by pairwise identifying the points in suitable annular regions around the two marked points, respectively. Having conformal blocks associated with two surfaces $\mathcal{C}_i$ with $n_i + 1$ punctures $P^i_0, P^i_1, \ldots, P^i_{n_i}$ one can construct a conformal block associated with the surface $\mathcal{C}_{12}$ obtained by gluing annular neighborhoods of P^i_0, $i = 1, 2$ as follows

$$\begin{aligned} \mathcal{F}_{\mathcal{C}_{12}}(v_1 \otimes \cdots \otimes v_{n_1} \otimes w_1 \otimes \cdots \otimes w_{n_2}) = \\ = \sum_{\nu \in \mathcal{I}_\beta} \mathcal{F}_{\mathcal{C}_1}(v_1 \otimes \cdots \otimes v_{n_1} \otimes v_\nu) \, \mathcal{F}_{\mathcal{C}_2}(\mathrm{e}^{2\pi i \tau L_0} v^\vee_\nu \otimes w_1 \otimes \cdots \otimes w_{n_2}) \ . \end{aligned} \tag{5.13}$$

The vectors v_ν and $v^\vee_\nu$ are elements of bases $\{v_\nu; \nu \in \mathcal{I}_\beta\}$ and $\{v^\vee_\nu; \nu \in \mathcal{I}_\beta\}$ for the representation $\mathcal{V}_\beta$ which are dual with respect to the invariant bilinear form $(.,.)_\beta$ on $\mathcal{V}_\beta$. The parameter τ in (5.13) is the modulus of the annular region used in the gluing construction of $\mathcal{C}_{12}$. The rest of the notations in (5.13) are hopefully self-explanatory. The case where P^i_0, $i = 1, 2$, are on a connected surface can be treated in a similar way.

A general Riemann surface $\mathcal{C}_{g,n}$ can be obtained by gluing $2g - 2 + n$ pairs of pants $\mathcal{C}^v_{0,3}$, $v = 1, \ldots, 2g - 2 + n$. It is possible to construct conformal blocks for the resulting Riemann

---

[16]This number is equal to the dimension of the Coulomb branch of the T_N gauge theory. Together with the $3(N - 1)$ parameters of the momenta α, it gives the $(N + 4)(N - 1)/2$ parameters of the T_N theory [76].
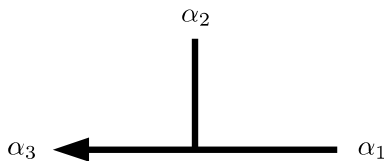
Figure 39. Vertex operator as an intertwiner of highest-weight representations $\mathcal{V}_{\alpha_i}$.

surface from the conformal blocks associated with the pairs of pants $\mathcal{C}^v_{0,3}$ by recursive use of the gluing construction outlined above. This yields families of conformal blocks parameterized by (i) the choices of representations $\mathcal{V}_\beta$ used in the gluing construction, and (ii) the choices of elements of the spaces $\mathrm{CB}(\mathcal{C}^v_{0,3})$, $v = 1, \ldots, 2g - 2 + n$.

Closely related to the gluing construction of conformal blocks are constructions of conformal blocks using chiral vertex operators. To any 3-point conformal block $\mathcal{F} \in \mathrm{CB}(\mathcal{C}_{0,3})$ we can associate a chiral vertex operator $V_{\mathcal{F}}\big(\begin{smallmatrix}\alpha_2\\\alpha_3\alpha_1\end{smallmatrix}\big)(v_2|z) : \mathcal{V}_{\alpha_1} \to \mathcal{V}_{\alpha_3}$ such that

$$\big(\, v_3\,,\, V_{\mathcal{F}}\big(\begin{smallmatrix}\alpha_2\\\alpha_3\alpha_1\end{smallmatrix}\big)(v_2|1)\, v_1 \,\big)_{\alpha_3} = \mathcal{F}(v_3 \otimes v_2 \otimes v_1) \tag{5.14}$$

holds for all $v_i \in \mathcal{V}_{\alpha_i}$, $i = 1, 2, 3$. The field $V_{\mathcal{F}}\big(\begin{smallmatrix}\alpha_2\\\alpha_3\alpha_1\end{smallmatrix}\big)(v_{\alpha_2}|z)$ associated with the highest-weight vector $v_{\alpha_2} \in \mathcal{V}_{\alpha_2}$ is called a primary field, and all other fields are called descendants. A graphical representation is given in figure 39. Conformal blocks associated with n-punctured spheres $\mathcal{C}_{0,n}$ can be constructed using compositions of chiral vertex operators in the form

$$\big(v_n\,,\, V_{\mathcal{F}_{n-1}}\big(\begin{smallmatrix}\alpha_{n-1}\\\alpha_n,\beta_{n-3}\end{smallmatrix}\big)(v_{n-1}|z_{n-1})\cdots V_{\mathcal{F}_2}\big(\begin{smallmatrix}\alpha_2\\\beta_1,\alpha_1\end{smallmatrix}\big)(v_2|z_2)\, v_1\big)_{\alpha_n}\,, \tag{5.15}$$

assuming that $z_n = \infty$ and $z_1 = 0$.

5.3 Free-field construction of chiral vertex operators

There is a useful way to construct chiral vertex operators in terms of the free fields $\varphi_j(z)$. Basic building blocks are the normal-ordered exponential fields

$$V_\alpha(\sigma) = \mathrm{e}^{(\alpha,\varphi(\sigma))}\,. \tag{5.16}$$

The normal-ordered exponential represents densely defined unbounded operators on $\mathcal{M} \equiv \mathcal{F} \otimes L^2(\mathbb{R}^{N-1})$ for $\mathrm{Im}(\sigma) > 0$, $\mathcal{F}$ being the Fock space generated by the oscillators a^i_n. Representing the momenta p_j as multiplication operators on $L^2(\mathbb{R}^{N-1})$ leads to a representation of the operators $\mathrm{e}^{(\alpha,q)}$ appearing in (5.16) as finite difference operators on functions $\psi(p)$. For our goals it will often suffice to adopt the closely related definition of the operators $\mathrm{e}^{(\alpha,q)}$ as formal shift operators mapping the highest-weight vector $v_\beta \in \mathcal{V}_\beta$ to $v_{\beta+\alpha} \in \mathcal{V}_{\alpha+\beta}$. The fields $V_\alpha(\sigma)$ can then be identified with the chiral primary fields $V\big(\begin{smallmatrix}\alpha\\\beta+\alpha,\beta\end{smallmatrix}\big)(z)$ for the algebra W_N via

$$V_\alpha(\sigma)v_\beta = z^{\Delta_\alpha}V\big(\begin{smallmatrix}\alpha\\\beta+\alpha,\beta\end{smallmatrix}\big)(z)v_\beta\,, \qquad\qquad v_\beta \in \mathcal{V}_\beta\,, \tag{5.17}$$

assuming that $z = \mathrm{e}^{i\sigma}$. For later use, let us note that the normal-ordered exponentials satisfy the exchange relations

$$V_\beta(\sigma')V_\alpha(\sigma) = \mathrm{e}^{-\pi\mathrm{i}(\alpha,\beta)\mathrm{sgn}(\sigma'-\sigma)}V_\alpha(\sigma)V_\beta(\sigma')\,. \tag{5.18}$$

An important role is furthermore played by the screening charges which are defined as

$$Q_i(\sigma) = \int_\sigma^{\sigma+2\pi} d\sigma' \, V_{be_i}(\sigma') \,. \tag{5.19}$$

Powers of the screening charges like $Q_i^n(\sigma) \equiv (Q_i(\sigma))^n$ make sense as unbounded self-adjoint operators on $\mathcal{M}$ if the power n is sufficiently small compared to b^{-2}. Higher powers can be defined by analytic continuation in b^2, and the result can be represented explicitly using suitable modifications of the contours of integration in (5.19). The key property of the screening charges $Q_i(\sigma)$ follows from the fact that the commutator of the fields $V_{be_i}(\sigma)$ with the generators of the W_N-algebra can be represented as a total derivative. This implies that the screening charges commute with the generators W_n^k.

More general primary fields can therefore be constructed by multiplying normal-ordered exponentials with monomials formed out of the screening charges. In the case $N = 2$ one may consider composite fields of the form $V_\alpha^s(\sigma) = V_\alpha(\sigma)Q^s(\sigma)$, $s \in \mathbb{Z}_{\geq 0}$. For $N = 3$ one could consider, more generally, fields of the form $V_\alpha Q_1^{s_1} Q_2^{s_2} Q_1^{s_3} Q_2^{s_4} \cdots$. One should note, however, that there exist many linear relations among these fields, as follows from the fact that the screening charges Q_i satisfy the Serre relations of the quantum group $\mathcal{U}_q(sl_N)$ [78],

$$Q_i^2 Q_j = (q + q^{-1})Q_i Q_j Q_i - Q_j Q_i^2 \,, \qquad \text{with} \quad |i - j| = 1 \,. \tag{5.20}$$

Using these relations it is elementary to show that in the case $N = 3$ arbitrary screened vertex operators can be expressed as linear combinations of

$$V_\alpha^{\mathbf{s}}(\sigma) = V_\alpha(\sigma)Q_1^{s_1-s}(\sigma)Q_2^{s_2-s}(\sigma)Q_{13}^s(\sigma) \,, \tag{5.21}$$

where $\mathbf{s} = (s_1, s_2, s)$, and

$$Q_{13}(\sigma) = Q_1 Q_2 - q Q_2 Q_1 = (1 - q^2)\int_\sigma^{\sigma+2\pi} d\sigma' \int_\sigma^{\sigma'} d\sigma'' V_{be_1}(\sigma')V_{be_2}(\sigma'') \,. \tag{5.22}$$

Indeed, the relations (5.20) can be rewritten as

$$Q_1 Q_{13} q^{-1} Q_{13} Q_1 \,, \qquad\qquad Q_2 Q_{13} = q Q_{13} Q_2 \,. \tag{5.23}$$

By making repeated use of these relations together with[17]

$$Q_1 Q_2^n = q^n Q_2^n Q_1 + [n]_q Q_2^{n-1} Q_{13} \,, \tag{5.24}$$

we can then express an arbitrary product of charges $Q_1^{s_1} Q_2^{s_2} Q_1^{s_3} Q_2^{s_4} \cdots$ as linear combination of monomials of the form $Q_1^{s_1-s} Q_2^{s_2-s} Q_{13}^s$, reducing any screened vertex operator to (5.21).

By using the screened vertex operators $V_\alpha^{\mathbf{s}}$ one can represent more general chiral vertex operators via

$$V_\alpha^{\mathbf{s}}(\sigma)v_\beta = z^{\Delta_\alpha} V_s\begin{pmatrix} \alpha \\ \beta'\beta \end{pmatrix}(z)v_\beta \,, \qquad \text{with} \quad \beta' = \beta + \alpha + b(s_1 e_1 + s_2 e_2) \,. \tag{5.25}$$

---

[17]Here we are using $[n]_q \equiv \frac{q^n - q^{-n}}{q - q^{-1}} = q^{n-1} + q^{n-3} + \cdots + q^{-n+1}$.

It is clear that we cannot represent the most general chiral vertex operators in terms of screened vertex operators using only integer values of s_1, s_2. It is therefore useful to observe that $Q_1(\sigma)$, $Q_2(\sigma)$ and $Q_{13}(\sigma)$ are proportional to positive self-adjoint operators, allowing us to consider also non-integer values for the powers s_1, s_2, s in (5.21). The arguments used in [69, 70] for the case $N = 2$ can easily be adapted to establish that $Q_1(\sigma)$ and $Q_2(\sigma)$ are positive self-adjoint. The operator $Q_{13}(\sigma)$ defined in (5.22) can be shown to be proportional to a positive operator by expressing it as an ordered double integral and normal-ordering the product $V_{be_1}(\sigma')V_{be_2}(\sigma'')$. Considering non-integer s_1, s_2 allows us to get arbitrary values for the weights (β', α, β) appearing in (5.25).

It is furthermore important to note that the difference between β' and β is independent of the parameter s in (5.21). By varying s one can therefore define via (5.25) an infinite family of chiral vertex operators $V_s\begin{pmatrix} \alpha \\ \beta'\beta \end{pmatrix}(z)$ intertwining between the same two representations β' and β. The correspondence (5.14) between chiral vertex operators and conformal blocks on the three-punctured sphere associates with each chiral vertex operator $V_s\begin{pmatrix} \alpha \\ \beta'\beta \end{pmatrix}(z)$ a conformal block $\mathcal{F}_s \in \mathrm{CB}(C_{0,3})$. It seems plausible that the conformal blocks $\mathcal{F}_s$ generate a basis for the physically relevant subspace of conformal blocks on $\mathcal{C}_{0,3}$.

To generalize these observations to $N > 3$ let us note that it directly follows from (5.20) that the space of screened vertex operators forms a module for the nilpotent sub-algebra of $\mathcal{U}_q(sl_N)$, with action of the generators E_i represented by right multiplication with Q_i. One can define screening charges $Q_{ij}(\sigma)$ associated with the generators E_{ij}, $j > i$ of $\mathcal{U}_q(sl_N)$ recursively via $Q_{i,i+1}(\sigma) \equiv Q_i(\sigma)$ together with

$$Q_{ij}(\sigma) = Q_{ik}(\sigma)Q_{kj}(\sigma) - qQ_{kj}(\sigma)Q_{ik}(\sigma), \quad 1 \leq i < k < j \leq N. \tag{5.26}$$

More general screened vertex operators can be constructed as

$$\begin{aligned} V_\alpha^{\mathbf{s}}(\sigma) = V_\alpha(\sigma)\big[Q_{12}^{s_{12}}(\sigma)Q_{13}^{s_{13}}(\sigma)\cdots Q_{1N}^{s_{1N}}(\sigma)\big] \times \cdots \\ \times \big[Q_{23}^{s_{23}}(\sigma)\cdots Q_{2N}^{s_{2N}}(\sigma)\big] \times \cdots \times [Q_{N-1,N}^{s_{N-1,N}}(\sigma)], \end{aligned} \tag{5.27}$$

where $\mathbf{s} = \{s_{ij}; i < j\}$. This can be extended to a module for the Borel-subalgebra of $\mathcal{U}_q(sl_N)$ with generators H_i and E_i by identifying H_i with the adjoint action of $-\mathrm{i}p^i/b$. For general α one can identify the resulting module with the Verma module of $\mathcal{U}_q(sl_N)$ with weight $\omega_\alpha = -\alpha/b$. The observations above imply a relation between screened vertex operators and representations of $\mathcal{U}_q(sl_N)$ on the level of vector spaces. This relation will be strengthened considerably below.

As before one can use the screened vertex operators $V_\alpha^{\mathbf{s}}(\sigma)$ to define chiral vertex operators via the obvious generalization of (5.25) to $N > 3$. Fixing the difference $\beta' - \beta$ defines a subspace in the space of parameters $\mathbf{s}$ of dimension $\frac{1}{2}(N - 1)(N - 2)$. This dimension coincides with half of the dimension of the moduli space of flat connections on $\mathcal{C}_{0,3}$, which was previously found to be equal to the dimension of the space of parameters labeling inequivalent elements in $\mathrm{CB}(\mathcal{C}_{0,3})$. This observation raises our hopes that the screened vertex operators $V_\alpha^{\mathbf{s}}(\sigma)$ can indeed be used to construct bases for $\mathrm{CB}(\mathcal{C}_{0,3})$.

Degenerate fields: for special values of α and $\mathbf{s}$ one may observe that the screened vertex operators satisfy certain differential equations relating derivatives of $V_\alpha^{\mathbf{s}}(\sigma)$ to the W_N-currents. These fields are called degenerate fields. The basic example for this phenomenon occurs in the case $\alpha = -b\omega_1$ when $[p^i, V_\alpha^{\mathbf{s}}(\sigma)] = \mathrm{i}bh_i V_\alpha^{\mathbf{s}}(\sigma)$, where h_i, $i = 1, \ldots, N$ are the weights of the fundamental representation. We will use the simplified notation $D^i(\sigma)$ for the screened vertex operators $V_\alpha^{\mathbf{s}}(\sigma)$ satisfying these conditions. They satisfy an Nth-order operator differential equation [79], which is essentially equivalent to the equations expressing the decoupling of null-vectors in the Verma module $\mathcal{V}_{-b\omega_1}$ within the framework of [73], see e.g. [68, 75]. State-operator correspondence in CFT relates the allowed values of β' to the so-called fusion rules, the rules determining the set of labels of the primary fields that can appear in the operator product expansion of fields $V_{-b\omega_1}(z_1)V_\beta(z_2)$.

The operator product expansion of degenerate fields generates further degenerate fields. It follows from the fusion rules that the screened vertex operators $V_{-b\lambda}^{\mathbf{s}}(\sigma)$ that can be generated by recursively by performing operator product expansions of the operators $D^i(\sigma)$ are labeled by the weights λ of finite-dimensional representations[18] M_λ of $\mathcal{U}_q(sl_N)$. The allowed powers of screening charges collected in $\mathbf{s} = \{s_{ij}, i < j\}$ are constrained by the fusion rules determining the fields $V_{\beta'}(z_2)$ appearing in the operator product expansion $V_{-b\lambda}(z_1)V_\beta(z_2)$. The s_{ij} have to be integers constrained by the condition that $\frac{1}{b}(\beta - \beta')$ coincides with one of the weights of the vectors in $\mathcal{R}_\lambda$.

5.4 Braiding and fusion of degenerate fields

It was shown in [79] that the degenerate fields $D^i(\sigma)$ satisfy exchange relations of the form

$$D^i(\sigma_2)D^j(\sigma_1) = \sum_{k,l=1}^N B^{\mathrm{D}}(p)_{kl}^{ij} D^k(\sigma_1)D^l(\sigma_2) \,. \tag{5.28}$$

Note that the matrix $B^{\mathrm{D}}(p)$ appearing in (5.28) is operator-valued in general, being dependent on the zero-mode operator $p = (p^1, \ldots, p^{N-1})$. The matrix $B^{\mathrm{D}}(p)$ satisfies a modified form of the Yang-Baxter equation called dynamical Yang-Baxter equation, and $B^{\mathrm{D}}(p)$ therefore represents an example of what is called a dynamical R-matrix. It was furthermore shown in [80] that there exist linear combinations $\tilde{D}^i(\sigma) = \sum_{j=1}^N c(p)_j^i D^j(\sigma)$ satisfying exchange relations of the form (5.28) with a matrix $\tilde{B}^{\mathrm{D}}(p)$ that is p-independent, and will therefore be denoted by $\tilde{B}$. The matrix $\tilde{B}$ is different from the standard braid-matrix R representing the braiding of two fundamental representations of the quantum group $\mathcal{U} \equiv \mathcal{U}_q(sl_N)$ (see appendix B.2 for the relevant background on $\mathcal{U}_q(sl_N)$). R can be obtained from the universal R-matrix $\mathcal{R}$ of $\mathcal{U}_q(sl_N)$ as
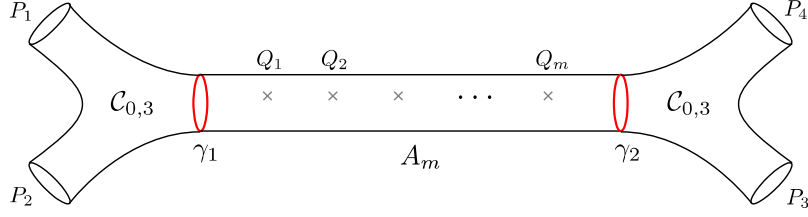
$$R = P(\pi_\Box \otimes \pi_\Box)(\mathcal{R}) \,, \tag{5.29}$$

where P is the operator permuting the two tensor factors of $\mathbb{C}^N \otimes \mathbb{C}^N$. The relation between $\tilde{B}$ and R was subsequently clarified in [81], where is was shown that $\tilde{B}$ can be obtained in a similar way as (5.29) from a universal R-matrix $\tilde{\mathcal{R}}$ that is related to $\mathcal{R}$ by a Drinfeld

---

[18] We identify $M_i \equiv M_{\omega_i}$ in our notations, with ω_i being the weight of the representation $\wedge^i \Box$.

Figure 40. Part of a decomposition of $\hat{\mathcal{C}}_{g,n+d}$ with n punctures P_r and d marked points Q_k into three-holed spheres $\mathcal{C}_{0,3}$ and annuli A_m with m marked points.

twist $\mathcal{J} \in \mathcal{U} \otimes \mathcal{U}$ such that $\tilde{\mathcal{R}} = \mathcal{J}_{21}^{-1} \mathcal{R} \mathcal{J}$. The twist $\mathcal{J}$ that relates $\mathcal{R}$ and $\tilde{\mathcal{R}}$ satisfies the cocycle condition

$$(\Delta \otimes \mathrm{id})(\mathcal{J}) \cdot \mathcal{J}_{12} = (\mathrm{id} \otimes \Delta)(\mathcal{J}) \cdot \mathcal{J}_{23} \,. \tag{5.30}$$

As explained in appendix B.3, one can extend the action of $\mathcal{J}$ to m-fold tensor products, allowing us to define operators

$$J_f^{(m)} := (\pi_f \otimes \cdots \otimes \pi_f)(\mathcal{J}^{(m)}) \,. \tag{5.31}$$

The cocycle condition (5.30) implies that $J_f^{(m)}$ is independent of the order in which tensor products are taken.

Let us consider the space VO_m spanned by the compositions of vertex operators $D^{i_m \ldots i_1}(\sigma_m, \ldots, \sigma_1) := \tilde{D}^{i_m}(\sigma_m)\tilde{D}^{i_{m-1}}(\sigma_{m-1}) \cdots \tilde{D}^{i_1}(\sigma_1)$ with $i_k \in \{1, \ldots, N\}$ for $k = 1, \ldots, m$. The space VO_m carries a representation of the braid group $\mathcal{B}_m$ with m strands represented in terms of the braid matrices $\tilde{B}$. It follows from the fact that $\mathcal{R}$ and $\tilde{\mathcal{R}}$ are related by the Drinfeld twist $\mathcal{J}$ that the linear operator $J_f^{(m)}$ maps the braid group representation on VO_m to the standard braid group representation on the m-fold tensor product of fundamental representations of $\mathcal{U}_q(sl_N)$.

By repeated use of the operator product expansion one can construct other degenerate vertex operators $D_\lambda^{\mathbf{s}}(\sigma)$ starting from the products $D^{i_m \ldots i_1}(\sigma_m, \ldots, \sigma_1)$. The vertex operators $D_\lambda^{\mathbf{s}}(\sigma)$ that can be obtained in this way have weights λ associated with the finite-dimensional irreducible representations of $\mathcal{U}_q(sl_N)$. It easily follows from the results described above that the braid group representation generated by products of the vertex operators $D_\lambda^{\mathbf{s}}(\sigma)$ is isomorphic to the braid group representation on the tensor product of the corresponding representations of $\mathcal{U}_q(sl_N)$. This implies, in particular, that the vector space spanned by the vertex operators $D_\lambda^{\mathbf{s}}(\sigma)$ with fixed λ is isomorphic to the space on which the finite-dimensional irreducible representation M_λ with highest weight λ is realized.

5.5 Conformal blocks with degenerate fields

Let us consider conformal blocks associated with a Riemann surface $\hat{\mathcal{C}}_{g,n+d}$ with $n + d$ punctures (see figure 40). We assume that fully degenerate representations $\mathcal{D}_k$ are associated with the punctures Q_k, $k = 1, \ldots, d$. The remaining n punctures P_r, $r = 1, \ldots, n$ are assumed not to be fully degenerate. We may alternatively consider Q_k, $k = 1, \ldots, d$, as a collection of distinguished points on the Riemann surface $\mathcal{C}_{g,n}$ which has punctures only at

P_r, $r = 1, \ldots, n$. We may start from a pants decomposition $\sigma = (\gamma, \Gamma)$ of the surface $\mathcal{C}_{g,n}$. Cutting $\mathcal{C}_{g,n}$ along the simple closed curves contained in $\gamma = \{\gamma_1, \ldots, \gamma_{3g-3+n}\}$ decomposes the surface into spheres $\mathcal{C}_{0,3}^v$ with three boundary components which can be holes or punctures. The trivalent graph Γ on $\mathcal{C}_{g,n}$ has exactly one vertex within each $\mathcal{C}_{0,3}^v$; it allows us to distinguish pants decompositions related by Dehn twists. The pants decomposition specified by $\sigma = (\gamma, \Gamma)$ can always be refined to a decomposition into a collection of annuli A^e and three-holed spheres T^v such that each of the fully degenerate punctures is contained in one of the annuli A^e. This can be done by cutting along additional simple closed curves on $\mathcal{C}_{g,n}$ which do not intersect any of the curves in γ, do not mutually intersect, and do not contain any Q_k, $k = 1, \ldots, d$. We furthermore need to cut out discs around the punctures P_r, $r = 1, \ldots, n$. A chosen orientation of the edges of Γ allows us to distinguish an incoming and an outgoing boundary component of each annulus A^e.

The gluing construction of conformal blocks allows us to construct families of conformal blocks out of two types of building blocks: the conformal blocks associated with the three-holed spheres, and the conformal blocks associated with the annuli A^e. Of particular interest for us will be the latter. Let $\mathrm{CB}(A_m)$ be the space of conformal blocks associated with an annulus with m marked points associated with fully degenerate representations, and incoming and outgoing boundary components associated with non-degenerate representations. We shall fix the representation associated with the incoming boundary component to be $\mathcal{V}_\beta$, and we assign fully degenerate representations $\mathcal{V}_{-b\lambda_1}, \ldots, \mathcal{V}_{-b\lambda_m}$ to the m marked points, respectively. The set of representations associated with the outgoing boundary component is then restricted by the fusion rules to a finite set. We will assign to the outgoing boundary component the direct sum of all representations allowed by the fusion rules.

It follows from the fusion rules that the resulting space of conformal blocks $\mathrm{CB}(A_m)$ is finite-dimensional. A basis for $\mathrm{CB}(A_m)$ can be constructed explicitly using the degenerate vertex operators defined above,

$$\mathcal{F}_{A_m}(v_{m+1} \otimes v_m \otimes \cdots \otimes v_1 \otimes v_0) = \left(v_{m+1}, \, D_{\lambda_m}^{\mathbf{s}_m}(v_m | \sigma_m) \, \cdots \, D_{\lambda_1}^{\mathbf{s}_1}(v_1 | \sigma_1) \, v_0 \right)_{\beta'}, \quad (5.32)$$

where $v_0 \in \mathcal{V}_\beta$, $v_{m+1} \in \mathcal{V}_{\beta'}$, and $D_{\lambda_k}^{\mathbf{s}_k}(v_k | \sigma_k)$ are the descendants of the degenerate vertex operators $D_{\lambda_k}^{\mathbf{s}_k}(\sigma_k)$ associated with vectors $v_k \in \mathcal{V}_{-b\lambda_k}$ for $k = 1, \ldots, m$.

It follows from the results discussed in the previous subsection that the space of conformal blocks $\mathrm{CB}(A_m)$ is naturally isomorphic (as a module for $\mathcal{B}_m$) to the tensor product of the m finite-dimensional representations $M_{\lambda_m}, \ldots, M_{\lambda_1}$ of the quantum group $\mathcal{U}_q(sl_N)$,

$$\mathrm{CB}(A_m) \simeq M_{\lambda_m} \otimes \cdots \otimes M_{\lambda_1}. \quad (5.33)$$

This isomorphism is realized by a linear operators $J_{\lambda_m \ldots \lambda_1}^{(m)}(p)$ that is constructed by combining the change of basis removing the p-dependence with the Drinfeld twist $\mathcal{J}$.

5.6 Verlinde network operators

Verlinde network operators are generalizations of Verlinde loop operators [41, 42] to Toda CFT of higher rank, and were previously studied in [82]. In order to define the Verlinde
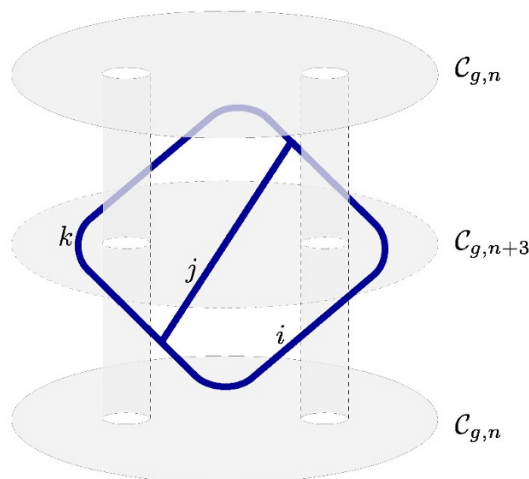
Figure 41. Verlinde network operator.

network operators one needs to consider conformal blocks associated with a Riemann surface $\mathcal{C}_{g,n+d}$, as above. Our definition will be based on certain relations between the spaces of conformal blocks with varying number d of fully degenerate insertions. In order to describe these relations we will employ the set-up introduced in the previous subsection, in particular the decomposition of $\mathcal{C}_{g,n+d}$ into three-holed spheres T_v and annuli A^e, and the isomorphism (5.33) which can be applied locally for each annulus A^e.

This needs to be combined with one further ingredient. We will conjecture that there exist exchange relations between fully degenerate chiral vertex operators and generic chiral vertex operators,

$$D^i(z_1)V_\alpha^{\mathbf{s}}(z_2) = \sum_j \sum_{\mathbf{s}'} B_{j,\mathbf{s}'}^{i,\mathbf{s}}(\alpha)V_\alpha^{\mathbf{s}'}(z_2)D^j(z_1)\,, \qquad (5.34)$$

where $|z_1| = |z_2|$, and furthermore operator product expansions of the form

$$D^i(w)\,V_\alpha^{\mathbf{s}}(z) = \sum_j \sum_{\mathbf{s}'} F_{j,\mathbf{s}'}^{i,\mathbf{s}}(\alpha)V_{\alpha-bh_j}^{\mathbf{s}'}\big(D^j(w-z)v_\alpha|z\big)\,, \qquad (5.35)$$

where h_s are the weights of the fundamental representation with highest weight ω_1. These relations would imply that there exist linear relations between the spaces of conformal blocks associated with surfaces $\mathcal{C}_{g,n+d}$ and $\mathcal{C}'_{g,n+d}$ related by moving a degenerate field from one annulus A^e to another one $A^{e'}$. So far we do not have a proof of these relations. We expect that such a direct proof should be possible using the free-field representation of the vertex operators. One may furthermore note that the relations (5.34), (5.35) follow from the results of [82] if the vertex operator $V_\alpha^{\mathbf{s}}$ is associated with a semi-degenerate representation $\mathcal{V}_\alpha$. Further generalizations of these braid relations were found in [20]. The general statement should follow from this special case if the operator product expansion of sufficiently many semi-degenerate vertex operators generates vertex operators associated with fully non-degenerate representations, as is generally expected.

By combining these ingredients we are now ready to define generalizations of the Verlinde loop operators as follows (see figure 41). The isomorphisms (5.33) allow us to associate

maps between spaces of conformal blocks with all the maps between tensor products of representations used in the Reshetikhin-Turaev construction. These maps can be composed with the moves (5.34), (5.35) describing the motion of a fully degenerate puncture from one annulus to another. One may in particular consider compositions of these two types of fusion and braiding operations for degenerate fields starting and ending with the space of conformal blocks associated with a surface $\mathcal{C}_{g,n}$ with no fully degenerate insertions. It is clear that such compositions can be labeled by networks of the same type as considered in the previous sections. The construction outlined above associates with each network an operator acting on the space $\text{CB}(\mathcal{C}_{g,n})$ of conformal blocks for a surface $\mathcal{C}_{g,n}$ with n non-degenerate punctures.

5.7 Relation to skein algebra

The Verlinde network operators generate an algebra $\mathcal{A}_V$ realized on the spaces $\text{CB}(C_{g,n})$. We are going to argue that this algebra is the same as the algebra of quantized functions on $\mathcal{M}_{g,n}^N$. Recall that the product of two networks is represented in terms of a network with crossings. It may be assumed that all crossings are located in annuli A^e. In order to describe the resulting algebraic relations we may therefore use the isomorphism (5.33) allowing us to describe the operations representing the crossing in terms of the intertwining maps used in the Reshetikhin-Turaev construction. All skein relations valid in the framework of the Reshetikhin-Turaev construction thereby carry over to the Verlinde network operators. In order to verify this claim it suffices to check that the basic skein relations are preserved by the twist $J_{\lambda_n \ldots \lambda_1}$ representing the isomorphism (5.33). Recall that the basic skein relations (2.41) take the form

$$
R_{ij} = \quad \vcenter{\hbox{\includegraphics{crossing}}} \quad = q^{\frac{ij}{2N}} \sum_{n=0}^{m} q^{-\frac{n}{2}} \quad \vcenter{\hbox{\includegraphics{square}}}
$$

(5.36)

with $m = \min\{i, j, N - i, N - j\}$. In the framework of Reshetikhin-Turaev one associates to both sides intertwining maps between the representations $M_j \otimes M_i$ and $M_i \otimes M_j$ of the Hopf algebra $\mathcal{U}_q(sl_N)$. The intertwining map on the left of (5.36) is represented by the operator R_{ij} defined in (2.43), the operators on the right of (5.36), in the following denoted as $C(n)_{ji}^{ij}$, are compositions of Clebsch-Gordan maps, as introduced in section 2.8. If the quasitriangular Hopf-algebra $\mathcal{U} = \mathcal{U}_q(sl_N)$ is replaced by a quasi-triangular Hopf-algebra $\tilde{\mathcal{U}}$ related to $\mathcal{U}$ by a Drinfeld twist, one can construct the intertwining maps $\tilde{C}(n)_{ji}^{ij}$ between representations of $\tilde{\mathcal{U}}$ from the intertwining maps $C(n)_{ji}^{ij}$ of $\mathcal{U}$ in a natural way, as is explained in appendix B. The construction is such that we have $\tilde{C}(n)_{ji}^{ij} = J_{ij}^{-1} C(n)_{ji}^{ij} J_{ji}$, provided that J_{ij} is the similarity transformation relating R_{ij} and $\tilde{B}_{ij}$ as $\tilde{B}_{ij} = J_{ij}^{-1} R_{ij} J_{ji}$. It follows immediately that $\tilde{C}(n)_{ji}^{ij}$ and $\tilde{B}_{ij}$ will satisfy a relation of the same form as (5.36).

One may in particular consider Verlinde network operators associated with networks that are confined to a disc $\mathbb{D}$ embedded in an annulus A^e. It is easy to see that such network

operators will act on $\mathrm{CB}(C_{g,n})$ as multiplication by a number. This number represents one of the link invariants obtained by using the Reshetikhin-Turaev construction. This construction is thereby recognized as a special case of the definition of the Verlinde network operators given above.

6 Spectrum

In the previous section we have found strong hints that the construction of loop and network operators using Fock-Goncharov coordinates defines an algebra isomorphic to the algebra generated by the Verlinde network operators in the Toda CFT. We had furthermore observed in subsection 2.6 that the resulting algebra shares some features with the algebra of operators in a quantum integrable model, containing large commutative sub-algebras. Simultaneously diagonalizing these sub-algebras defines natural representations. The next natural step in our program is to compare the representations resulting from the quantization of the Fock-Goncharov coordinates, and from Toda conformal field theory. As an outlook, we collect here a few observations and conjectures concerning this problem.

6.1 Spectrum in Toda field theory

In order to determine the set of representations of the algebra W_N appearing in the spectrum of Toda field theory one may follow the example of Liouville theory. For studying the spectral problem of Toda field theories it is natural to consider canonical quantization on a spacetime having the geometry of a two-dimensional cylinder with time coordinate t and a spatial coordinate $\sigma \sim \sigma + 2\pi$. At time $t = 0$ one can decompose the fields $\phi(\sigma) \equiv \phi(0, \sigma)$ as $\phi(\sigma) = \phi_0 + \chi(\sigma)$, where the zero mode is defined as the average $\phi_0 = \frac{1}{2\pi} \int_0^{2\pi} \mathrm{d}\sigma \, \phi(\sigma)$. One may then observe that the interaction term $\int_0^{2\pi} \mathrm{d}\sigma \, \mathrm{e}^{b(e_i, \phi(\sigma))}$ in the Hamiltonian is equal to $2\pi \, \mathrm{e}^{b(e_i, \phi_0)}$ up to terms of order b^2. This means that zero modes and oscillators completely decouple in the limit $b^2 \to 0$. Canonical quantization of the oscillators yields a Hamiltonian of the form

$$H = H_0 + \mathsf{N} + \bar{\mathsf{N}} + \mathcal{O}(b^2), \qquad \text{with} \quad H_0 = \frac{1}{2}(p, p) + 2\pi\mu \mathrm{e}^{b(e_i, \phi_0)}, \qquad (6.1)$$

which is defined on the Hilbert space $\mathcal{H} = L^2(\mathbb{R}^{N-1}) \otimes \mathcal{F}$ by choosing the Schrödinger representation on $L^2(\mathbb{R}^{N-1})$ for the operators p_i and ϕ_0^j satisfying $[\phi_0^i, p_j] = \mathrm{i}\delta_j^i$, and by realizing two sets of oscillators a_n^i and $\bar{a}_n^i$, $i = 1, \ldots, N-1$, $n \in \mathbb{Z} \setminus \{0\}$, on the Fock space $\mathcal{F}$ in the usual way. The operator N satisfies $[\mathsf{N}, a_n^i] = -na_n^i$, and commutes with $\bar{a}_n^i$, and similarly for $\bar{\mathsf{N}}$.

The problem of determining the spectrum of the Hamiltonian H therefore reduces in the limit $b^2 \to 0$ to the problem of finding the spectrum of the quantum-mechanical system with Hamiltonian H_0. This system is a well-known quantum integrable model called the open Toda chain, and its spectrum is known exactly [83–85]. The spectrum is purely continuous, with generalized eigenstates in one-to-one correspondence with the orbits of vectors $\mathfrak{p} \in \mathbb{R}^{N-1}$ under the Weyl group of $\mathrm{SU}(N)$. This suggests that the spectrum of Toda field theory will be purely continuous.

Observing furthermore that the interaction terms $\int_0^{2\pi} d\sigma \, e^{b(e_i, \phi(\sigma))}$ are closely related to the screening charges of the free-field realization of the algebra W_N, it becomes straightforward to generalize the arguments used in [86] to determine the spectrum of Liouville theory to Toda field theories with $N > 2$, leading to the conclusion that the spectrum has the form

$$\mathcal{H} = \int_{\mathbb{S}} d\beta \, \mathcal{V}_\beta \otimes \bar{\mathcal{V}}_\beta \,, \tag{6.2}$$

where $\mathcal{V}_\beta$ and $\bar{\mathcal{V}}_\beta$ are representations of the algebra W_N generated by holomorphic currents $W^k(z)$ and their anti-holomorphic counterparts $\bar{W}^k(\bar{z})$, respectively, $\mathbb{S}$ denotes the set of Weyl-orbits of vectors of the form $\beta = Q + i\mathfrak{p}$, with $\mathfrak{p} \in \mathbb{R}^{N-1}$ and $Q = \rho(b + b^{-1})$. It follows from this form of the spectrum that correlation functions such as

$$\langle \, \alpha_\infty \, | \, V_{\alpha_2}(z_2, \bar{z}_2) \, V_{\alpha_1}(z_1, \bar{z}_1) \, | \, \alpha_0 \, \rangle \,, \tag{6.3}$$

can be represented in the form

$$\begin{aligned}
\langle \, \alpha_\infty \, | & \, V_{\alpha_2}(z_2, \bar{z}_2) \, V_{\alpha_1}(z_1, \bar{z}_1) \, | \, \alpha_0 \, \rangle \\
&= \int_{\mathbb{S}} d\beta \int_{\mathbb{V}} ds_1 ds_2 d\bar{s}_1 d\bar{s}_2 \; C_{s_2 \bar{s}_2}(\alpha_\infty, \alpha_2, \beta) C_{s_1 \bar{s}_1}(Q - \beta, \alpha_1, \alpha_0) \\
&\quad \times \mathcal{F}\big[{}^{\alpha_2}_{\alpha_\infty} {}^{s_2}|\beta|{}^{s_1}_{\alpha_0} \big](z_2, z_1) \bar{\mathcal{F}}\big[{}^{\alpha_2}_{\alpha_\infty} {}^{\bar{s}_2}|\beta|{}^{\bar{s}_1}_{\alpha_0} \big](\bar{z}_2, \bar{z}_1) \,,
\end{aligned} \tag{6.4}$$

where

$$\mathcal{F}\big[{}^{\alpha_2}_{\alpha_\infty} {}^{s_2}|\beta|{}^{s_1}_{\alpha_0} \big](z_2, z_1) = \big(v_{\alpha_\infty}, \, V_{s_2}\big({}^{\alpha_2}_{\alpha_\infty \beta}\big)(z_2) \, V_{s_1}\big({}^{\alpha_1}_{\beta \alpha_0}\big)(z_1) \, v_{\alpha_0} \big)_{\alpha_\infty} \,. \tag{6.5}$$

In order to arrive at the expansion (6.4) we have inserted a complete set of intermediate states from $\mathcal{H}$ between the two vertex operators $V_{\alpha_2}(z_2, \bar{z}_2)$ and $V_{\alpha_1}(z_1, \bar{z}_1)$, and we have furthermore assumed that the resulting matrix elements can be expanded as

$$\begin{aligned}
\langle \, Q - \alpha_3 \, | \, V_{\alpha_2}(z, \bar{z}) \, | \, \alpha_1 \, \rangle &= \\
&= \int_{\mathbb{V}} ds \, d\bar{s} \; C_{s\bar{s}}(\alpha_3, \alpha_2, \alpha_1) \, \big(v_{\alpha_3}, V_s\big({}^{\alpha_2}_{\alpha_3 \alpha_1}\big)(z) \, v_{\alpha_1} \big)_{\alpha_3} \big(v_{\alpha_3}, V_{\bar{s}}\big({}^{\alpha_2}_{\alpha_3 \alpha_1}\big)(\bar{z}) \, v_{\alpha_1} \big)_{\alpha_3} \,.
\end{aligned} \tag{6.6}$$

The assumption (6.6) will hold for any set of chiral vertex operators $V_s\big({}^{\alpha_2}_{\alpha_3 \alpha_1}\big)(z)$ labeled by an index s taking values in the set $\mathbb{V}$ with measure ds which may be continuous or discrete allowing us to define a basis for the space $\text{CB}(\mathcal{C}_{0,3})$ via (5.14). If the index set $\mathbb{V}$ or measure ds depends nontrivially on the choice of α_i, one will have to modify (6.4) in an obvious way.

It seems likely that the usual consistency conditions of the conformal bootstrap can only be satisfied if the conformal blocks with $\beta \in \mathbb{S}$ form a basis for the space of conformal blocks $\text{CB}(\mathcal{C}_{0,4})$ on the four-punctured sphere $\mathbb{P}^1 \setminus \{0, z_1, z_2, \infty\}$, as is known to be the case for $N = 2$ (Liouville theory) [25]. It is furthermore easy to show that the Verlinde loop operators associated with the curve γ_s separating punctures z_1 and 0 from z_2 and ∞ act diagonally in this basis, with eigenvalues parameterized in terms of $\beta = Q + i\mathfrak{p}$. The formulas for the eigenvalues look simplest if one represents the vectors $\mathfrak{p} \in \mathbb{R}^{N-1}$ in terms of vectors $\mathfrak{a} \in \mathbb{R}^N$ lying on the plane $\sum_k a_k = 0$, where a_k are the components of $\mathfrak{a}$ with respect to an orthonormal basis for $\mathbb{R}^N$. The eigenvalues $\lambda_{\omega_1}(a)$ of the Verlinde loop

operator associated with the curve γ_s and the degenerate fields D^i, for example, can then be represented as

$$\lambda_{\omega_1}(a) \,=\, \sum_{i=1}^{N} \mathrm{e}^{-2\pi \mathrm{i} b a_i}\,. \tag{6.7}$$

The considerations above motivate us to propose that the Hilbert space of Toda conformal blocks has the form

$$\mathrm{HCB}(\mathcal{C}_{g,n}) \,=\, \int_{\mathbb{S}} \prod_{\text{edges } e} \mathrm{d}\beta_e \bigotimes_{\text{vertices } v} \mathrm{HCB}(\mathcal{C}_{0,3}^v)\,. \tag{6.8}$$

Here $\mathrm{HCB}(\mathcal{C}_{0,3}^v)$ is the Hilbert space of conformal blocks on the three-punctured spheres $\mathcal{C}_{0,3}^v$, with $v = 1, \ldots, 2g - 2 + n$, that appear in the pants decomposition of $\mathcal{C}_{g,n}$. The conformal blocks constructed by gluing will diagonalize the Verlinde loop operators for the cutting curves in the pants decomposition.

It should be noted that our conjecture (6.8) appears to be necessary for having consistency conditions of the conformal bootstrap like crossing symmetry, modular invariance, or locality realized in the usual way. Let us consider, for example, the condition of mutual locality of the vertex operators $V_\alpha(z, \bar{z})$ within correlation functions such as

$$\big\langle\, \alpha_\infty \,|\, V_{\alpha_2}(z_2, \bar{z}_2)\, V_{\alpha_1}(z_1, \bar{z}_1)\, |\, \alpha_0\, \big\rangle = \big\langle\, \alpha_\infty \,|\, V_{\alpha_1}(z_1, \bar{z}_1)\, V_{\alpha_2}(z_2, \bar{z}_2)\, |\, \alpha_0\, \big\rangle. \tag{6.9}$$

Such relations would hold if (i) the conformal blocks satisfy braid relations of the form

$$\begin{aligned}
\mathcal{F}\big[{}^{\alpha_2}_{\alpha_\infty} s_2 | \beta | s_1 {}^{\alpha_1}_{\alpha_0}\big](z_2, z_1) &= \\
&= \int_{\mathbb{S}} \mathrm{d}\beta' \int_{\mathbb{T}} \mathrm{d}t_2 \mathrm{d}t_1 \; B_{\beta\beta'}\big[{}^{\alpha_2}_{\alpha_\infty}\, {}^{\alpha_1}_{\alpha_0}\big]{}^{t_2 t_1}_{s_2 s_1}\; \mathcal{F}\big[{}^{\alpha_1}_{\alpha_\infty} t_1 | \beta | t_2 {}^{\alpha_2}_{\alpha_0}\big](z_1, z_2)\,,
\end{aligned} \tag{6.10}$$

and (ii) kernels $B_{\beta\beta'}\big[{}^{\alpha_2}_{\alpha_\infty}\, {}^{\alpha_1}_{\alpha_0}\big]{}^{t_2 t_1}_{s_2 s_1}$ and structure functions $C_{s\bar{s}}(\alpha_3, \alpha_2, \alpha_1)$ appearing in (6.4) satisfy suitable orthogonality relations. Equations (6.10) may then be interpreted as relations between two different bases for the space of conformal blocks $\mathrm{HCB}(\mathcal{C}_{0,4})$. The spectrum (6.2) thereby gets related to the spectrum (6.8) of Verlinde loop operators on the space of conformal blocks.

6.2   Spectrum of quantized trace functions

We have explained in section 2.6 that a maximal set of commuting Hamiltonians on the symplectic moduli space $\bar{\mathcal{M}}_{g,n}^N$ (with fixed holonomies around the punctures) consists of the cutting loops that specify a pants decomposition of $\mathcal{C}_{g,n}$ together with the corresponding pants networks. This implies that all these loop and network operators can be simultaneously diagonalized.

We are going to argue that the spectrum of the Hamiltonians associated with the cutting curves coincides with the expected spectrum of the corresponding Verlinde loop operators. To this aim we are going to observe that some essential features of the spectrum can be anticipated without solving the eigenvalue problem explicitly.

Example for $N = 2$: as a warm-up, let us consider the case of SL(2)-connections on $\mathcal{C}_{1,1}$. In the polarization $\mathsf{p} = \frac{1}{2}(\hat{B} + \hat{C})$ and $\mathsf{q} = -\frac{1}{2}(\hat{B} - \hat{C})$ with $[\mathsf{p}, \mathsf{q}] = -i\hbar$, the A-cycle operator (4.53) becomes

$$\hat{A} = 2\cosh\mathsf{p} + \mathrm{e}^{-\mathsf{q}}, \tag{6.11}$$

which defines a positive self-adjoint, but unbounded operator on $L^2(\mathbb{R})$. A complete set of eigenfunctions for this difference operator is known [87, 88]. The spectrum is purely continuous, and supported in the semi-infinite interval $(2, \infty)$. The (generalized) eigenvalues are non-degenerate and can therefore be parameterized in terms of a parameter $s \in \mathbb{R}^+$ as $2\cosh(s)$.

Without having solved the spectral problem explicitly one could still note that the term $\mathrm{e}^{-\mathsf{q}}$ appearing in the definition of $\hat{A}$ decays exponentially for $\mathsf{q} \to \infty$, and that the term $2\cosh\mathsf{p}$ can be seen as a "deformation" of the usual term p^2 in Schrödinger operators. One may therefore expect that the spectral problem for $\hat{A}$ will in some respects be similar to the spectral problem for the Liouville quantum mechanics with Hamiltonian H_0 (6.1). The extent to which this is the case was clarified in [88]. In the Schrödinger representation with q represented on wave-functions $\psi(q)$ as an operator of multiplication with q one can construct two linearly independent Jost solutions, eigenfunctions $f_s^\pm(q)$ of H_0 that behave for $q \to \infty$ as $f_s^\pm(q) = \mathrm{e}^{\pm \frac{i}{\hbar} sq} + o(1)$ [88]. The Jost solutions grow exponentially at the opposite end $q \to -\infty$. One can, however, find a function $R(s)$ such that the linear combination $\psi_s(q) = f_s^+(q) + R(s)f_s^-(q)$ decays rapidly for $q \to -\infty$. Only this linear combination may appear in the spectral decomposition of $\hat{A}$. Note that $\psi_{-s}(q)$ is related to $\psi_s(q)$ by a relation of the form $\psi_{-s}(q) = R(s)\psi_s(q)$, analogous to the case of a Schrödinger operator with repulsive potential.

The fact that the spectrum is bounded from below by 2 follows from the observation that $\hat{A}$ is the sum of two positive self-adjoint operators, and its spectrum therefore bounded from below by the spectrum of $2\cosh\mathsf{p}$.

Example for $N = 3$: although we will not be able to find explicit diagonal representations for the A-cycle operators for higher rank, we can anticipate features of their spectra by a similar reasoning. In order to see how the observation above generalize, let us next consider the quantization of the trace functions associated with SL(3)-connections on $\mathcal{C}_{1,1}$.

In order to represent the trace functions associated with A- and B-cycles in a form that will be convenient for the quantization, let us start by fixing the eigenvalues of the holonomy $\mathbf{M}$ around the puncture in terms of constants $\gamma_1 = a_1 a_2 b_1 b_2 c_1 c_2$ and $\gamma_2 = xy$:

$$\left\{ \frac{1}{a_1 a_2 b_1 b_2 c_1 c_2 xy}, \frac{1}{xy}, a_1 a_2 b_1 b_2 c_1 c_2 x^2 y^2 \right\} = \left\{ \frac{1}{\gamma_1 \gamma_2}, \frac{1}{\gamma_2}, \gamma_1 \gamma_2^2 \right\} . \tag{6.12}$$

We must then choose a polarization with momenta P_i and positions Q_j satisfying $\{P_i, Q_j\} = \delta_{ij} P_i Q_j$. The nice Poisson bracket (4.58) between the monomials α_i and β_j appearing in

the A- and B-cycle suggests the following choice:

$$P_1 = \alpha_1 = b_1 c_1 x, \qquad Q_1 = \prod_i \beta_i^{-\kappa_{1i}^{-1}} = a_1^{-\frac{2}{3}} a_2^{-\frac{1}{3}} b_1^{-\frac{2}{3}} b_2^{-\frac{1}{3}} x^{-\frac{1}{3}} y^{-\frac{2}{3}},$$

$$P_2 = \alpha_2 = b_2 c_2 y, \qquad Q_2 = \prod_i \beta_i^{-\kappa_{2i}^{-1}} = a_1^{-\frac{1}{3}} a_2^{-\frac{2}{3}} b_1^{-\frac{1}{3}} b_2^{-\frac{2}{3}} x^{-\frac{2}{3}} y^{-\frac{1}{3}},$$

$$P_3 = x, \qquad Q_3 = (a_2 b_2 c_2)^{-1}. \tag{6.13}$$

The A-cycle trace functions are then expressed as

$$A_1 = P_1^{\frac{1}{3}} P_2^{\frac{2}{3}} + \frac{P_1^{\frac{1}{3}}}{P_2^{\frac{1}{3}}} + \frac{1}{P_1^{\frac{2}{3}} P_2^{\frac{1}{3}}} + \frac{P_1^{\frac{1}{3}} P_2^{\frac{2}{3}} P_3}{\gamma_1 \gamma_2^2 Q_1 Q_2} + P_1^{\frac{1}{3}} P_2^{\frac{2}{3}} \frac{Q_1 Q_3}{Q_2^2} \left(1 + \frac{1}{\gamma_2}\right) + \frac{P_1^{\frac{1}{3}} Q_2 (1 + P_3)}{\gamma_1 \gamma_2 P_2^{\frac{1}{3}} Q_1^2 Q_3},$$

$$A_2 = P_1^{\frac{2}{3}} P_2^{\frac{1}{3}} + \frac{P_2^{\frac{1}{3}}}{P_1^{\frac{1}{3}}} + \frac{1}{P_1^{\frac{1}{3}} P_2^{\frac{2}{3}}} + \frac{P_2^{\frac{1}{3}} Q_1 Q_3}{P_1^{\frac{1}{3}} P_3 Q_2^2} + \frac{P_2^{\frac{1}{3}} Q_1 Q_3}{P_1^{\frac{1}{3}} Q_2^2} \left(\frac{1}{P_3} + \frac{1}{\gamma_2}\right) + \frac{P_1^{\frac{2}{3}} P_2^{\frac{1}{3}} Q_2}{\gamma_1 \gamma_2 Q_1^2 Q_3} (1 + P_3).$$

If we take the limit $Q_1, Q_2 \to \infty$ with Q_1/Q_2 finite we see that only the first three terms survive. The quantization of these expressions is straightforward following our discussions above, allowing us to define operators $\hat{A}_i$, $i = 1, 2$.

By generalizing the arguments used in the case $N = 2$ above one finds that the eigenvalues A_i' of the operators $\hat{A}_i$ can be parameterized in terms of a vector $(s_1, s_2) \in \mathbb{R}^2$ as follows

$$A_1' = \xi_1 + \xi_2 + \xi_3, \qquad A_2' = \frac{1}{\xi_1} + \frac{1}{\xi_2} + \frac{1}{\xi_3}, \tag{6.14}$$

where ξ_a are defined for $a = 1, 2, 3$ as

$$\left(\xi_1, \xi_2, \xi_3\right) = \left(e^{\frac{1}{3}(s_1 + 2s_2)}, \; e^{\frac{1}{3}(s_1 - s_2)}, \; e^{-\frac{1}{3}(2s_1 + s_2)}\right). \tag{6.15}$$

The expressions for the eigenvalues A_i' are manifestly invariant under Weyl symmetry permuting the ξ_a.

Furthermore, it seems likely that the repulsive nature of the dependence on Q_1, Q_2 will imply that the spectrum is parameterized by the Weyl-orbits of vectors $\mathfrak{s} = (s_1, s_2) \in \mathbb{R}^2$. In order to see this, let $\psi_{\mathfrak{s}}(\mathfrak{q})$, $\mathfrak{q} = (q_1, q_2)$, be a joint eigenfunction of the operators $\hat{A}_i$, $i = 1, 2$, in a Schrödinger-type representation where the quantum operators corresponding to the classical variables $\log Q_i$ are diagonal with eigenvalues q_i. The wave-function $\psi_{\mathfrak{s}}(\mathfrak{q})$ will be of the form

$$\psi_{\mathfrak{s}}(\mathfrak{q}) = \psi_{\mathfrak{s}}^0(\mathfrak{q}) + \mathcal{O}\left(e^{-\frac{1}{2}(q_1 + q_2)}\right), \tag{6.16}$$

where $\psi_{\mathfrak{s}}^0(\mathfrak{q})$ is an eigenfunction of the operators

$$\hat{A}_1^0 = \mathsf{P}_1^{\frac{1}{3}} \mathsf{P}_2^{\frac{2}{3}} + \mathsf{P}_1^{\frac{1}{3}} \mathsf{P}_2^{-\frac{1}{3}} + \mathsf{P}_1^{-\frac{2}{3}} \mathsf{P}_2^{-\frac{1}{3}}, \qquad \hat{A}_2^0 = \mathsf{P}_1^{\frac{2}{3}} \mathsf{P}_2^{\frac{1}{3}} + \mathsf{P}_1^{-\frac{1}{3}} \mathsf{P}_2^{\frac{1}{3}} + \mathsf{P}_1^{-\frac{1}{3}} \mathsf{P}_2^{-\frac{2}{3}},$$

where $\mathsf{P}_i = e^{\frac{\hbar}{i} \frac{\partial}{\partial q_i}}$. A joint eigenfunction of $\hat{A}_i^0$ is given by $e^{\frac{i}{\hbar}(s_1 q_1 + s_2 q_2)} \equiv e^{\frac{i}{\hbar}(\mathfrak{s}, \mathfrak{q})}$, where $(\mathfrak{s}, \mathfrak{q})$ denotes the standard scalar product of the vectors $\mathfrak{s}$ and $\mathfrak{q}$ in $\mathbb{R}^2$. The Weyl-invariance of the eigenvalues of $\hat{A}_i^0$ implies that other joint eigenfunctions of $\hat{A}_i^0$ are given by the functions

$\mathrm{e}^{\frac{\mathrm{i}}{\hbar}(w(\mathfrak{s}),\mathfrak{q})}$, where $w(\mathfrak{s})$ is the vector obtained by the action of the element w of the Weyl-group $\mathcal{W}$ of SL(3) on $\mathfrak{s} \in \mathbb{R}^2$. It follows that the most general joint eigenfunction of the $\hat{A}_i^0$ has the form

$$\psi_{\mathfrak{s}}^0(\mathfrak{q}) = \sum_{w \in \mathcal{W}} C_w(\mathfrak{s}) \mathrm{e}^{\frac{\mathrm{i}}{\hbar}(w(\mathfrak{s}),\mathfrak{q})} \, . \tag{6.17}$$

The exponential growth of the terms in $\hat{A}_i$ depending on $q_i \equiv \log Q_i$ will imply that the wave-functions $\psi_{\mathfrak{s}}(\mathfrak{q})$ have to decay very rapidly when $q_1, q_2 \to \infty$. This will imply that $\psi_{\mathfrak{s}}(\mathfrak{q})$ has to satisfy two reflection relations that must be compatible with the structure (6.17) of the $\psi_{\mathfrak{s}}^0(\mathfrak{q})$. The reflection relations must therefore be of the form

$$\psi_{w_i(\mathfrak{s})}(\mathfrak{q}) = R_i(\mathfrak{s})\psi_{\mathfrak{s}}(\mathfrak{q}) \, , \qquad i = 1, 2 \, , \tag{6.18}$$

with w_i two different elements of $\mathcal{W}$. By composition of the Weyl reflections w_i, one can generate reflection relations corresponding to all elements of the Weyl group $\mathcal{W}$. The resulting relations will determine the coefficients $C_w(\mathfrak{s})$ in (6.17) completely up to an overall normalization. We are thereby lead to the conclusion that the spectrum is indeed parameterized by the Weyl-orbits of vectors $\mathfrak{s} \in \mathbb{R}^2$.

A very similar structure is found for the trace functions B_i associated with the B-cycles. The explicit expressions turn out to be of the form

$$B_1 = Q_2 + \frac{Q_1}{Q_2} + \frac{1}{Q_1} + \mathcal{O}\big((P_1P_2)^{\frac{1}{6}}\big), \quad B_2 = \frac{1}{Q_2} + \frac{Q_2}{Q_1} + Q_1 + \mathcal{O}\big((P_1P_2)^{\frac{1}{6}}\big), \tag{6.19}$$

suggesting that the eigenvalues can be parameterized in terms of real positive numbers ζ_a, $a = 1, 2, 3$, satisfying $\zeta_1\zeta_2\zeta_3 = 1$, as

$$B_1 \to \zeta_1 + \zeta_2 + \zeta_3 \, , \qquad B_2 \to \frac{1}{\zeta_1} + \frac{1}{\zeta_2} + \frac{1}{\zeta_3} \, . \tag{6.20}$$

Our observations above suggest that the spectrum of the trace-functions A_1 and B_1 coincides with the spectrum (6.7) of the corresponding Verlinde loop operators.

Higher rank: the remarks above seem to generalize to cases with $N > 3$. In the case $N = 4$, for example, one may note that the trace function A_2 of the A-cycle holonomy in the second antisymmetric representation (see (4.65)) has a similar structure as observed in the case $N = 3$ above, with the following leading term:

$$A_2^0 = 2\cosh\frac{1}{2}(p_1 + p_3) + 2\cosh\frac{1}{2}(p_1 - p_3) + 2\cosh\frac{1}{2}(p_1 + 2p_2 + p_3) \, , \tag{6.21}$$

where we defined $p_i \equiv \log P_i$. This further strengthens our confidence that the spectra of quantized trace functions will coincide with the spectra of the Verlinde loop operators in Toda CFT.

6.3 Concluding remarks

One of the most important problems is clearly to find useful bases for the space of conformal blocks $\mathrm{CB}(\mathcal{C}_{0,3})$. A natural possibility would be to define such bases by diagonalizing a

maximal set of commuting Verlinde network operators. Natural as it may be, it seems technically much harder to analyze the spectrum of network operators along similar lines as described above. As an example let us consider the pants network N_1 on $\mathcal{C}_{0,3}$ in the case $N = 3$. We can use the coordinates

$$p_1 = a_1, \qquad q_1 = y, \qquad (6.22)$$

and denote the eigenvalues of $\mathbf{A}$ by $\tilde{\alpha}_1 = \alpha_1^{1/3}\alpha_2^{2/3}$ and $\tilde{\alpha}_2 = \alpha_1^{1/3}\alpha_2^{-1/3}$, and similarly for $\mathbf{B}$ and $\mathbf{C}$. The pants network function can then be represented as

$$N_1 = \frac{p_1}{\tilde{\beta}_1\tilde{\gamma}_1\tilde{\gamma}_2}\left[1 + \frac{2\tilde{\beta}_1^2\tilde{\gamma}_1^2\tilde{\gamma}_2^3}{\tilde{\alpha}_1 p_1^3} + \tilde{\alpha}_1\tilde{\beta}_1\tilde{\gamma}_1 \right. \qquad (6.23)$$

$$+ \frac{1}{p_1^2}\left(\frac{\tilde{\beta}_1\tilde{\gamma}_1^2\tilde{\gamma}_2^2}{\tilde{\alpha}_1\tilde{\alpha}_2} + \frac{\tilde{\beta}_1^2\tilde{\gamma}_1^2\tilde{\gamma}_2^3}{\tilde{\alpha}_1} + \frac{\tilde{\beta}_1^2\tilde{\gamma}_1\tilde{\gamma}_2}{\tilde{\alpha}_1} + \tilde{\alpha}_2\tilde{\beta}_1\tilde{\gamma}_1^2\tilde{\gamma}_2^2 + \tilde{\beta}_1^2\tilde{\beta}_2\tilde{\gamma}_1\tilde{\gamma}_2^2 + \frac{\tilde{\beta}_1\tilde{\gamma}_1\tilde{\gamma}_2^2}{\tilde{\beta}_2} \right)$$

$$+ q_1\left(\frac{\tilde{\alpha}_2\tilde{\beta}_1^2\tilde{\beta}_2\tilde{\gamma}_1^2\tilde{\gamma}_2^4}{\tilde{\alpha}_1 p_1^3} + \frac{\tilde{\alpha}_2\tilde{\beta}_1^2\tilde{\beta}_2\tilde{\gamma}_1\tilde{\gamma}_2^2}{\tilde{\alpha}_1 p_1^2} + \frac{\tilde{\beta}_1\tilde{\beta}_2\tilde{\gamma}_1^2\tilde{\gamma}_2^3}{\tilde{\alpha}_1 p_1^2} + \frac{\tilde{\beta}_1\tilde{\beta}_2\tilde{\gamma}_1\tilde{\gamma}_2}{\tilde{\alpha}_1 p_1} + \frac{\tilde{\alpha}_2\tilde{\beta}_1\tilde{\gamma}_1\tilde{\gamma}_2^3}{p_1^2} + \frac{\tilde{\alpha}_2\tilde{\beta}_1\tilde{\gamma}_2}{p_1} + \frac{\tilde{\gamma}_1\tilde{\gamma}_2^2}{p_1} + 1 \right)$$

$$+ \left. \frac{1}{q_1}\left(\frac{\tilde{\beta}_1^2\tilde{\gamma}_1^2\tilde{\gamma}_2^2}{\tilde{\alpha}_1\tilde{\alpha}_2\tilde{\beta}_2 p_1^3} + \frac{\tilde{\beta}_1^2\tilde{\gamma}_1^2\tilde{\gamma}_2^2}{\tilde{\alpha}_1\tilde{\alpha}_2\tilde{\beta}_2 p_1^2} + \frac{\tilde{\alpha}_1\tilde{\beta}_1\tilde{\gamma}_1}{p_1} + \tilde{\alpha}_1\tilde{\beta}_1\tilde{\gamma}_1 + \frac{\tilde{\beta}_1^2\tilde{\gamma}_1\tilde{\gamma}_2}{\tilde{\alpha}_2 p_1^2} + \frac{\tilde{\beta}_1^2\tilde{\gamma}_1\tilde{\gamma}_2}{\tilde{\alpha}_2 p_1} + \frac{\tilde{\beta}_1\tilde{\gamma}_1^2\tilde{\gamma}_2}{\tilde{\beta}_2 p_1^2} + \frac{\tilde{\beta}_1\tilde{\gamma}_1^2\tilde{\gamma}_2}{\tilde{\beta}_2 p_1} \right) \right].$$

We see that there is no limit in which the terms depending on q_1 vanish. This might indicate that the spectrum of the corresponding quantum operator is discrete rather than continuous. It would be very interesting if one could describe the spectrum of this operator more precisely.

One may also note that the free-field construction of chiral vertex operators gave us families of conformal blocks labeled by a space of parameters which has the same dimension as Lagrangian subspaces of $\mathcal{M}_{0,3}^N$. This indicates that the conformal blocks that can be obtained in this way may represent a basis for $\mathrm{CB}(\mathcal{C}_{0,3})$.

Let us finally note that the geometric engineering of gauge theories of class $\mathcal{S}$, combined with the topological vertex technique has led to a prediction for the structure functions $C_{s\bar{s}}(\alpha_3, \alpha_2, \alpha_1)$ appearing in (6.4), see [89, 90]. The labels s for a basis of $\mathrm{CB}(\mathcal{C}_{0,3})$ would thereby be identified with geometric data of the local Calabi-Yau manifold used in the geometric engineering of the class $\mathcal{S}$ theories associated with $\mathcal{C}_{0,3}$. It would be very interesting to identify the meaning of this parameter within conformal field theory, or within the quantum theory obtained by quantizing $\mathcal{M}_{0,3}^N$.

Acknowledgments

A   Fock-Goncharov coordinates

In [30], Fock and Goncharov constructed coordinates systems on the moduli space of flat connections over a punctured surface $\mathcal{C}_{g,n}$. They assume that the surface is hyperbolic, that is $\chi(\mathcal{C}_{g,n}) = 2 - 2g - n < 0$, and has at least one puncture, $n \geq 1$. Their approach consists in "localizing" flat connections on the triangles of an ideal triangulation of $\mathcal{C}_{g,n}$ (in which the vertices of the triangles are at punctures). However, since a triangle is contractible, any flat connection on it is trivial. This difficulty can be overcome by considering *framed* flat connections, which means adding on each puncture a flag that is invariant under the holonomy around the puncture.

A.1   Coordinates associated with N-triangulations

Let us review how to build coordinates on the moduli space of framed flat connections over a punctured surface $\mathcal{C}_{g,n}$ (We mostly follow section 4 in [67], and appendix A in [23]). Given an SL(N)-vector bundle with a framed flat connection over $\mathcal{C}_{g,n}$, each triangle of an ideal triangulation of $\mathcal{C}_{g,n}$ gives rise to a (generic) configuration of three flags $\{A, B, C\}$ associated with the vertices. A flag A in an N-dimensional complex vector space V_N is a collection of nested subspaces

$$A: \qquad 0 = A_0 \subset A_1 \subset A_2 \subset \cdots \subset A_N = V_N\,, \tag{A.1}$$

with $\dim[A_a] = a$. An N-triangulation consists in a further decomposition of each triangle into small triangles, whose vertices are at the $\binom{N+2}{2}$ lattice points p_{abc} with

$$a + b + c = N\,, \qquad\qquad a, b, c \in \mathbb{Z}_{\geq 0}\,. \tag{A.2}$$

See figure 42 for an example with $N = 3$. There are N^2 small triangles for each ideal triangle, $\binom{N+1}{2}$ of which are "upright" (white) and labeled by the solutions of $a + b + c = N - 1$, while $\binom{N}{2}$ are "upside-down" (black) and labeled by the solutions of $a + b + c = N - 2$. To every white triangle we associate a line l_{abc} in V_N arising as the intersection of the corresponding subspaces of the flags $\{A, B, C\}$. More explicitly, writing $A^a \equiv A_{N-a}$ with $\text{codim}[A^a] = a$, we have

$$l_{abc} = A^a \cap B^b \cap C^c\,, \qquad\qquad a + b + c = N - 1\,. \tag{A.3}$$

Similarly, we associate to every black triangle a plane P_{abc}, and to every internal lattice point with $a + b + c = N - 3$ a 3-space V_{abc}:

$$\begin{aligned} P_{abc} &= A^a \cap B^b \cap C^c\,, & a + b + c &= N - 2\,, \\ V_{abc} &= A^a \cap B^b \cap C^c\,, & a + b + c &= N - 3\,. \end{aligned} \tag{A.4}$$
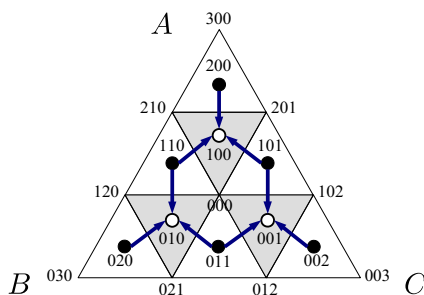
Figure 42. N-triangulation of a triangle (here for $N = 3$). The triples of non-negative integers a, b, c sum to 3 on lattice points p_{abc}, to 2 on white triangles associated with lines l_{abc} (black dots), and to 1 on black triangles associated with planes P_{abc} (white dots). The internal lattice point is associated with the 3-space V_{000}. Arrows between dots indicate incidence relations.

The plane P_{abc} on a black triangle contains all three lines $l_{(a+1)bc}$, $l_{a(b+1)c}$, and $l_{ab(c+1)}$ on the adjacent white triangles. In turn, the 3-space V_{abc} on an internal lattice point contains all three planes on the surrounding black triangles, and thus all six lines on the surrounding white triangles.

This collection of subspaces on the N-triangulation allows us to associate coordinates to every lattice point (excluding the vertices at the punctures). We can define coordinates x_{abc} associated with the internal lattice points p_{abc} with $a+b+c = N-3$ as the triple-ratio of the six surrounding lines contained in V_{abc} (the neighborhood of an internal lattice point looks like the 3-triangulation shown in figure 42). The 3-space V_{abc} contains the three flags

$$
\begin{aligned}
\tilde{A} : \quad & 0 \subset l_{(a+2)bc} \subset P_{(a+1)bc} \subset V_{abc} , \\
\tilde{B} : \quad & 0 \subset l_{a(b+2)c} \subset P_{a(b+1)c} \subset V_{abc} , \\
\tilde{C} : \quad & 0 \subset l_{ab(c+2)} \subset P_{ab(c+1)} \subset V_{abc} .
\end{aligned}
\tag{A.5}
$$

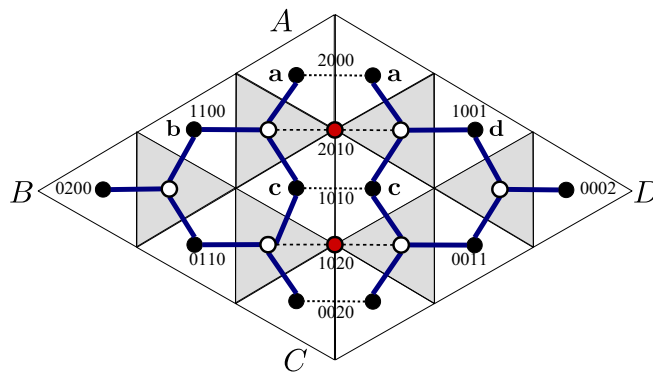Fixing the flags to be $\tilde{A} = (\mathbf{a_1}, \mathbf{a_1} \wedge \mathbf{a_2})$, with $\mathbf{a_i}$ vectors in V_{abc}, we can write the triple-ratio as

$$
x_{abc} = \frac{\langle \mathbf{a_1} \wedge \mathbf{a_2} \wedge \mathbf{b_1} \rangle \langle \mathbf{b_1} \wedge \mathbf{b_2} \wedge \mathbf{c_1} \rangle \langle \mathbf{c_1} \wedge \mathbf{c_2} \wedge \mathbf{a_1} \rangle}{\langle \mathbf{a_1} \wedge \mathbf{a_2} \wedge \mathbf{c_1} \rangle \langle \mathbf{b_1} \wedge \mathbf{b_2} \wedge \mathbf{a_1} \rangle \langle \mathbf{c_1} \wedge \mathbf{c_2} \wedge \mathbf{b_1} \rangle} .
\tag{A.6}
$$

Here the notation $\langle \mathbf{v_1} \wedge \mathbf{v_2} \wedge \mathbf{v_3} \rangle$ means the determinant of the matrix expressing the vectors $\mathbf{v_1}, \mathbf{v_2}, \mathbf{v_3}$ in a unimodular basis for the 3-space containing them (this triple-ratio is the inverse of the one originally defined by Fock and Goncharov, see appendix A in [23]).

It remains to define coordinates for the lattice points on the edges of the ideal triangulation. Along the common edge of two glued N-triangulated triangles, adjacent white triangles are associated with the same lines, and adjacent black triangles to the same planes (see figure 43). A lattice point on an edge is thus surrounded by four lines, which allows us to define a cross-ratio coordinate. For example, at the point p_{2010} on figure 43, we choose four vectors $\mathbf{a} \in l_{2000}$, $\mathbf{b} \in l_{1100}$, $\mathbf{c} \in l_{1010}$, $\mathbf{d} \in l_{1001}$, all contained in the plane P_{1000}, which give the cross-ratio

$$
x_{2010} = \frac{\langle \mathbf{a} \wedge \mathbf{b} \rangle \langle \mathbf{c} \wedge \mathbf{d} \rangle}{\langle \mathbf{a} \wedge \mathbf{d} \rangle \langle \mathbf{b} \wedge \mathbf{c} \rangle} .
\tag{A.7}
$$

Figure 43. Two 3-triangulated triangles ABC and ACD glued along the edge AC. The quadruples of non-negative integers a, b, c, d sum to 3 on lattice points p_{abcd}, and to 2 on white triangles associated with lines l_{abcd}. Lines and planes adjacent across the edge are identical. Each edge point is surrounded by four lines.
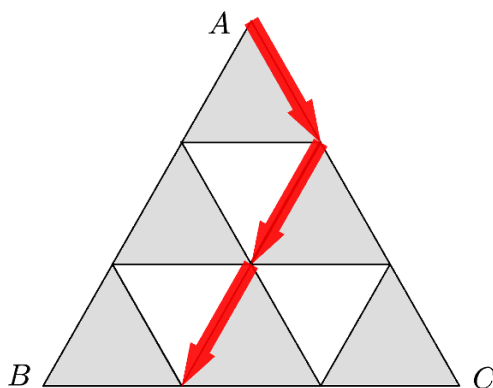
Figure 44. Example of a snake on the $(N-1)$-triangulation of a triangle (here for $N = 4$).

An ideal triangulation of the surface $\mathcal{C}_{g,n}$ has $-2\chi(\mathcal{C}_{g,n})$ triangles and $-3\chi(\mathcal{C}_{g,n})$ edges. There are $\binom{N-1}{2}$ internal lattice points in each triangle and $N-1$ lattice points on each edge, so the total number of independent coordinates provided by triple-ratios and cross-ratios is

$$\#\{x\text{-coordinates}\} = -\chi(\mathcal{C}_{g,n})\dim[\mathrm{SL}(N,\mathbb{C})] \ . \tag{A.8}$$

This agrees with the dimension (2.3) of the moduli space of flat $\mathrm{SL}(N,\mathbb{C})$-connections on $\mathcal{C}_{g,n}$.

A.2 Snakes and projective bases

Fock and Goncharov showed how to construct projective bases in the N-dimensional vector space V_N related to three flags A, B, C at the vertices of a triangle. Each basis is represented by a *snake*, that is an oriented path on the edges of the $(N-1)$-triangulation from one vertex to the opposite side (see figure 44 for an example). Notice that in the $(N-1)$-triangulation the vertices correspond to lines, and the upright (black) triangles to planes. Each segment of the snake goes from a line l_1 to a line l_2, and the plane they define also

Figure 45. Segment of a snake along an edge of a black triangle in an $(N-1)$-triangulation. The vertices of the triangles correspond to 3 coplanar lines l_1, l_2, l_3. Picking a vector $\mathbf{v}_1 \in l_1$ at the start of the segment determines $\mathbf{v}_2 \in l_2$ by the rule that $\mathbf{v}_2 \pm \mathbf{v}_1 \in l_3$ depending on whether the segment is oriented clockwise or counterclockwise around the triangle.

contains a third line l_3 at the third vertex of the black triangles. Given a vector $\mathbf{v}_1 \in l_1$, a vector $\mathbf{v}_2 \in l_2$ is determined by the rule that $\mathbf{v}_2 + \mathbf{v}_1 \in l_3$ if the segment is oriented clockwise around the black triangle, and $\mathbf{v}_2 - \mathbf{v}_1 \in l_3$ if it is oriented counterclockwise (see figure 45). To construct the projective basis $\{\mathbf{v}_1, \mathbf{v}_2, \cdots, \mathbf{v}_N\}$ defined by a snake, we can choose any vector $\mathbf{v}_1$ at the first vertex of the snake and use this rule to determine all the subsequent vectors.

A projective basis can be transformed into another one by a sequence of simple moves. The moves I and II shown in figure 46 can be expressed in terms of two types of elementary $GL(N)$ matrices. Let $\varphi_i : \mathrm{SL}(2) \to GL(N)$ be the canonical embedding corresponding to the ith root $\lambda_i - \lambda_{i+1}$. Then the two types of elementary matrices can be written as

$$F_i = \varphi_i \begin{pmatrix} 1 & 0 \\ 1 & 1 \end{pmatrix}, \qquad H_i(x) = \mathrm{diag}(\underbrace{1, \cdots, 1}_{i \text{ times}}, x, \cdots, x) . \tag{A.9}$$

For example, for $N = 3$ we have the following elementary matrices:

$$F_1 = \begin{pmatrix} 1 & 0 & 0 \\ 1 & 1 & 0 \\ 0 & 0 & 1 \end{pmatrix}, \qquad\qquad F_2 = \begin{pmatrix} 1 & 0 & 0 \\ 0 & 1 & 0 \\ 0 & 1 & 1 \end{pmatrix},$$

$$H_1(x) = \begin{pmatrix} 1 & 0 & 0 \\ 0 & x & 0 \\ 0 & 0 & x \end{pmatrix}, \qquad\qquad H_2(x) = \begin{pmatrix} 1 & 0 & 0 \\ 0 & 1 & 0 \\ 0 & 0 & x \end{pmatrix} . \tag{A.10}$$

Note that F_i and $H_j(x)$ commute unless $i = j$.

Move I flips the last segment of a snake across a black triangle, which according to the rule in figure 45 transforms the projective basis as

$$\begin{pmatrix} \mathbf{v}_1 \\ \vdots \\ \mathbf{v}_{N-1} \\ \mathbf{v}_N \end{pmatrix} \mapsto \begin{pmatrix} \mathbf{v}_1 \\ \vdots \\ \mathbf{v}_{N-1} \\ \mathbf{v}_N + \mathbf{v}_{N-1} \end{pmatrix} = F_{N-1} \begin{pmatrix} \mathbf{v}_1 \\ \vdots \\ \mathbf{v}_{N-1} \\ \mathbf{v}_N \end{pmatrix} . \tag{A.11}$$

Move II takes any two consecutive segments of a snake across a pair of adjacent black and white triangles, see figure 46. For a choice of vector $\mathbf{a}$ at their first common vertex, the
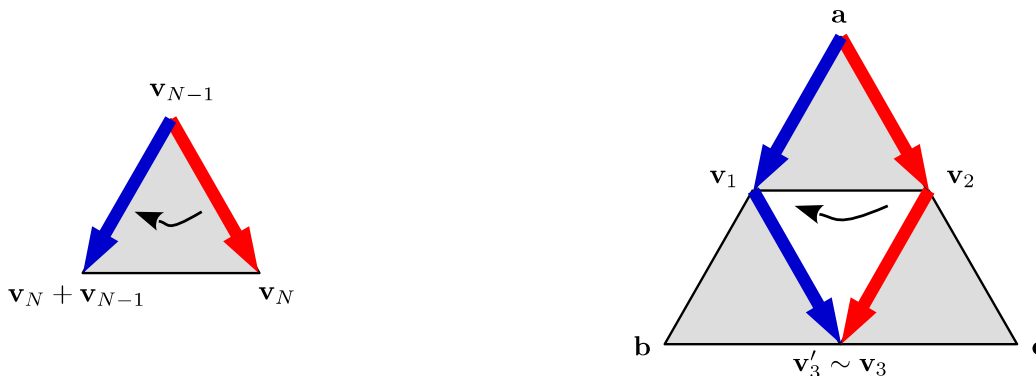
Figure 46. Elementary moves for segments of a snake. *Left*: move I can only occur on the last segment of a snake. *Right*: move II can occur on any two consecutive segments of a snake.

initial and final snakes define two vectors $\mathbf{v}_3$ and $\mathbf{v}_3'$ spanning the line at the vertex where the snakes meet again. The proportionality function is precisely the coordinate x_{abc} for the internal lattice point associated with the white triangle

$$\mathbf{v}_3' = x_{abc}\mathbf{v}_3 \ . \tag{A.12}$$

This can be checked by writing down the triple-ratio (A.6) for the choice of flags $A = (\mathbf{a}, \mathbf{v}_1)$, $B = (\mathbf{b}, \mathbf{v}_3)$, $C = (\mathbf{c}, \mathbf{v}_2)$ and using the relations provided by the black triangles as in figure 45 (that is $\mathbf{v}_1 = \mathbf{v}_2 + \mathbf{a}$, $\mathbf{b} = \mathbf{v}_3' + \mathbf{v}_1$, $\mathbf{c} = \mathbf{v}_3 - \mathbf{v}_2$). The transformation between the bases associated with the two snakes in figure 46 acts as

$$\begin{pmatrix} \mathbf{a} \\ \mathbf{v}_2 \\ \mathbf{v}_3 \end{pmatrix} \mapsto \begin{pmatrix} \mathbf{a} \\ \mathbf{v}_1 \\ \mathbf{v}_3' \end{pmatrix} = F_1 H_2(x_{abc}) \begin{pmatrix} \mathbf{a} \\ \mathbf{v}_2 \\ \mathbf{v}_3 \end{pmatrix} \ . \tag{A.13}$$

More generally, we can see that moving the ith segment of snake across a black triangle corresponds to acting with a matrix F_i, while moving it across a white triangle corresponds to acting with a matrix $H_i(x)$, where x is the face coordinate associated with the white triangle. An important snake transformation consists in moving a snake from one edge of a triangle across the entire face to the next edge, rotating clockwise around the initial vertex (see figure 47). For $N = 2$ this gives simply $\mathcal{F} = F_1$. For $N = 3$, this gives
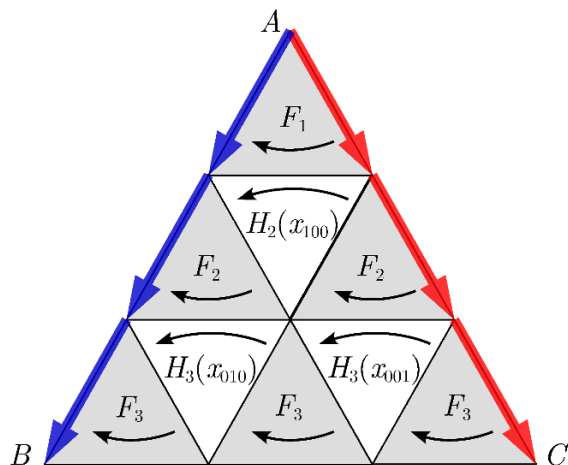
$$\mathcal{F} = F_2 F_1 H_2(x_{000}) F_2 = \begin{pmatrix} 1 & 0 & 0 \\ 1 & 1 & 0 \\ 1 & 1 + x_{000} & x_{000} \end{pmatrix} \ . \tag{A.14}$$

For $N = 4$ as in figure 47 this gives

$$\mathcal{F} = F_3 F_2 H_3(x_{010}) F_3 F_1 H_2(x_{100}) F_2 H_3(x_{001}) F_3 \ . \tag{A.15}$$

Another type of move is the reversal of the orientation of a snake along an edge of a triangle, see figure 48. This reverses the order of the basis vectors, and changes the sign of

Figure 47. Elementary matrices F_i and $H_i(x)$ in an $(N-1)$-triangulation (here for $N=4$). The transformation $\mathcal{F}$ from the snake along the edge AC to the snake along AB can be decomposed into a sequence of moves across the black and white triangles, corresponding to matrices F_i and $H_i(x)$.
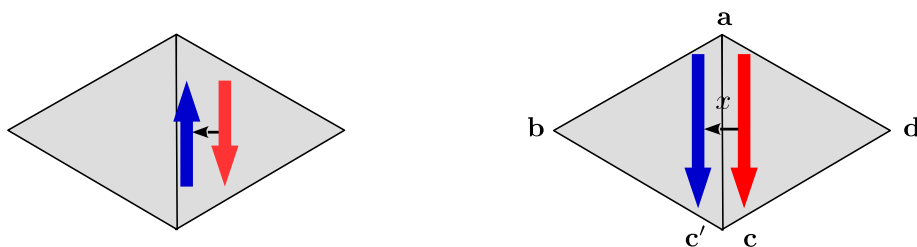
Figure 48. *Left*: reversal of the orientation of the snake along an edge of a triangle. *Right*: snake crossing an edge of a triangle with a cross-ratio coordinate x.

every even-numbered vector, thus multiplying by an anti-diagonal matrix

$$
S = \begin{pmatrix} \cdots & 0 & 0 & 1 \\ \cdots & 0 & -1 & 0 \\ \cdots & 1 & 0 & 0 \\ \cdots & \vdots & \vdots & \vdots \end{pmatrix} . \tag{A.16}
$$

Finally, we can move a snake from one triangle to another across their common edge. If the coordinates along the edge followed by the snake are $\{x_1, x_2, \ldots, x_{N-1}\}$ (in this order), this transformation acts as

$$
H_1(x_1)H_2(x_2)\cdots H_{N-1}(x_{N-1}) = \mathrm{diag}(1, x_1, x_1 x_2, \ldots, x_1 x_2 \cdots x_{N-1}) . \tag{A.17}
$$

This can again be checked by writing down the cross-ratio (A.7) for the edge coordinate x in figure 48 and using the relations provided by the black triangles as in figure 45.

B Background on sl(N) and $\mathcal{U}_q(\mathrm{sl}_N)$

B.1 Lie algebra conventions

The vectors e_i with $i = 1, \ldots, N-1$ are the simple roots of the Lie algebra sl(N) and $(\cdot, \cdot)$ denotes the scalar product on the Cartan subalgebra of sl(N), with the Cartan matrix given by $\kappa_{ij} = (e_i, e_j)$. It is often useful to represent the root/weight subspace of sl(N) as a hyperplane in $\mathbb{R}^N$, allowing us to represent the simple roots as $e_i = u_i - u_{i+1}$ with u_i a unit vector of $\mathbb{R}^N$. The simple roots are dual to the fundamental weights ω_i in the sense that $(e_i, \omega_j) = \delta_{ij}$. In general they can be written as $\omega_i = \sum_{j=1}^{i} u_j - \frac{i}{N} \sum_{k=1}^{N} u_k$. Their inner product is given by the inverse Cartan matrix $(\omega_i, \omega_j) = \kappa_{ij}^{-1}$ and their sum is the Weyl vector $\rho = \sum_i \omega_i$. The weights of the fundamental representation of sl(N) with highest weight ω_1 are $h_i = \omega_1 - \sum_{j=1}^{i-1} e_j$, with $i = 1, \ldots, N$ and $(h_i, h_j) = \delta_{ij} - \frac{1}{N}$.

B.2 Basic definitions

We review some basic notions about quantum groups that are relevant here. For a complete background and set of axioms we refer the reader to some of the standard references [91].

Abstractly, a *Hopf algebra* is a collection $(\mathcal{U}, m, \eta, \Delta, \epsilon, S)$, with unit $\eta : \mathbb{C}(q) \to \mathcal{U}$, product $m : \mathcal{U} \otimes \mathcal{U} \to \mathcal{U}$, coproduct $\Delta : \mathcal{U} \to \mathcal{U} \otimes \mathcal{U}$, counit $\epsilon : \mathcal{U} \to \mathbb{C}(q)$ and an algebra antiautomorphism called antipode $S : \mathcal{U} \to \mathcal{U}$. The triple $(\mathcal{U}, m, \eta)$ is a unital associative algebra and $(\mathcal{U}, \Delta, \epsilon)$ is a counital associative coalgebra. Δ, ϵ are unital algebra homomorphisms and satisfy the following relations

$$
\begin{aligned}
(\Delta \otimes \mathrm{id}) \circ \Delta &= (\mathrm{id} \otimes \Delta) \circ \Delta && \text{(co-associativity)} \\
(\epsilon \otimes \mathrm{id}) \circ \Delta &= (\mathrm{id} \otimes \epsilon) \circ \Delta = \mathrm{id} \\
m \circ (S \otimes \mathrm{id}) \circ \Delta &= \eta \circ \epsilon = m \circ (\mathrm{id} \otimes S) \circ \Delta && \text{(pentagon) .}
\end{aligned}
\tag{B.1}
$$

The quantum group $\mathcal{U} = \mathcal{U}_q(\mathrm{sl}_N)$ is an example of a Hopf algebra, generated as an associative algebra over $\mathbb{C}(q)$ by E_i, F_i, $K_i^{\pm 1}$ for $i = 1, \ldots, N-1$ satisfying

$$
K_i K_i^{-1} = 1 = K_i^{-1} K_i, \ K_i E_j = q^{(i,j)} E_j K_i, \ K_i F_j = q^{-(i,j)} F_j K_i \quad \text{for} \quad i, j = 1, \ldots, N-1,
$$

where $(i, j) \in \{2, -1, 0\}$ when $|i - j| = 0, 1$ or ≥ 2, and

$$
[E_i, F_j] = \delta_{ij} \frac{K_i - K_i^{-1}}{q - q^{-1}}, \ i, j = 1, \ldots, N-1, \qquad [E_i, E_j] = 0, \ [F_i, F_j] = 0, \ |i - j| \geq 2 .
$$

For $|i - j| = 1$, the generators satisfy the quantum Serre relations

$$
E_i^2 E_j - (q + q^{-1}) E_i E_j E_i + E_j E_i^2 = 0 \quad , \quad F_i^2 F_j - (q + q^{-1}) F_i F_j F_i + F_j F_i^2 = 0 .
$$

The Hopf algebra structure is given by $\epsilon(K_i) = 1$, $\epsilon(E_i) = 0 = \epsilon(F_i)$,

$$
\Delta(K_i) = K_i \otimes K_i \quad , \quad \Delta(E_i) = E_i \otimes K_i + 1 \otimes E_i \quad , \quad \Delta(F_i) = F_i \otimes 1 + K_i^{-1} \otimes F_i
$$

and

$$
S(K_i) = K_i^{-1} \quad , \quad S(E_i) = -E_i K_i^{-1} \quad , \quad S(F_i) = -K_i F_i .
$$

A *quasitriangular* Hopf algebra $\mathcal{U}$ additionally has an invertible element $\mathcal{R} \in \mathcal{U} \otimes \mathcal{U}$, the universal R-matrix of $\mathcal{U}$, which satisfies a set of relations. For example, $\mathcal{R}\Delta(a) = \Delta'(a)\mathcal{R}$ for any $a \in \mathcal{U}$, where $\Delta'(a) = P \circ \Delta(a)$ and P is the permutation homomorphism mapping $P(a \otimes b) = (b \otimes a)$.

With each algebra $\mathcal{U}$, we can associate the category Rep$\mathcal{U}$ of its finite dimensional linear representations, with objects V, W, ... that are finitely generated left $\mathcal{U}$-modules and with morphisms that are $\mathcal{U}$-linear homomorphisms. The action of $\mathcal{U}$ on an $\mathcal{U}$-module V induces a representation $\pi_V : \mathcal{U} \to \text{End } V$.

The coproduct in a quasitriangular Hopf algebra $\mathcal{U}$ induces the tensor product in Rep$\mathcal{U}$, where for $\mathcal{U}$-modules U, V and $\forall a \in \mathcal{U}$, $\pi_{U \otimes V}(a) = (\pi_U \otimes \pi_V)(\Delta(a))$. The unit object in Rep$\mathcal{U}$ is the ground field $\mathbb{C}(q)$ equipped with the action of $\mathcal{U}$ by means of the counit ϵ. Furthermore, there exist associativity and left and right action homomorphisms that make Rep$\mathcal{U}$ a monoidal category (see for example [53]). Moreover, for any $\mathcal{U}$-modules V, W there is a mapping called braiding

$$R_{VW} = P \circ (\pi_V \otimes \pi_W)(\mathcal{R}) : V \otimes W \to W \otimes V \,, \tag{B.2}$$

which is a morphism of Rep$\mathcal{U}$ and turns this into a braided monoidal category.

For triples of $\mathcal{U}$-modules U, V, W, where $U \subset V \otimes W$, a Clebsch-Gordan map $C^U_{VW} : V \otimes W \to U$ intertwines the actions on $V \otimes W$ and U,

$$C^U_{VW}(\pi_V \otimes \pi_W)\Delta(x) = \pi_U(x)C^U_{VW}, \qquad x \in \mathcal{U} \,. \tag{B.3}$$

Clebsch-Gordan maps are represented graphically as trivalent vertices in figure 49. We note that the representations V, W and U may be reducible, in general. We may, in particular, consider cases that V, W and U can be tensor products of representations such as $V = V_1 \otimes \cdots \otimes V_m$, for example. Such Clebsch-Gordan maps C^U_{VW} can be constructed as compositions of Clebsch-Gordan maps intertwining the respective representations on the tensor factors. Avoiding cases where q is a root of unity, one can find any irreducible finite-dimensional representation in a sufficiently high tensor power of the fundamental representation.

The conjugate Clebsch-Gordan maps $C^{VW}_U : U \to V \otimes W$ satisfy the property

$$C^{VW}_U \pi_U(x) = (\pi_V \otimes \pi_W)\Delta(x)C^{VW}_U \,. \tag{B.4}$$

A special subset of intertwiners are the *cap* and *cup* maps intertwining between a tensor product $V \otimes \bar{V}$ and the trivial representation $\mathbf{1} \simeq \mathbb{C}(q)$, respectively, where $\bar{V}$ is the conjugate representation to V. In the Reshetikhin-Turaev construction, one considers general morphisms M in Rep$\mathcal{U}$ between tensor products of modules $V_1 \otimes \ldots \otimes V_m$ and $W_1 \otimes \ldots \otimes W_n$.

B.3 Twisted (compositions of) Clebsch-Gordan maps

Two quasitriangular Hopf algebras $\mathcal{U}$ and $\tilde{\mathcal{U}}$ are related by a Drinfeld twist $\mathcal{J} \in \mathcal{U} \otimes \mathcal{U}$ if the co-products and R-matrices are related by

$$\tilde{\Delta}(\cdot) = \mathcal{J}^{-1}\Delta(\cdot)\mathcal{J}, \qquad \tilde{\mathcal{R}}_{12} = \mathcal{J}^{-1}_{21}\mathcal{R}_{12}\mathcal{J}_{12} \,. \tag{B.5}$$
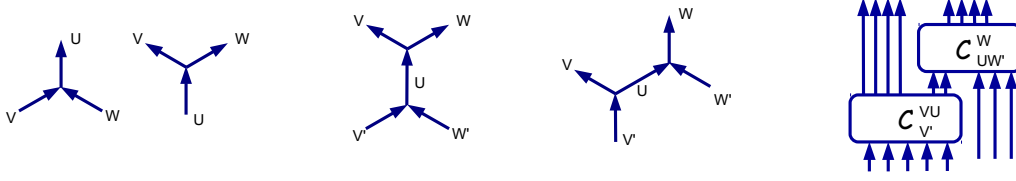
Figure 49. (*Left*): Clebsch-Gordan maps. (*Middle*): gluing of vertices. (*Right*): generic network.

Here we are using leg-numbering notation where the subscripts refer to tensor factors. The twist will preserve co-associativity if

$$(\Delta \otimes \mathrm{id})(\mathcal{J}) \cdot \mathcal{J}_{12} = (\mathrm{id} \otimes \Delta)(\mathcal{J}) \cdot \mathcal{J}_{23} \,, \tag{B.6}$$

The action of $\mathcal{J}$ can be extended to m-fold tensor products by defining recursively

$$\mathcal{J}^{(k+1)} := (\mathrm{id}^{\otimes(k-1)} \otimes \Delta)(\mathcal{J}^{(k)}) \cdot (\mathrm{id}^{\otimes(k-1)} \otimes \mathcal{J}) \,, \qquad \mathcal{J}^{(2)} := \mathcal{J} \,. \tag{B.7}$$

The condition (B.6) ensures that the operator

$$J^{(m)}_{V_m \otimes \cdots \otimes V_1} := (\pi_{V_m} \otimes \cdots \otimes \pi_{V_1})(\mathcal{J}^{(m)}) \,, \tag{B.8}$$

is independent of the order in which tensor products are taken.

Given a Clebsch-Gordan map $C^U_{VW} : V \otimes W \to U$ one may define

$$\tilde{C}^U_{VW} := C^U_{VW} \cdot J_{VW} \,, \qquad J_{VW} := (\pi_V \otimes \pi_W)(\mathcal{J}) \,. \tag{B.9}$$

It is easy to see that $\tilde{C}^U_{VW}$ is a Clebsch-Gordan map intertwining the representation defined on $V \otimes W$ using the twisted coproduct $\tilde{\Delta}$ with the representation U. Similarly, by defining $\tilde{C}^{VW}_U := J^{-1}_{VW} C^{VW}_U$ one can show that $\tilde{C}^{VW}_U \pi_U(x) = (\pi_V \otimes \pi_W)\tilde{\Delta}(x)\tilde{C}^{VW}_U$.

Given a general intertwining map $C : V_1 \otimes \ldots \otimes V_m \to W_1 \otimes \ldots \otimes W_n$ it seems natural to define

$$\tilde{C} := (J^{(n)}_{W_1 \otimes \ldots \otimes W_n})^{-1} \cdot M \cdot J^{(m)}_{V_1 \otimes \ldots \otimes V_m} \,. \tag{B.10}$$

If M is represented as the composition of "more elementary" Clebsch-Gordan maps one needs to verify the consistency of definition (B.10) with (B.9). This boils down to the consideration of two cases, as will be discussed in the following.

Twisting composite intertwiners (I): let $C^{UVW}_T : T \to U \otimes V \otimes W$ be constructed as $C^{UV}_S C^{SW}_T$. This composition may be re-expressed in terms of $\tilde{C}^{UV}_S \tilde{C}^{SW}_T$ by using

$$C^{UV}_S C^{SW}_T = C^{UV}_S J_{SW} J^{-1}_{SW} C^{SW}_T = C^{UV}_S J_{SW} \tilde{C}^{SW}_T \,. \tag{B.11}$$

Decomposing $J_{SW} = \sum_k \pi_S(x_k) \otimes \pi_W(x^k)$, one can use the intertwining property satisfied by C^{UV}_S to calculate

$$C^{UV}_S J_{SW} = C^{UV}_S \cdot \sum_k \pi_S(x_k) \otimes \pi_W(x^k) =$$

$$= \sum_k (\pi_U \otimes \pi_V)(\Delta(x_k)) \otimes \pi_W(x^k) \cdot C^{UV}_S = J_{(U \otimes V) \otimes W} C^{UV}_S \,.$$

Noting that $C_S^{UV} = J_{UV}\tilde{C}_S^{UV}$, we arrive at

$$C_S^{UV}C_T^{SW} = J_{(U\otimes V)\otimes W}J_{UV}\tilde{C}_S^{UV}\tilde{C}_T^{SW}\ . \tag{B.12}$$

In a similar way one can verify that $C_S^{VW}C_T^{US} = J_{U\otimes(V\otimes W)}J_{VW}\tilde{C}_S^{VW}\tilde{C}_T^{US}$.

Twisted compositions (II): Clebsch-Gordan maps of the type C_U^{VW} and C_{VW}^{U} can also be composed in the following ways

$$C_{V'W'}^{VW} := C_U^{VW}C_{V'W'}^{U}\quad ,\quad C_{V'W'}^{VW} := C_{UW'}^{W}C_{V'}^{VU}\ . \tag{B.13}$$

The second type of composition is diagrammatically represented in figure 49.

Recall that the representations $\pi_V,\pi_U,\dots$ are not necessarily irreducible. As such, the blocks in figure 49 should themselves be thought of as networks with a general number of incoming and outgoing legs and iterated compositions of Clebsch-Gordan maps inside each block. Compositions of the first type in equation (B.13) are twisted trough

$$\tilde{N}_{V'W'}^{VW} = \tilde{C}_U^{VW}\tilde{C}_{V'W'}^{U} = J_{VW}^{-1}C_U^{VW}C_{V'W'}^{U}J_{V'W'}\ . \tag{B.14}$$

Compositions of the second type

$$\hat{N}_{V'W'}^{VW} = C_{UW'}^{W}C_{V'}^{VU} = \tilde{C}_{UW'}^{W}J_{UW'}^{-1}J_{VU}\tilde{C}_{V'}^{VU} \tag{B.15}$$

also transform by conjugation with the J-factors of equation (B.14). To show that $\hat{N}_{V'W'}^{VW}$ is twisted by acting on its free legs as

$$\hat{N}_{V'W',\text{twist}}^{VW} = J_{VW}^{-1}\hat{N}_{V'W'}^{VW}J_{V'W'}\, , \tag{B.16}$$

we insert the identity in (B.15)

$$\hat{N}_{V'W',\text{twist}}^{VW} = J_{VW}^{-1}C_{UW'}^{W}J_{V(U\otimes W')}J_{V(U\otimes W')}^{-1}J_{(V\otimes U)W'}J_{(V\otimes U)W'}^{-1}C_{V'}^{VU}J_{V'W'}\ .$$

$J_{V(U\otimes W')}$ and $J_{(V\otimes U)W'}^{-1}$ can be shifted past $C_{UW'}^{W}$ and $C_{V'}^{VU}$ to cancel J_{VW}^{-1} and $J_{V'W'}$

$$C_{UW'}^{W}J_{V(U\otimes W')} = C_{UW'}^{W}\sum_k \pi_V(x_k)\otimes(\pi_U\otimes\pi_{W'})\Delta(x^k) = \sum_k \pi_V(x_k)\otimes\pi_W(x^k)C_{UW'}^{W}\, ,$$

where $\sum_k \pi_V(x_k)\otimes\pi_W(x^k)C_{UW'}^{W} = J_{VW}C_{UW'}^{W}$ and similarly for $J_{(V\otimes U)W'}^{-1}$. So we find

$$\hat{N}_{V'W',\text{twist}}^{VW} = C_{UW'}^{W}J_{V(U\otimes W')}^{-1}J_{(V\otimes U)W'}C_{V'}^{VU} = \tilde{C}_{UW'}^{W}J_{UW'}^{-1}J_{V(U\otimes W')}^{-1}J_{(V\otimes U)W'}J_{VU}\tilde{C}_{V'}^{VU}\ .$$

By the cocycle condition (B.6) $J_{UW'}^{-1}J_{V(U\otimes W')}^{-1}J_{(V\otimes U)W'}J_{VU}$ reduces to the identity evaluated on the tensor product of modules $V\otimes U\otimes W'$ and

$$\hat{N}_{V'W',\text{twist}}^{VW} = \tilde{C}_{UW'}^{W}\tilde{C}_{V'}^{VU} \tag{B.17}$$

as claimed. Therefore general networks $\hat{N}_{V'W'}^{VW}$, constructed as iterated compositions of Clebsch-Gordan maps, are twisted by J-factors which act on their external free legs.

References

[1] J. Teschner, *Exact results on $\mathcal{N} = 2$ supersymmetric gauge theories*, [arXiv:1412.7145](https://arxiv.org/abs/1412.7145) [INSPIRE].

[2] D. Gaiotto, *$\mathcal{N} = 2$ dualities*, *JHEP* **08** (2012) 034 [arXiv:0904.2715] [INSPIRE].

[3] D. Gaiotto, G.W. Moore and A. Neitzke, *Wall-crossing, Hitchin Systems and the WKB Approximation*, *Adv. Math.* **234** (2013) 239 [arXiv:0907.3987] [INSPIRE].

[4] L.F. Alday, D. Gaiotto and Y. Tachikawa, *Liouville Correlation Functions from Four-dimensional Gauge Theories*, *Lett. Math. Phys.* **91** (2010) 167 [arXiv:0906.3219] [INSPIRE].

[5] N. Wyllard, *A_{N-1} conformal Toda field theory correlation functions from conformal $\mathcal{N} = 2$ SU(N) quiver gauge theories*, *JHEP* **11** (2009) 002 [arXiv:0907.2189] [INSPIRE].

[6] F. Passerini, *Gauge Theory Wilson Loops and Conformal Toda Field Theory*, *JHEP* **03** (2010) 125 [arXiv:1003.1151] [INSPIRE].

[7] C. Kozçaz, S. Pasquetti and N. Wyllard, *A & B model approaches to surface operators and Toda theories*, *JHEP* **08** (2010) 042 [arXiv:1004.2025] [INSPIRE].

[8] S. Kanno, Y. Matsuo and S. Shiba, *Analysis of correlation functions in Toda theory and AGT-W relation for* SU(3) *quiver*, *Phys. Rev.* **D 82** (2010) 066009 [arXiv:1007.0601] [INSPIRE].

[9] J. Gomis and B. Le Floch, *'t Hooft Operators in Gauge Theory from Toda CFT*, *JHEP* **11** (2011) 114 [arXiv:1008.4139] [INSPIRE].

[10] N. Wyllard, *W-algebras and surface operators in $\mathcal{N} = 2$ gauge theories*, *J. Phys.* **A 44** (2011) 155401 [arXiv:1011.0289] [INSPIRE].

[11] N. Wyllard, *Instanton partition functions in $\mathcal{N} = 2$ SU(N) gauge theories with a general surface operator and their W-algebra duals*, *JHEP* **02** (2011) 114 [arXiv:1012.1355] [INSPIRE].

[12] N. Drukker and F. Passerini, *(de)Tails of Toda CFT*, *JHEP* **04** (2011) 106 [arXiv:1012.1352] [INSPIRE].

[13] Y. Tachikawa, *On W-algebras and the symmetries of defects of 6d $\mathcal{N} = (2, 0)$ theory*, *JHEP* **03** (2011) 043 [arXiv:1102.0076] [INSPIRE].

[14] V.A. Fateev and A.V. Litvinov, *Integrable structure, W-symmetry and AGT relation*, *JHEP* **01** (2012) 051 [arXiv:1109.4042] [INSPIRE].

[15] B. Estienne, V. Pasquier, R. Santachiara and D. Serban, *Conformal blocks in Virasoro and W theories: Duality and the Calogero-Sutherland model*, *Nucl. Phys.* **B 860** (2012) 377 [arXiv:1110.1101] [INSPIRE].

[16] H. Zhang and Y. Matsuo, *Selberg Integral and* SU(N) *AGT Conjecture*, *JHEP* **12** (2011) 106 [arXiv:1110.5255] [INSPIRE].

[17] S. Shiba, *Notes on 3-point functions of A_{N-1} Toda theory and AGT-W relation for* $\mathrm{SU}(N)$ *quiver*, *JHEP* **12** (2011) 108 [arXiv:1111.1899] [InSPIRE].

[18] S. Kanno, Y. Matsuo and H. Zhang, *Extended Conformal Symmetry and Recursion Formulae for Nekrasov Partition Function*, *JHEP* **08** (2013) 028 [arXiv:1306.1523] [InSPIRE].

[19] M. Aganagic, N. Haouzi and S. Shakirov, A_n-*Triality*, arXiv:1403.3657 [InSPIRE].

[20] J. Gomis and B. Le Floch, *M2-brane surface operators and gauge theory dualities in Toda*, arXiv:1407.1852 [InSPIRE].

[21] D. Gaiotto, G.W. Moore and A. Neitzke, *Four-dimensional wall-crossing via three-dimensional field theory*, *Commun. Math. Phys.* **299** (2010) 163 [arXiv:0807.4723] [InSPIRE].

[22] D. Gaiotto, G.W. Moore and A. Neitzke, *Framed BPS States*, *Adv. Theor. Math. Phys.* **17** (2013) 241 [arXiv:1006.0146] [InSPIRE].

[23] D. Gaiotto, G.W. Moore and A. Neitzke, *Spectral Networks and Snakes*, *Annales Henri Poincaré* **15** (2014) 61 [arXiv:1209.0866] [InSPIRE].

[24] A. Neitzke, *Hitchin systems in* $\mathcal{N} = 2$ *field theory*, arXiv:1412.7120 [InSPIRE].

[25] J. Teschner and G.S. Vartanov, *Supersymmetric gauge theories, quantization of* $\mathcal{M}_{\mathrm{flat}}$ *and conformal field theory*, *Adv. Theor. Math. Phys.* **19** (2015) 1 [arXiv:1302.3778] [InSPIRE].

[26] J. Teschner, *Supersymmetric gauge theories, quantisation of moduli spaces of flat connections and Liouville theory*, arXiv:1412.7140 [InSPIRE].

[27] O. Aharony, N. Seiberg and Y. Tachikawa, *Reading between the lines of four-dimensional gauge theories*, *JHEP* **08** (2013) 115 [arXiv:1305.0318] [InSPIRE].

[28] Y. Tachikawa, *On the* 6d *origin of discrete additional data of* 4d *gauge theories*, *JHEP* **05** (2014) 020 [arXiv:1309.0697] [InSPIRE].

[29] C. Córdova and A. Neitzke, *Line Defects, Tropicalization and Multi-Centered Quiver Quantum Mechanics*, *JHEP* **09** (2014) 099 [arXiv:1308.6829] [InSPIRE].

[30] V. Fock and A. Goncharov, *Moduli spaces of local systems and higher Teichmuller theory*, *Publ. Math. IHES* **103** (2006) 1 [math.AG/0311149].

[31] S. Gukov and E. Witten, *Gauge theory, ramification, and the geometric Langlands program*, in *Current developments in mathematics*, International Press, Somerville U.S.A. (2008), pp. 35–180.

[32] Y. Ito, T. Okuda and M. Taki, *Line operators on* $S^1 \times \mathbb{R}^3$ *and quantization of the Hitchin moduli space*, *JHEP* **04** (2012) 010 [arXiv:1111.4221] [InSPIRE].

[33] V. Pestun, *Localization of gauge theory on a four-sphere and supersymmetric Wilson loops*, *Commun. Math. Phys.* **313** (2012) 71 [arXiv:0712.2824] [InSPIRE].

[34] J. Gomis, T. Okuda and V. Pestun, *Exact Results for 't Hooft Loops in Gauge Theories on* S^4, *JHEP* **05** (2012) 141 [arXiv:1105.2568] [InSPIRE].

[35] N. Hama and K. Hosomichi, *Seiberg-Witten Theories on Ellipsoids*, *JHEP* **09** (2012) 033 [arXiv:1206.6359] [InSPIRE].

[36] Y. Tachikawa, *A review on instanton counting and W-algebras*, arXiv:1412.7121 [InSPIRE].

[37] N. Nekrasov and E. Witten, *The Omega Deformation, Branes, Integrability and Liouville Theory*, *JHEP* **09** (2010) 092 [arXiv:1002.0888] [InSPIRE].

[38] N.A. Nekrasov, *Seiberg-Witten prepotential from instanton counting*, *Adv. Theor. Math. Phys.* **7** (2004) 831 [hep-th/0206161] [INSPIRE].

[39] N. Nekrasov, A. Rosly and S. Shatashvili, *Darboux coordinates, Yang-Yang functional and gauge theory*, *Nucl. Phys. Proc. Suppl.* **216** (2011) 69 [arXiv:1103.3919] [INSPIRE].

[40] O. Chacaltana and J. Distler, *Tinkertoys for Gaiotto Duality*, *JHEP* **11** (2010) 099 [arXiv:1008.5203] [INSPIRE].

[41] L.F. Alday, D. Gaiotto, S. Gukov, Y. Tachikawa and H. Verlinde, *Loop and surface operators in $\mathcal{N} = 2$ gauge theory and Liouville modular geometry*, *JHEP* **01** (2010) 113 [arXiv:0909.0945] [INSPIRE].

[42] N. Drukker, J. Gomis, T. Okuda and J. Teschner, *Gauge Theory Loop Operators and Liouville Theory*, *JHEP* **02** (2010) 057 [arXiv:0909.1105] [INSPIRE].

[43] W.M. Goldman, *Trace Coordinates on Fricke spaces of some simple hyperbolic surfaces*, arXiv:0901.1404.

[44] A.S. Sikora, *Generating sets for coordinate rings of character varieties*, arXiv:1106.4837.

[45] S. Lawton, *Generators, Relations and Symmetries in Pairs of 3x3 Unimodular Matrices*, math.AG/0601132.

[46] M. Audin, *Lectures on gauge theory and integrable systems*, in *Gauge Theory and Symplectic Geometry*, J. Hurtubise, F. Lalonde and G. Sabidussi eds., *NATO Sci. Ser.*, **C 488** Springer, Netherlands (1997), pp. 1–48.

[47] W. Goldman, *Invariant functions on Lie groups and Hamiltonian flows of surface group representations*, *Invent. Math.* **85** (1986) 263.

[48] S. Lawton, *Poisson Geometry of* SL(3, C)*-Character Varieties Relative to a Surface with Boundary*, math.SG/0703251.

[49] G. Kuperberg, *Spiders for rank 2 Lie algebras*, q-alg/9712003.

[50] V.G. Turaev, *Skein quantization of poisson algebras of loops on surfaces*, *Ann. Sci. École Norm. S.* **24** (1991) 635.

[51] E. Witten, *Quantum Field Theory and the Jones Polynomial*, *Commun. Math. Phys.* **121** (1989) 351 [INSPIRE].

[52] E. Witten, *Gauge Theories, Vertex Models and Quantum Groups*, *Nucl. Phys.* **B 330** (1990) 285 [INSPIRE].

[53] N. Yu. Reshetikhin and V.G. Turaev, *Ribbon graphs and their invariants derived from quantum groups*, *Commun. Math. Phys.* **127** (1990) 1 [INSPIRE].

[54] A.S. Sikora, *Skein theory for* SU(n)*-quantum invariants*, math/0407299.

[55] H. Murakami, T. Ohtsuki, and S. Yamada, *Homfly Polynomial via an Invariant of Colored Plane Graphs*, *Enseign. Math.* **44** (1998) 325.

[56] D. Kim, *Graphical Calculus on Representations of Quantum Lie Algebras*, math.QA/0310143.

[57] S. Morrison, *A Diagrammatic Category for the Representation Theory of $U_q(\mathrm{sl}_n)$*, arXiv:0704.1503.

[58] S. Cautis, J. Kamnitzer and S. Morrison, *Webs and quantum skew Howe duality*, *Math. Ann.* **360** (2014) 351.

[59] Y. Tachikawa and N. Watanabe, *On skein relations in class S theories*, *JHEP* **06** (2015) 186 [`arXiv:1504.00121`] [ɪɴSPIRE].

[60] Y. Teranishi, *The ring of invariants of matrices*, *Nagoya Math. J.* **104** (1986) 149.

[61] T. Dimofte and S. Gukov, *Chern-Simons Theory and S-duality*, *JHEP* **05** (2013) 109 [`arXiv:1106.4550`] [ɪɴSPIRE].

[62] D. Xie, *Higher laminations, webs and $\mathcal{N} = 2$ line operators*, `arXiv:1304.2390` [ɪɴSPIRE].

[63] S. Lawton, *Obtaining the One-Holed Torus from Pants: Duality in an* SL(3, C)*-Character Variety*, `arXiv:0803.3489`.

[64] S. Lawton, *Minimal Affine Coordinates for* SL(3, C) *Character Varieties of Free Groups*, `arXiv:0709.4403`.

[65] S. Lawton, *Algebraic Independence in* SL(3, C) *Character Varieties of Free Groups*, `arXiv:0807.0798`.

[66] N. Saulina, *Spectral networks and higher web-like structures*, `arXiv:1409.2561` [ɪɴSPIRE].

[67] T. Dimofte, M. Gabella and A.B. Goncharov, *K-Decompositions and 3d Gauge Theories*, `arXiv:1301.0192` [ɪɴSPIRE].

[68] V.A. Fateev and A.V. Litvinov, *Correlation functions in conformal Toda field theory. I.*, *JHEP* **11** (2007) 002 [`arXiv:0709.3806`] [ɪɴSPIRE].

[69] J. Teschner, *Liouville theory revisited*, *Class. Quant. Grav.* **18** (2001) R153 [`hep-th/0104158`] [ɪɴSPIRE].

[70] J. Teschner, *A Lecture on the Liouville vertex operators*, *Int. J. Mod. Phys.* **A 19S2** (2004) 436 [`hep-th/0303150`] [ɪɴSPIRE].

[71] P. Bouwknegt and K. Schoutens, *W symmetry in conformal field theory*, *Phys. Rept.* **223** (1993) 183 [`hep-th/9210010`] [ɪɴSPIRE].

[72] E. Frenkel and D. Ben-Zvi, *Vertex algebras and algebraic curves*, American Mathematical Society (2004).

[73] A.A. Belavin, A.M. Polyakov and A.B. Zamolodchikov, *Infinite Conformal Symmetry in Two-Dimensional Quantum Field Theory*, *Nucl. Phys.* **B 241** (1984) 333 [ɪɴSPIRE].

[74] J. Teschner, *Quantization of moduli spaces of flat connections and Liouville theory*, `arXiv:1405.0359` [ɪɴSPIRE].

[75] P. Bowcock and G.M.T. Watts, *Null vectors, three point and four point functions in conformal field theory*, *Theor. Math. Phys.* **98** (1994) 350 [`hep-th/9309146`] [ɪɴSPIRE].

[76] C. Kozçaz, S. Pasquetti and N. Wyllard, *A & B model approaches to surface operators and Toda theories*, *JHEP* **08** (2010) 042 [`arXiv:1004.2025`] [ɪɴSPIRE].

[77] L. Bao, V. Mitev, E. Pomoni, M. Taki and F. Yagi, *Non-Lagrangian Theories from Brane Junctions*, *JHEP* **01** (2014) 175 [`arXiv:1310.3841`] [ɪɴSPIRE].

[78] P. Bouwknegt, J.G. McCarthy and K. Pilch, *Quantum Group Structure in the Fock Space Resolutions of* sl(n) *Representations*, *Commun. Math. Phys.* **131** (1990) 125 [ɪɴSPIRE].

[79] A. Bilal and J.-L. Gervais, *Systematic Construction of Conformal Theories with Higher Spin Virasoro Symmetries*, *Nucl. Phys.* **B 318** (1989) 579 [ɪɴSPIRE].

[80] E. Cremmer and J.-L. Gervais, *The Quantum Group Structure Associated With Nonlinearly Extended Virasoro Algebras*, *Commun. Math. Phys.* **134** (1990) 619 [INSPIRE].

[81] E. Buffenoir, P. Roche and V. Terras, *Quantum Dynamical coBoundary Equation for finite dimensional simple Lie algebras*, `math.QA/0512500`.

[82] M. Bullimore, *Defect Networks and Supersymmetric Loop Operators*, *JHEP* **02** (2015) 066 [`arXiv:1312.5001`] [INSPIRE].

[83] M. Semenov-Tian-Shansky, *Quantization of open toda lattices*, in *Dynamical Systems VII*, V. Arnol'd and S. Novikov eds., *Encyclopaedia of Mathematical Sciences* **16**, Springer, Berlin Heidelberg (1994), pp. 226–259.

[84] N. Wallach, *Real reductive groups II*, Academic Press (1992).

[85] K.K. Kozlowski, *Unitarity of the SoV Transform for the Toda Chain*, *Comm. Math. Phys.* **334** (2014) 223 [`arXiv:1306.4967`].

[86] T.L. Curtright and C.B. Thorn, *Conformally Invariant Quantization of the Liouville Theory*, *Phys. Rev. Lett.* **48** (1982) 1309 [*Erratum ibid.* **48** (1982) 1768].

[87] R.M. Kashaev, *On the spectrum of Dehn twists in quantum Teichmüller theory*, in *Physics and Combinatorics*, A.N. Kirillov, A. Tsuchiya and H. Umemura eds., World Scientific (2001), pp. 63–81 [`math/0008148`] [INSPIRE].

[88] L.D. Faddeev and L.A. Takhtajan, *On the spectral theory of one functional-difference operator from conformal field theory*, `arXiv:1408.0307` [INSPIRE].

[89] V. Mitev and E. Pomoni, *Toda 3-Point Functions From Topological Strings*, *JHEP* **06** (2015) 049 [`arXiv:1409.6313`] [INSPIRE].

[90] M. Isachenkov, V. Mitev and E. Pomoni, *Toda 3-Point Functions From Topological Strings II*, `arXiv:1412.3395` [INSPIRE].

[91] V. Chari and A. Pressley, *A guide to quantum groups*, Cambridge University Press (1994).